Investigation on the ultrasound intensification of a leaching process applied to copper recycling

Auteur : Antunes Simão, Miguel
Promoteur(s) : Gaydardzhiev, Stoyan
Faculté : Faculté des Sciences appliquées
Diplôme : Cours supplémentaires destinés aux étudiants d'échange (Erasmus, ...)
Année académique : 2021-2022
URI/URL : http://hdl.handle.net/2268.2/15714

Master thesis

Investigation on the ultrasound intensification of a leaching process applied to copper recycling

by

Miguel Simão

In collaboration with Faculty of Applied Sciences, ArGEnCo Department, and GeMMe Research Group

Pr. Dr. Ir. Stoyan **Gaydardzhiev**, Advisor

Pr. Dr. Ir. Eric **Pirard**, Committee member

Prof. Dr. Ir. Léonard **Grégoire**, Committee member

Ir. Mohamed **Aâtach**, Committee member

ULiège

22 August 2022

Acknowledgments

This work was directly made possible by a few individuals. To Professor Stoyan Gaydardzhiev thank you for having both made the topic available and encouraging this choice, but also for the continuous support and supervision throughout the semester. To Engineer Mohamed Aâtach, thank you, for not only sharing your wealth of knowledge, but for always doing it with an extremely contagious enthusiasm, for the meetings at egregious times, and for the constant concern not only academically but also emotionally. Thank you to Sabrina and Sébastien Blasuitig, for a lot of the technical laboratory knowledge, and for the analysis of God-knows how many (109) samples.

This work was also indirectly made possible by many individuals. To the whole GeMMe group, thank you for the great barbecues, stories, and welcoming. To the professors of ULiège, whose great professionalism and competences made life at times challenging, but always rewarding, thank you for uncovering so much about metallurgy, recycling, raw materials and so many fascinating topics. To the high school teachers, thank you for the commitment to your students, for the life lessons, for the humanity.

To the badminton players, thank you for the adrenaline filled games that so many times made all the hardships purposeful, and for the warm welcoming, which made Home seem a little closer. To the AMIR and Erasmus students thank you for great moments, the best of luck in your personal and professional (ad)ventures, you will change the world for the better. To the more-legs-than-torso queen, to the matlab lord, to the Archimedes of calisthenics, and to the tall genius with a lot of hair, thank you for the life changing journey that was getting an academic degree. To Mariana and Bruna, thank you for encouraging me to take this path and so many others. To Mário and Luísa, thank you for the always kind words, and for taking such good care of your loved ones.

This work was made by a meat and bones vehicle, in which the brain takes the driving seat. That brain has been completely shaped by the love, patience, and knowledge given by its creators. Mom and Dad, thank you, this work is more yours than mine, I'm a puppet of your education, and I'm forever grateful and proud of that. To Marta, thank you for your existence, which completes my own. To grandmas, thank you for being the pillars. To grandpas, thank you for being with me, now and always.

To the old lady that waited by the river…

Contents

1. Introduction 1

1.1 Ultrasounds & Cavitation 1

1.1.1 Bubble dynamics and cavitation effects 1

1.1.2 Transducers 3

1.1.3 Use cases for ultrasounds 5

1.1.4 Ultrasonic characterization 8

1.1.4.1 Calorimetry 9

1.1.4.2 Chemical dosimetry 10

1.1.4.3 Setup and comparison of calorimetry and iodide dosimetry 11

1.1.4.4 Weissler, Fricke and terephthalic dosimetry methods 11

1.1.5 Discussion on the effectiveness of each method 13

1.1.6 Conclusion on characterization methods 13

1.2 Leaching 14

1.2.1 Selection of parameters 17

1.3 Copper cementation 19

1.3.1 Kinetics of leaching – Chemical vs Diffusion control 20

1.3.2 Calculating activation energy 23

1.3.3 Reaction order 23

1.3.4 Reaction parameters 23

1.3.5 Copper production 24

1.4 Objectives 25

2. Methodology 27

2.1 Safety and good practices regard 27

2.2 ICP-MS analysis 27

2.2.1 Sample preparation/procedure 27

2.2.2 Working principle 28

2.3 Iron titration 28

2.3.2 Sample preparation/procedure 28

2.3.3 Working principle 29

2.4 Resonance frequency determination 30

2.4.1 Working principle 30

2.4.1 Measurement setup 31

2.5 Characterization of the vessel-transducer system – Calorimetry 31
2.6 Control reaction – Cementation of copper on steel balls 33
2.7 U.S. assisted reaction – Cementation of copper on steel balls 34
2.8 Calibration of the measuring equipment 35
3. Results and discussion 36
3.1 Calorimetry 36
3.1.1 Discussion on calorimetry results 38
3.2 Iron titration 40
3.2.1 Iron titration 42
3.3 Resonance frequency determination 44
3.3.1 Discussion on resonance frequency (RF) determination results 45
3.4 Silent copper recovery 46
3.4.1 pH effects at low temperature & low RPM (40°C & 200 RPM): 46
3.4.1.1 Discussion on pH effects at low temperature & low RPM (40°C & 200 RPM): 47
3.4.2 pH effects at high temperature & low RPM (60°C & 200 RPM) 49
3.4.2.1 Discussion on pH effects at low temperature & low RPM (40°C & 200 RPM): 49
3.4.3 pH effects at low temperature & high RPM (40°C & 500 RPM) 50
3.4.3.1 Discussion on pH effects at low temperature & low RPM (40°C & 200 RPM): 51
3.4.1 pH effects at high temperature & high RPM (60°C & 500 RPM) 52
3.4.1.1 Discussion on pH effects at low temperature & low RPM (40°C & 200 RPM): 52
3.5 US assisted copper recovery 55
3.5.1 Influence of the cavitation effects 58
3.5.2 Influence of RPM 61
3.5.3 Influence of resonance frequency 62
3.5.4 Energetic consumption 65
3.6 Optical observation of the cemented copper and of the fine powder 68
4. EiT Chapter 69
4.1 Life cycle analysis – Environmental benefits of sonication in cementation 72
4.4.1 Structure of sonicated assay emissions 74
4.4.1 Structure of silent assay emissions 74
4.4.2 Limitations of the life cycle assessment 75
4.2 Techno-economic analysis 75
4.2.1 Conversion from lab to industrial scale – Considerations 76
4.3 Entrepreneurial prospects – Business plan and SWOT analysis 77
5. Conclusion 79

Bibliography **81**
Annexes **85**

List of figures

Figure 1 Diagram of a Langevin-type transducer (Fragassa & Ippoliti, 2016) 4
Figure 2 Ideal US frequencies for different applications. Dark colors indicate higher intensity process. (Kiss et al., 2018) 8
Figure 3 Major characterization methods and respective description (Dong et al., 2020) 14
Figure 4 Pourbaix diagram of CuO-H2O system. Increase in temperature (left to right,) results in dissolution at lower potential (Yagi, 2011) 18
Figure 5 Pourbaix diagram of Fe-H2O system (Perry et al., 2020) 18
Figure 6 Copper cementation process setup, used for copper production (Habashi, 2006) 25
Figure 7 Left, solution is one titrating agent's drop away from equilibrium; Right, after equilibrium was reached 29
Figure 8 Complete setup for US assays and res freq. determination 31
Figure 9 Calorimetric data at 20, 40, and 60 kHz. Frame 2 was used, and the initial temperature of the water in the vessel was not regulated. Significant dispersion between results is observed. 36
Figure 10 Calorimetric data at 20, 40, and 60 kHz. Frame 2 was used and the initial temperature of the water in the vessel was regulated. 37
Figure 11 Calorimetric data at 20, 40, and 60 kHz. Frame 1 was used and the initial temperature of the water in the vessel was regulated 37
Figure 12 Statistical data calculated with SPSS software. Left, the correlations, or the degree of influence between variables is seen. Right, the amount of change caused by one variable (B), along with significance (Sig.). Data from unregulated initial temperature and frame 2 38
Figure 13 Left, the correlations, or the degree of influence between variables is seen. Right, the amount of change caused by one variable (B), along with significance (Sig.). Data from regulated initial temperature and frame 1 39
Figure 14 Assay 91's evolution of ferrous and ferric ions in solution, along with a dashed line showing the physical limit, indicating an error. 41
Figure 15 Assay 90's evolution of ferrous and ferric ions in solution, along with a dashed line showing the physical limit, well above the total iron obtained. 41
Figure 16 Evolution of the Fe^{3+} ion concentration in solution in silent and sonicated conditions 42
Figure 17 Left, resistance and reactance measurements of transducer 1 alone; Right, same measurements for the setup transducer 1 and frame 1 44
Figure 18 Left, resistance and reactance measurements of transducer 2 alone; Right, same measurements for the setup transducer 2 and frame 2 44

Figure 19 Copper recovery and PPT evolution of assay 3. pH 2.5, 40°C and 200 RPM..... 46
Figure 20 Copper recovery and PPT evolution of assay 8. pH 2.0, 40°C and 200 RPM..... 46
Figure 21 Eh evolution of assay 03..... 46
Figure 22 Eh evolution of assay 8..... 46
Figure 23 Activation energy of copper cementation at 200 RPM and pH 2, measurements taken at 40 and 60°C..... 48
Figure 24 Copper recovery and PPT evolution of assay 13. pH 2.5, 60°C and 200 RPM..... 49
Figure 25 Copper recovery and PPT evolution of assay 19. pH 2.0, 60°C and 200 RPM..... 49
Figure 26 Eh evolution of assay 13..... 49
Figure 27 Eh evolution of assay 19..... 49
Figure 28 Copper recovery and PPT evolution of assay 05. pH 2.5, 40°C and 500 RPM..... 50
Figure 29 Copper recovery and PPT evolution of assay 10. pH 2.0, 40°C and 500 RPM..... 50
Figure 30 Eh evolution of assay 05..... 50
Figure 31 Eh evolution of assay 10..... 50
Figure 32 Copper recovery and PPT evolution of assay 16. pH 2.5, 60°C and 500 RPM..... 52
Figure 33 Copper recovery and PPT evolution of assay 22. pH 2.0, 60°C and 500 RPM..... 52
Figure 34 Eh evolution of assay 16..... 52
Figure 35 Eh evolution of assay 22..... 52
Figure 36 Left, solid residue from assay 8 obtained after filtration (fine residue was separated). The beads are strongly stuck together in the shape formed at the bottom of the reactor; Right, solid residue from assay 93..... 54
Figure 37 Activation energy of copper cementation at 500 RPM and pH 2, measurements taken at 40 and 60°C..... 55
Figure 38 Copper recovery and PPT evolution of assay 90. pH 2.0, 60°C and 500 RPM..... 56
Figure 39 Cu recov. and PPT evolution of assay 91, pH 2.0, 60°C, 500 RPM, 20 kHz and Pcal=4.7±0.3W..... 56
Figure 40 Eh evolution of assay 90..... 56
Figure 41 Eh evolution of assay 91..... 56
Figure 42 Cu recov. and PPT evolution of assay 92, pH 2.0, 60°C, 200 RPM, 20 kHz and Pcal=4.7±0.3W..... 57
Figure 43 Cu recov. and PPT evolution of assay 93, pH 2.0, 60°C, 200 RPM, 40 kHz and Pcal=4.7±0.3W..... 57
Figure 44 Eh evolution of assay 93..... 57

Figure 45 Photos of silent assay 90, taken 5 and 30 minutes into the reaction (left and right image, respectively). Beads can be seen at the bottom of the vessel, brownish in color. 58
Figure 46 Photos of US assay 91, taken 5 and 30 minutes into the reaction (left and right image, respectively). Copper particles make the solution opaque. On the right, crests and troughs of the modulated wave signal are seen. 59
Figure 47 Recovery rates plotted as ln(1-X), with X being recovered fraction. Steeper slope means faster cementation. 63
Figure 48 Agglomeration of the beads, cemented together, seen in assay 92 (left) and 93 (right). 64
Figure 49 Assay 92, little over 11 minutes into the reaction 65
Figure 50 Energetic/power consumption estimates for silent (assay 90) and sonicated trials (assay 92)… 67
Figure 51 CO2 emissions embedded in global trade in 2019. Positive values (red) represent net importers of CO2, and negative values (blue) represent exporters (Ritchie et al., 2020, p. 2). 69
Figure 52 Left, cost/benefit plot for copper removal techniques; Right, cumulative copper which "sequestrated" within the steel supply chain, in line blue. In orange is the copper which needs to be removed from the same supply chain. (Daehn et al., 2017) 71
Figure 53 CRM assessment map. Materials above and to the right of the red dotted line are considered critical. Copper is highlighted, and it's not a CRM (European Commission, 2020). 72
Figure 54 Calculated values for impact indicators of silent and US cementation of 1 kg of copper at 80% efficiency 73
Figure 55 Relative comparison between the previously obtained results for the different eco indicators.. 74
Figure 56 Relative contribution of the sonicated process components on the GWP 74
Figure 57 Relative contribution of the silent process components on the GWP 74
Figure 58 Predicted cost of operation in a laboratory setting at different handling scales 75
Figure 59 Dangers of US exposure of in terms of frequency and decibels (Moyano et al., 2022) 76

List of tables

Table 1 Calculated conversion factors for the characterization of the ultrasonic setup with regulated initial temperature 40
Table 2 Different growth rates of Fe3+ concentration, for assays 90 & 91 42
Table 3 Determined resonance frequencies in transducer and reactor 44
Table 4 Experimental results low temperature low RPM 46
Table 5 Experimental results high temperature low RPM 49
Table 6 Experimental results at low temperature and high RPM 50

Table 7 Experimental results at high temperature and high RPM 52
Table 8 Calculated Ea for every non-sonicated scenario. A comparative scale is presented, to help identify which controlling category each scenario falls into 53
Table 9 Compilation of pH, temperature, stirring, US freq, and time parameters used in the sonicaated assays 56
Table 10 Compilation of experimental results obtained with US intensification 57
Table 11 Energetic consumption of the equipment used for copper cementation, silent and sonicated 65
Table 12 Optical characteristics of cemented copper. Left images are the filter aspect after filtration; right images show copper covered beads. (RPM, pH, kHz) 68
Table 13 Swot analysis of a simulated start-up focused on sonicated Cu cementation and US cleaning ... 78

Nomenclature

c, concentration, or molarity

CRM, critical raw material

Ea, activation energy

GWP, global warming potential

M, molar mass

m, mass

Pin, power input

Pcal, calorimetric power

PPT, precipitant factor

RPM, rotations per minute

RF, resonance frequency

US, ultrasounds/ ultrasonic

Abstract

A langevin type transducer was used to produce US waves, these create cavitation bubbles that generate micro-events of extreme pressure and temperature. Such conditions change how the electrochemical copper cementation reaction works. Silent (no US) and sonicated (with US) assays were done to measure the degree of influence of the sonication on the reaction. Calorimetric characterization, resonance frequency determination, iron titration, and activation energy (Ea) measurements were performed. Increased initial temperature of solution was found to negatively impact calorimetry reproducibility, contrarily to literature findings. Sonication at 20 kHz did not increase radical species concentration significantly when compared to silent tests. Silent rate of leaching was found to be highest at 60°C, pH 2, and 500 RPM with maximum cu recovery at 83% after 4h, and the reaction to be an intermediate controlled process, regarding Ea. When US were applied to same previous parameters, max, cu recovery was 96% after 1h30 min, with similar precipitant factor at 1.09. Reducing RPM from 500 to 200 while using US did **not** change the behavior of the reaction. Copper nanoparticles might have been produced during sonication at 20 kHz. Cementation at resonance frequency (~40.5 kHz) damaged the reaction efficiency. Power consumption (Wh) per 80% of cu recovery was lower to substantially lower when US was used. A preliminary LCA study was performed, and the sonication process was shown to be more environmentally friendly in terms of global warming potential and ozone layer depletion.

Chapter 1

1. Introduction

1.1 Ultrasounds & Cavitation

The manipulation of pressure waves has long been used in our world. The Aztecs built structures that interacted with sound waves and changed them to mimic animals. Later, in the Alps, long and hollow wooden tubes were used to create sounds that could be heard deep into the mountain ranges. Today and forever, sound will be a part of the lives of all of us, but perhaps not in the ways most of us expect.

Starting at 20 kHz and up to a few GHz, these frequencies of the sound spectrum correspond to the ultrasonic domain, where the frequency is too high for humans to hear, for the most part. They have been used in various activities and fields, from imaging, diagnosing, and surgery techniques, amongst many others. In 2021 alone, PubMed and ULiège library both reported over 10 000 articles with titles related to ultrasonic technologies/processes.

When an ultrasound producing device transmits its mechanical energy through an elastic medium, a fascinating phenomenon happens. One that has been known for over a century: cavitation. However, it didn't start with ultrasounds, it started by degrading and reducing the lifespan of ship's motor blades. Powerful micro-events were happening under water and slowly chipping away at propellers. These were cavitation events, and they are caused by bubbles formed by negative pressures inside the liquid. In the case of propellers, it's their physical displacement of water that generates differential pressure in the wake of the blade, causing hydrodynamic cavitation. When ultrasounds generate cavitation, it's called acoustic cavitation (Pflieger et al., 2019).

1.1.1 Bubble dynamics and cavitation effects

Either in acoustic or hydrodynamic events, when the bubble forms, it's made of vapor of the host liquid. This vapor, unlike the liquid, can be compressed or expanded, and according to these two actions, the radius of the bubble varies with time, and this can be defined as R(t), radius, and t, time. The liquid pressure far away from the bubble is $p_\infty(t)$. This is composed by the hydrostatic pressure p_0 and any external acoustic pressure caused by sound fields used to generate the bubbles. This latter pressure is what dictates the behavior of the bubbles. If there is no external pressure, or $p_\infty(t) = p_0$ the bubble is in equilibrium and has a radius at equilibrium R_0.

In any liquid, stabilized entities at nano scale, non-condensable gases, are diffused throughout. They are called nuclei and are the origin point of cavitation bubbles. How many of these exist depends on factors such as the handling of the liquid, temperature, and amount of dissolved gas (here handling of the liquid refers to whether it was degassed or filtered previously, either of which will decrease number and size of nuclei). As soon as the conditions allow bubbles to form, nucleation, also called activation, takes place. For this to happen, a cavitation threshold needs to be crossed, and this is also influenced by some factors such as impurities present, type of vessel walls, and dissolved gas (Pflieger et al., 2019).

After a bubble is formed, the acoustic energy will change its R_0. If it decreases, the internal pressure then increases, consequently expanding the bubble and the R_0, which then decreases internal pressure, and the cycle repeats. The volume of the bubble enters an oscillating system, with a resonance radius R_{res}:

$$Rres = \frac{1}{2\pi f}\left(\frac{3\gamma p_0}{\rho}\right)^{\frac{1}{2}} \tag{1.1}$$

Here f is the linear resonance of a bubble, p_0 is the ambient pressure, liquid density is ρ, and polytropic exponent of the ideal gas γ. However, this oscillating system is not linear because the expansion and compression restoring forces are not equal in strength. So, the system becomes anharmonic in its oscillations, which ultimately results in the bubble collapse. As the liquid fills the gap left by the bubble, the air inside is quickly heated up and compressed to very high pressures as the bubbles implodes. One collapse can result in several implosions, each consecutively weaker in temperature and pressure conditions. These conditions, which reach up to five thousand kelvin and five hundred bar, can intensify chemical reactions, and make the gas emit light, in what is known as sonochemistry and sonoluminescence.

It was said previously that the oscillation of the bubble is not harmonic. However, not always do the bubbles collapse, which is the case in stable bubbles or stable cavitation. If the maximum radius of the bubble is less than 2 to 3 times that of the equilibrium radius, no implosion occurs, which makes these much more lasting, and with no energy release. In contrast, intense cavitation occurs when the ratio of maximum over equilibrium ratio is higher than 2 to 3, in so called inertial or transient bubbles. When using high driving frequencies to produce cavitation (500 kHz) it was found that the resulting bubbles are of significantly lower size compared to lower driving frequencies (20 kHz).

Besides bubble type, implosion can also be of different types. Stream jets occur when one of the bubble walls collapses inward, creating a jet of liquid that is propelled in the same direction as the imploding wall. This effect can happen while the bubble is in movement in the liquid, and the jet is usually in the direction of the movement. The reaction is less intense in temperature and pressure than a traditional cavitation event but can have beneficial secondary effects such as increased mixing and transport caused by vortex flows.

When bubbles are collapsing near a solid boundary, the jet tends to strike towards that solid, increasing erosion. This is one of the mechanisms on which ultrasonic cleaning devices rely for cleaning, and which might be beneficial to some of the copper cementation nuanced characteristics, explained further below.

The complete movement and implosion dynamics, in depth physical and mechanical properties, complex mathematical simulations, and much more regarding the fascinating world of tiny air-filled pockets should be consulted in the work done by Pflieger et al., 2019.

1.1.2 Transducers

They all start with one type of material, a piezoelectric. These convert an electrical current into a longitudinal deformation in their physical structure. These deformations are synchronized to the "shape" of the electrical current supplied. If the current is modeled to oscillate with a frequency of 20 kHz, 20 thousand times per second, the piezoelectric will deform at a rate of 20 kHz. This vibration is converted into mechanical energy that propagates through the transducer itself and into the desired subject. A piezoelectric can be a naturally occurring material such as quartz, but due to stability and resilience, they are not used nowadays. Instead, ceramics with low mechanical and dielectric losses are used.

Currently there are two types of ultrasonic producing devices being utilized. Piezoelectric plate based, and Langevin-type reactors. The former is used for very low ultrasonic power procedures, which is not in the scope of this work. At higher powers, Langevin are the most used, and they work particularly well at low frequencies of US. They are made of two piezoelectric ceramic rings joined face to face. A heavy mass (usually iron) is placed in the back of the ceramics, and a light mass (usually aluminium) is placed in front. This difference in mass causes a preferential direction to be taken by the US waves. Additionally, they work as heat sinks in which the heat from the piezoelectric pieces can dissipate in. The masses and ceramic disks are clamped together with a bolt that crosses the structure, as seen in figure 1 (Fragassa & Ippoliti, 2016). This bolt provides the mechanical bias necessary for resonance to occur in the entirety of the structure (Moreno et al., 2005). A modifier called sonotrode can be used to further focus the sonic energy on a smaller point.

Finally, the transducer must be in contact with the subject. This can be done indirectly, through liquids, usually water. The water serves as an intermediary that carries the US power to the reactor, which is inside the liquid, in what are called ultrasonic batch reactors. This method has its pros and cons but that is outside the reach of this work. Direct coupling was the connection method used. Epoxy is used to glue the surface of the transducer to the bottom of the reactor. This method is more efficient in ultrasonic energy transportation. As the epoxy is a permanent glue, one way to increase its flexibility is to glue the transducer to a piece of material with low attenuation that can then be used as a bottom in vessels of different types.

One drawback of the direct coupling is that the heat produced in the transducer is directly conducted to the reactor. If the powers at play are large enough, typical cooling solutions such as fans might not be enough. In these cases, pulsed ultrasonic waves should be used. This has been reported to not reduce acoustic effects, while diminishing the increase of reactor temperature from 7°C to less than 1°C (Dong et al., 2020), while also benefitting from reduced energy consumption.

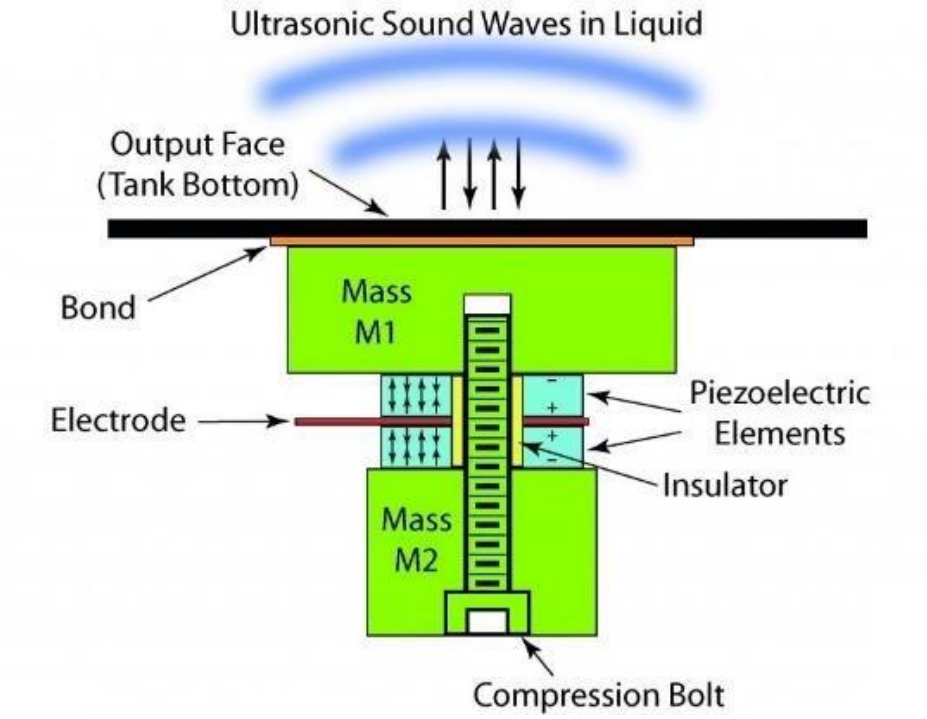

Figure 1 Diagram of a Langevin-type transducer (Fragassa & Ippoliti, 2016)

Within the piezoelectric type reactors just described, there are a few variations used at lab scale. Most common are the ultrasonic horn, and the ultrasonic bath. The horn is a direct contact equipment that works in batches. It's a long and thin tool that is submerged in the solution to a specific depth. Due to its direct contact with cavitation, and due to solutions often being hot and acid, its material needs to be resistant to extreme conditions, and titanium is usually the choice material. Nonetheless, probe erosion is inevitable, leading to extra costs and lower efficiency, and contamination of the solution (Castro & Capote, 2007). These drawbacks made horns unsuitable for this investigation on copper cementation.

Ultrasonic bath is an indirect batch type method, where several transducers are placed beneath a stainless-steel container. It's usually filled with water, and the reactor is placed inside the water. Because ultrasonic baths are widely used for ultrasonic cleaning, they are easily accessible and omnipresent in ultrasonic research. They are cheap and come mostly ready to use. However, significant power can be lost to the medium, reducing usable power to less than 5 W/cm^2. In cheaper products, power control is very limited,

if existent, and can have significant operating frequency variations, hurting reproducibility. When building an US bath, an efficient way to test if enough US fields are being generated is to place an aluminium foil on top of the water while using US for about 30 seconds. In a working setup, the cavitations will repeatedly pierce the surface of the foil (Castro & Capote, 2007). Due to the lower power

Flow reactors are usually made of a piezoelectric plate glued to a plate microreactor. So far, they are reserved for low volume and power experiments, mostly at lab scale. They provide good control of the flow dynamics and have higher heat and mass transfer rates. However, two important downsides widely reported in the literature make them unsuitable for a reaction such as copper cementation, the weak convective mixing and the difficulty handling solid residue (Dong et al., 2020).

1.1.3 Use cases for ultrasounds

Wastewater treatment

In the wake and growth of human civilization, innumerous processes were and are being created to develop all areas of human life, such as health, comfort, and technology. These are often processes unique to human activities and otherwise non-existent in nature. This means that any of nature's creations, such as all living species, have not had time to adapt to these ever-changing processes . This leads to many negative scenarios such as global warming, air pollution, pronounced increase in cancer incidences, in chronic illnesses, all despite an apparent increase in quality of life. Copper poisoning by drinking water is one of those examples. It has been a health concern for some time, as copper tubing is often used for drinking water distribution. Both short- and long-term effects are nefarious to humans, although not very frequent, and warrant technologies to decrease copper contamination of drinking water (Taylor et al., 2020). This explains why one of the biggest sectors of copper removal is in wastewaters and tailings purification.

Recycling streams treatment

Copper is a dangerous contaminant to recycled metal. It decreases the quality and mechanical properties of steel. Additionally, it's difficult to remove from the host metal, economically, once it has dissolved (Hayes, 2021). One solution proposed in the literature is to improve the sorting processes being utilized in recycling facilities. But this might be too little, as in many products the copper is deeply imbedded and inaccessible to workers and machine. Using leaching to selectively dissolve the copper after the sorting stage, following by cementing it under the right conditions, on the iron present in the original stream or in a separate one could mitigate the problem, especially if ultrasonic energy is being supplied to disperse the cemented copper and alter its morphology into specific and valuable products such as nanoparticles. This could offset the costs of the purification and encourage further recycling.

Reducing hold up time

As mentioned previously ((its mentioned after, so don't forget to change order)), hydrometallurgical processes are frequently done at concentrations of solute lower than 1 mol / l. To make a ton of copper, for example, that would require over 200 bathtubs of solute. If 200 bathtubs are needed at each step of the process, a lot of money is held up in the system. The faster the process is done, from leaching to high purity recovery, the smaller the plant needs to be, as the "bathtubs" are dispatched more quickly. By improving purification times of PLS, ultrasonic energy can help decrease held up costs and plant size.

Cementing impurities from zinc leach solutions – Using ultrasounds

When working with roast-leach-electrowinning process for Zn production (Chen et al., 2022), zinc PLS has too many impurities, which reduce energy efficiency, and contaminate and re-dissolve cemented Zn, which prevent it from being used as electrolyte for the EW process right away. By introducing active metals (Zn powder) in the PLS, the more stable impurities precipitate. A problem of this purification step is that the consumed Zn is in great excess of the stoichiometric necessity, making it expensive and cumbersome due the great amount of material needed. Furthermore, not all the introduced Zn is consumed as it is retained along with the impurities in the solid residue, which sometimes form compact layers that hinder the cementation agents from dissolving, and therefore hurting the efficiency of the cementation.

Hydrogen evolution is a reaction that takes place in water in electrochemical reactions, and forms H_2. It occurs on the surface of the Zn powder, and it locally increases the pH of the surrounding area. This allows the formation of Zn crystals which probably further decrease access to the Zn surface, preventing its dissolution.

Clearing the Zn surface of the cemented metals and crystals could prove very beneficial. Chen et al. studied the effects of applied ultrasounds on the morphology and composition of the unwanted cemented products. Temperature varied from 20-60°C, 800 ml of solution, and ultrasounds produced by a titanium horn at 20-kHz, with output power ranging from 0 to 2 kW. There was no stirring.

During silent assays, copper cementation was greatly increased by increasing the temperature from 20 to 60°C (for 4h, at pH 4.5). The influence of pH was tested (at 60°C) and at pH 3 it showed densely packed Cu deposition on the Zn layer. At pH 2, the deposition was highly porous and not very homogeneous, and at pH 1 most of the Zn surface was exposed, with very inhomogeneous, porous, and sparse disposition of Cu. This was probably caused by hydrogen evolution, in which H_2 bubbles are formed at the surface and decrease contact from the contaminants with the Zn.

During titanium horn sonicated (20 kHz for 4 hours) assays at 60°C, increasing the intensity from 400 to 2000 W resulted in a loosely attached and porous cementation layer. Additionally, by removing H_2 bubbles

from the Zn surface, it increased hydrogen evolution, which as seen previously increases local pH and salt formation. These salts negatively impact Cu cementation by limiting access to Zn.

US assisted extraction

When transferring solute from one immiscible liquid to another, ultrasounds were found to, together with micro channeling (small pathways for the liquid to move through), increase the mass transfer between the two phases. In an experiment to remove acetic anhydride from an organic stream with water, US were applied at a frequency of 42 kHz and a voltage 590 mV (for a total applied power of 20 W). Reaction time was reduced by a factor of 22 to achieve an extraction of 86%, compared to the same procedure but silent (Kiss et al., 2018).

US assisted crystallization

Due to its impacts on crystal growth rates and agglomeration effects, this application has been extensively studied, for the food industry specifically. When freezing foods with intact cellular walls, the induced ice crystal growth can rupture them. By using US, the crystal size is decreased, and the cellular structure is better preserved, which preserves more food properties. Crystal morphology, which is also impacted by US, impacts food sensations in a process known as the organoleptic sensation, important in icy products. The lack of a well understood and researched large-scale approach is probably inhibiting further adoption of the technology. The emphasis on the possible decrease of energetic consumption by sonicating reactions might also be negatively impacting adoption, as a more reasonable focus should be on the rate enhancing effects rather than the energy saving ones (Kiss et al., 2018).

Industrial applications

Just like the transducers used in this work, most of the commercially available ones have the main purpose of deep cleaning at frequencies between 20, 40 or 60 kHz. The low frequencies favor more intense cavitation effects. However, not every process requires these effects, so the ideal parameters vary according to application, as seen on figure 2 (Kiss et al., 2018). Importantly, the interaction between reactor, mixing conditions and specific gravity all change the interaction between the effects of cavitation and the system. Generally, the size of the bubbles, speed of their collapse and of the jet streams generated, at their peak intensity between 20 and 100 kHz. 40 kHz has been reported as the best frequency for nucleation and sono-fragmentation, but all the setup parameters mentioned before will affect this value.

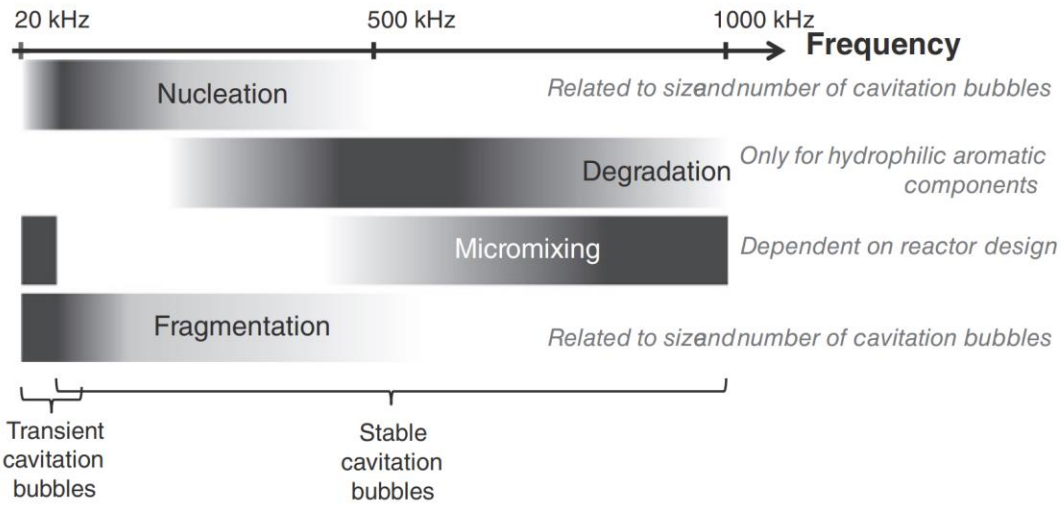

Figure 2 Ideal US frequencies for different applications. Dark colors indicate higher intensity process. (Kiss et al., 2018)

Degradation of some pharmaceutical compounds has been found to be faster with US application. Specifically, paracetamol will best degrade between 165 and 850 kHz. But this only works with hydrophilic aromatic components, like paracetamol, which degrade via radical chain reactions at the bubble-solution interface. Volatile aromatics, however, degrade at lower frequencies, around 20 kHz. Additionally, further research in pulsed ultrasounds has been recommended in the literature. This method has shown, in some cases, to produce similar effects to continuous US, but with 90% energy reduction.

Regarding the scale up of the ultrasonic technology, it should be stated that it has already been done. With a good enough understanding of the sonochemical processes, it can be done. Either a batch either a flow type system can be used, or even a mixture of both. As Castro & Capote, 2007 put it wonderfully, "the first question to be answered in scaling up (…) is whether the reaction is sonochemical or just the result of an ultrasonically induced mechanical effect". Depending on the answer, US can be used in a preliminary processing plant or for the complete duration of the process. The equipment used resemble ultrasonic baths and probes, but larger and more powerful. One example is the UIP16000, standing at 0.6 m x 1.2 m, and supplying 16 kW of continual power (Castro & Capote, 2007). As per the manufacturer, Hielscher, when combined in a 4x16 kW system, is can process anywhere from 0.2 to 50 m^3/hour, depending on the purpose.

1.1.4 Ultrasonic characterization

Several methods are found in the literature to characterize acoustic power delivered from a sound source, into a liquid. However, given the wide range of applications and the maturity of U.S. technologies, the lack of standardized characterization becomes apparent. To properly compare between experiments and results

from the literature, an amount of U.S. power needs to be measured. To this end there are several characterization methods, some of which are summarized here. Measuring the vibration amplitude with a vibration meter is one of them, however, under a cavitation regime, it loses reliability. This happens because cavitation bubbles sharply change the compressibility of the medium, which becomes comparable to that of a gas, but not its density. This reduces the speed of sound by up to two orders of magnitude and creates large measurement errors when using a vibration meter. Another method is calculating the acoustic intensity with the formula:

$$I = k \times f \times U^2 \times (p_L c_L) \tag{1.2}$$

With k being a conversion coefficient, which depends on the transducer, U the voltage of the transducer, f the frequency of the U.S. waves, and (pL cL) being the acoustic impedance of the medium. This approach, however, is highly dependable on the setup and is of high complexity. Piezoelectric sensors can also be used to measure the sound absorption and heating of a calibrated "sticky drop", although there is not much literature on this method. Optical measurements are also possible on specifically shaped vessels, as long as cavitation is not fully established, restrictions which make it a very cumbersome option. Measuring radiation pressure has also been utilized, but the reflecting sound waves and jet streams from cavitation interfere with the measurements. To eliminate this issue a specific setup is required, where no cavitation occurs, the liquid is degassed, focused radiators are needed, as well as acoustic screens. All these methods require the challenging determination of pLcL, and therefore all suffer from cavitation interference with compressibility (Margulis & Margulis, 2005). For these reasons, these methods are not very common. The most common characterization techniques are now explained in greater detail.

1.1.4.1 Calorimetry

This is considered a simple method of characterizing the efficiency of the sonochemical reactor. It measures the conversion of acoustic energy into heat, and it does not require specific information about the medium or equipment being used (Rochebrochard d'Auzay et al., 2010). Estimates say that 1-20% of acoustic energy is transformed to cavitation energy, with a higher fraction of that occurring at higher frequencies (300 to 1000 kHz).

The setup usually consists of a thermocouple, a temperature measuring system, a thermally insulated vessel, and the heating medium, usually deionized water. In this method, the heating of the liquid is measured in a sufficiently long-time interval (at least 5 and up to 30 minutes, to achieve a ΔT of 5-20°C according to Margulis' work). The absorbed power (W_{US}) is calculated with the relation:

$$W_{US} = c_V \, m \, \frac{\Delta T_{US}}{t_{US}} \tag{1.3}$$

In which c_V is the specific heat ($J\,K^{-1}kg^{-1}$) of water, m is its mass (kg) and ΔT_{US} is the temperature difference (K) after the time (s) t_{US} elapsed. This method presents some disadvantages, namely the heat transfer to the setup components such as the vessel or transducer, and even to the surrounding atmosphere. Additionally, the system as a whole has a c_V which can be much higher than water's c_V. In most experiments, a homogeneous distribution of heat in the liquid is assumed. However, Margulis reports that in some experiments, the cavitation and overall U.S. influence is not enough to homogenize the liquid, reason for which a stirrer is recommended. Additionally, if t_{US} is over 90 seconds, heat generated in the transducer can be transferred to the liquid. These conditions mean that the measured acoustic power will lie somewhere between the electric power consumed by the transducer and the actual absorbed energy.

These drawbacks can be eliminated by the comparative calorimetric method. In this variation, U.S. heating of a liquid is done just like previously. Then, after cooling, a heater is turned on and used in a manner to replicate the heating curve of the U.S. The power lost by the heater is then assumed to be the acoustic power absorbed in the volume of liquid (Margulis & Margulis, 2005).

1.1.4.2 Chemical dosimetry

This chemical method needs to be adapted to different setups, and it uses different reaction systems that quantify radical production (which are a by-product of ultrasonic energy). Some of the systems are the Fricke reaction, the Weissler reaction, HNO_2 and HNO_3 formation, TPPS, and terephthalate dosimetry. Of these, Weissler's appears to be the most common, for its simplicity (Rochebrochard d'Auzay et al., 2010).

As mentioned previously, US can lead to increased radical formations, caused by the phenomena of cavitation. This phase is responsible for generating extreme temperatures and pressures, up to 5200 K and 500 atm. These conditions break apart molecules in a process called sonolysis. In water, this leads to one of the main chemical reactions observed ('))' meaning that the reaction was sonicated, and 'Δ' meaning that heat was supplied):

$$H_2O \xrightarrow[)))]{\Delta} HO^{\cdot} + H^{\cdot} \tag{1.4}$$

And it's been reported to be responsible for 80% of $HO^{\cdot}$ and $H^{\cdot}$ radicals. By measuring the quantity of these, one can know how much ultrasonic energy was given to a system and then compare between experiments. However, in the literature, it's this comparison step that is not always easy, due to the several characterization methods. Nevertheless, water is the medium of preference. And for its sonolysis, frequencies in the range of 200 to 500 kHz are the most effective.

1.1.4.3 Setup and comparison of calorimetry and iodide dosimetry

Rochebrochard et al. also provide detailed information on a possible setup for different characterizations. Simply put, a wave generator, an amplifier, and the transducer (in these, ideally, the output impedance should be measured, along with reflected electric powers in the circuit). A reaction cell, fans to cool down the transducers, and a cooling system for the cells were also used. For the transducer preparation, both a Pyrex and a stainless-steel disk were used as protective surfaces for two different transducers. They were glued with a low vapor pressure epoxide resin.

For calorimetry, water purified by reverse osmosis was used. No mixing was used, and sonification done in 10 min intervals. Experiments were repeated four to five times.

For dosimetry, the potassium iodide reaction was chosen. The radicals generated from water sonolysis oxidize the iodide ions, producing iodine, which leads to the formation of I_3^- species according to equation (1.5). It follows the Weissler reaction.

$$2HO^{\cdot} + 3I^- \rightarrow 2HO^- + I_3^- \tag{1.5}$$

Which happens according to the reactions:

$$2\,HO^{\cdot} \rightarrow H_2O_2 \tag{1.6}$$

$$2H^{\cdot} \rightarrow H_2 \tag{1.7}$$

$$H_2O_2 + 2\,I^- \rightarrow I_2 + 2\,HO^- \tag{1.8}$$

$$I_2 + I^- \rightarrow I_3^- \tag{1.9}$$

Analyzing the data showed that iodide dosimetry was reliable when compared with UV spectrophotometry for nitrite and nitrate ion formation. Calorimetry however, had limited usefulness, as part of the acoustic energy was used for the reactions measured by the dosimeters (Rochebrochard d'Auzay et al., 2010). In this work, these reactions are considered to be negligeable due to ferric ion measurements revealing little radical formation.

1.1.4.4 Weissler, Fricke and terephthalic dosimetry methods

Being the most common methods for radical determination found in the literature, they should be further explained and differentiated (Rajamma et al., 2021).

Weissler dosimetry

As seen just before, triiodide complexes (I_3^-) are formed in the reaction, after which they are measured. Hence, a potassium iodide (KI) reagent is needed. In (Rajamma et al., 2021), 1 ml of both reagents A (0.4 M KI, 0.05 M NaOH, 1.6×10^{-4} M $(NH_4)_6Mo_7O_{24}{\cdot}4H_2O$) and B (0.1 M $KHC_8H_4O_4$) were mixed with 1 ml of sonicated water. Then the sample is measured for triiodide absorption at 350 nm in a spectrophotometer. As can be seen in equations (1.3) and (1.6), the amount of $HO^{\cdot}$ can be determined by doubling the yield of I_3^- or H_2O_2. As predicted, Rajamma's work found that increased sonication time or power resulted in linear increase of $HO^{\cdot}$ yield (at 490 kHz and 40 W).

Fricke dosimetry

Here it's the ferric ions (Fe_3^+) which are measured. For that, once again using Rajamma's work as reference, 0.392 g of FeSO4(NH4)2SO4·6H2O (1.0 × 10− 3 M), 41.1 g of 96% H2SO4 (0.4 M) and NaCl (0.0585 g, 1.0 × 10− 3 M) were dissolved in 15 ml of distilled water. The sample was sonicated, and the absorbance of the ferric ions taken at 304 nm in a spectrophotometer. The $HO^{\cdot}$ and H_2O_2 formed from eq. (1.4) and (1.6) oxidize ferrous ions into ferric ones according to the reactions:

$$HO^{\cdot} + Fe^{2+} + H^+ \rightarrow Fe^{3+} + \mathrm{H2O} \tag{1.10}$$

$$\mathrm{H2O2} + Fe^{2+} + H^+ \rightarrow Fe^{3+} + \mathrm{H2O} + HO^{\cdot} \tag{1.11}$$

H2SO4 is added to prevent the oxidation of Fe^{2+} by air, as dissolved oxygen can be a catalyst of that reaction. It prevents it by increasing the pH and "pushing" the reaction equilibrium to the left, preventing oxidation. Just like with the Weisser's dosimetry and using the same conditions, an increase in sonication time or power resulted in increased $HO^{\cdot}$ yield.

Terephthalic acid dosimetry

Again, using the same Rajamma's work as reference, 0.33 g of terephthalic acid (TA) at 2×10^{-3} M and sodium hydroxide (0.20 g, 5 × 10− 3 M) were added to a phosphate buffer. The emission spectra of the sonicated samples were recorded at 310 nm (excitation wavelength) and 425 nm (emission wavelength) with a fluorescence spectrophotometer.

This process depends on the hydroxylation of the TA by $HO^{\cdot}$. The product of this reaction, 2-hydroxyterephthalate ion (HTA), is highly fluorescent and can therefore be observed with the suitable equipment (Rajamma et al., 2021).

1.1.5 Discussion on the effectiveness of each method

In the results of Rajamma, it was noted that in both TA and Weissler methods there is a deterioration of the linear growth of $HO^{\cdot}$ yield with sonication time. In Weissler's this is because H_2O_2 is somewhat unstable, and after ~20 minutes it can decompose to possibly form H_2O and O_2. In TA, some decomposition products accumulate in the cavitation bubbles and reduce their temperature. Therefore, these methods should be used with caution for long duration sonication (over 20 minutes) high power (above 40 W).

Additionally, Weissler and Fricke dosimetry resulted in similar values for $HO^{\cdot}$ yield, 1.2 - 1.4 for the former and 0.96 - 1.2 μM min^{-1} W^{-1} for the latter. TPA showed values at best 17 times lower, and at worst 30 times lower than the previous methods. Nonetheless, individually, these methods can be used to quantify the effects of independent variables on sonication results.

On a side note, it has been famously reported that 80% of radical formation is momentaneous and leads to recombination inside cavitation bubbles to form water very shortly after formation, with only 20% remaining in its radical form (Henglein, 1987). The phenomenon is common to all dosimetry methods, which despite influencing absolute measurements, makes it neglectable for purposes of comparison between said methods.

1.1.6 Conclusion on characterization methods

The most relevant methods were presented previously, but a more digestible table was built with those mentioned and a few others relevant in the literature (Dong et al., 2020).

Method	Type of Method	Objectives	Materials
Sonochemiluminescence of luminol	Experimental, Chemical, Qualitative	Observation of cavitation activity distribution	Aqueous solution of luminol and sodium hydroxide.
Dosimetries: salicylic acid, Fricke, Weissler, terephthalic acid	Experimental, Chemical, Qualitative	General cavitation activity measurement, cavitation yield	Analysis method: spectrophotometry, HPLC analysis.
Hydrophone measurement	Experimental, Physical, Quantitative	Acoustic pressure mapping. Observation of standing waves.	Hydrophone probe, oscilloscope.
Temperature mapping	Experimental, Physical, Qualitative	Temperature mapping to observe hot spots.	Thermal camera.
Calorimetric measurement	Experimental, Physical, Quantitative	Temperature rise measurements. Estimation of power density.	Temperature probe.
Impedance measurement	Experimental, Physical, Quantitative	Resonance conditions: resonance and anti-resonance frequency.	Impedance analyzer
Pressure acoustic mapping	Numerical, Quantitative	Helmholtz equation	Numerical simulation software
Simulation of primary and secondary effect	Numerical, Quantitative	Temperature, bubble yield	Numerical simulation software

Figure 3 Major characterization methods and respective description (Dong et al., 2020)

Now with a better understanding of the multiple characterization methods, calorimetric measurements appear to be the most adequate for this work, and likely for most of other similar works. The physical nature of this measurement makes it less susceptible to variations in the type of reaction and reactants used. It uses the simplest materials and procedure, which incentivizes reproducibility and characterization. It was often found in the literature, especially in publications not focused on the US themselves, that transducers were 'characterized' only by their nominal power, which is makes comparison of results extremely hard. The shortcomings of this technique are easily overcome by cooling the transducer with a fan or using pulsed mode; preventing heat from escaping the reactor by covering it with insulating material; and repeating the measurements repeatedly to ensure reproducibility, and in case the results change with time, for example obtaining less calorimetric power after each run, parasitic heat conduction/losses are happening and the duration of the tests should be reduced to minimize their effects. That being said, redundancy is welcome, and performing more than one characterization is ideal.

1.2 Leaching

In the field of extractive metallurgy, metal is obtained through pyro or metallurgical processes, or a combination of both. Pyro comes from the Greek word of "fire", which is a clue to the nature of the process.

High temperatures are used change the chemistry and structure of metals, to improve mass transport and chemical reactions, and to enable separations via liquid and gas phases. A combination of these factors allows to produce and recycle metals. Most of these processes occur between 300 and 2000°C.

One of the biggest differences between hydro and pyro is the difference between process streams. The latter is used in dense streams, like copper smelting at 20.000 mol/m^3, or zinc at 32.000 mol/m^3 (in smelting and roasting operations, respectively). Hydrometallurgy, however, processes those metals at 20 and 770 mol/m^3 (in heap and pressure leaching, respectively). The high cost of running pyro processes due to complex infrastructure, high energetic and raw material consumption, forces their streams to be highly concentrated, and therefore valuable. Other ways to minimize energy expenditure are by using the chemical energy released from exothermic reactions, by using heat recovery systems, and overall efficient reactors with great thermal insulation.

With hydrometallurgy there is more flexibility and accuracy regarding selectivity of metals processing, which allows lower grade ores to be used in its processes. To understand what makes this happen, let's consider a reaction:

$$aA + bB \rightarrow cC + dD \tag{1.12}$$

Its "will power" to create products (C and D) must be measured. And it's given by the variation of the Gibbs Free Energy (ΔG). This characteristic is measured in joules (J) and given by the formula:

$$\Delta G = \Delta G^0 + RTln\frac{a_C^c \times a_D^d}{a_A^a \times a_B^b} \tag{1.13}$$

Where ΔG^0 is the standard Gibbs Free Energy, R is the gas constant (8.314 J/mol), T is the absolute temperature (K), "μ" are the chemical activities of the components A, B, C, and D, and a, b, c, and d being their stoichiometric coefficients. The ratio of these chemical activities is often simplified to K_{eq}, or equilibrium constant of the chemical reaction at hand. At equilibrium, $\Delta G = 0$, which simplifies the previous formula to:

$$\Delta G^0 = -RTln\, K_{eq} \tag{1.14}$$

With Keq being:

$$K_{eq} = \frac{\mu_C^c \times \mu_D^d}{\mu_A^a \times \mu_B^b} \tag{1.15}$$

And these relationships show that there is a link between temperature, chemical concentration, and pressure. This link is incredibly exploited across most hydro processes, as well as in the present work.

An additional characteristic is that part of the reactants and of the products are in ionic form. In such conditions, spontaneous electrochemical reactions take place, where electrons (hence 'electro') are usually transferred from a reductor (sacrificial metal) to the desired ionic metal, in cementation reactions. In leaching reactions, it's the desired metal that is oxidized by an oxidizing agent. The Gibbs free energy of an electrochemical reactions can be calculated by:

$$\Delta G = -zF\Delta E \left(\frac{J}{mol}\right) \tag{1.15}$$

With z being the number of electrons transferred in the reaction, F being Faraday's constant (96487 coulombs) and ΔE being the voltage drop between the final and initial electrons state. Importantly, a reaction is given forward momentum, that is, incentivizes product production, when ΔG is negative. From the previous equation its seen that the voltage drop must be positive for forward bias or momentum. Additionally, the electrical potential becomes a crucial variable to determine the equilibrium of a reaction.

With the influencing parameters of a hydrometallurgical reaction being defined, one must understand at which point of the process the present work will overlap. Usually, the leaching process follows the steps:

- Choosing the adequate leaching agents, which should be highly selective to the desired material, and non-overly toxic to humas and the environment. It should also be inexpensive and allow simple and cheap further extraction once the material is dissolved in the agent.
- The ore/waste in which the metal is present is comminuted to smaller sized particles, which favor the process with higher superficial area and easier access to the wanted mental. The extent of this process highly depends on the source and materials involved.
- The source stream is leached with the chosen agent. The setup can take different forms. In mining locations in the form of in-situ leaching; in waste/tailing storage facilities, where heaps of such waste are made, and to which acid is dumped at the top and collected at the bottom; autoclave leaching, where high pressures and temperatures are used; tank leaching, which consists of atmospheric pressure and low-medium temperatures and often are stirred. The valuable metal will be dissolved in the solution, which is called pregnant leach solution (PLS) after the leaching process. Along with the valuable, other contaminants will be present at high concentrations in this solution.
    - The PLS must often be purified/refined and sometimes concentrated. Counter current decantation is a very common technique in industrial setups to purify the pregnant stream, whereas the refinement is frequently done through Precipitation – Manipulating PLS parameters until the dissolved species surpasses solubility limit; Cementation –

Electrochemical reaction of ion exchange between a sacrificial metal and a dissolved species, which is reduced by the sacrificial metal; or Solvent extraction.

- To obtain a high purity and valuable metal in solid form, electrowinning is generally used last.

This basic description of leaching is helpful to understand the cementation process, which encompasses the third step of the process described above and will be fully explained in the next chapter. There the precipitant metal is leached as part of the electrochemical reaction that takes place.

1.2.1 Selection of parameters

When planning a leaching experiment, researchers guide themselves with Pourbaix diagrams. They show the regions of stability of the desired molecules with regards to the pH and oxidation-reduction potential (Eh) of the medium. Beforehand, the metallic species (and non-metallic ones, if it's the case) and the medium must be selected. In practice, the pH is adjusted with the addiction of acidic or basic compounds, and the Eh by the addition of oxidants or reducing agents, or by an applied electric potential. Several leaching reactions can be made, but for the purpose of this work, only water solvation of metallic ions is relevant. A general example of such reaction is:

$$MeX_{(s)} \Leftrightarrow {Me^{2+}}_{(aq)} + {X^{2-}}_{(aq)} \tag{1.16}$$

These reactions can be used to solubilize certain minerals, but in this case, it was used to solubilize an artificially made copper containing salt, Copper (II) sulphate pentahydrate. Its chemical formula and leaching reaction are as follows:

$$CuSO_4.5H_2O \tag{1.17}$$

$$CuSO_{4(s)} \Leftrightarrow {Cu^{2+}}_{(aq)} + {SO_4^{2-}}_{(aq)} \tag{1.18}$$

This dissolution serves as a simulation of any other type of real-life leaching that would solubilize copper into cupric ions, and it's used as a supplier of a constant and predictable source of cupric ions, on which the experiments can be carried out. For the purpose this work, the source of the copper is not being studied.

On the next step another leaching experiment takes place. An acid attacks takes place on the sacrificial metal, the iron, and it follows the following reaction:

$$Fe_{(s)} + H_2SO_{4\,(aq)} \Leftrightarrow H_{2\,(g)} + FeSO_{4\,(aq)} \tag{1.19}$$

As well as iron oxidation and copper reduction, in the following electrochemical reaction:

$$CuSO_{4\,(aq)} + Fe_{(s)} \Leftrightarrow FeSO_{4\,(aq)} + Cu_{(s)} \tag{1.20}$$

These reactions occur in the right direction if the products are more stable than the reagents. pH diagrams are used to know what parameters will accomplish stability, as seen in the figures below (Yagi, 2011) and (Perry et al., 2019).

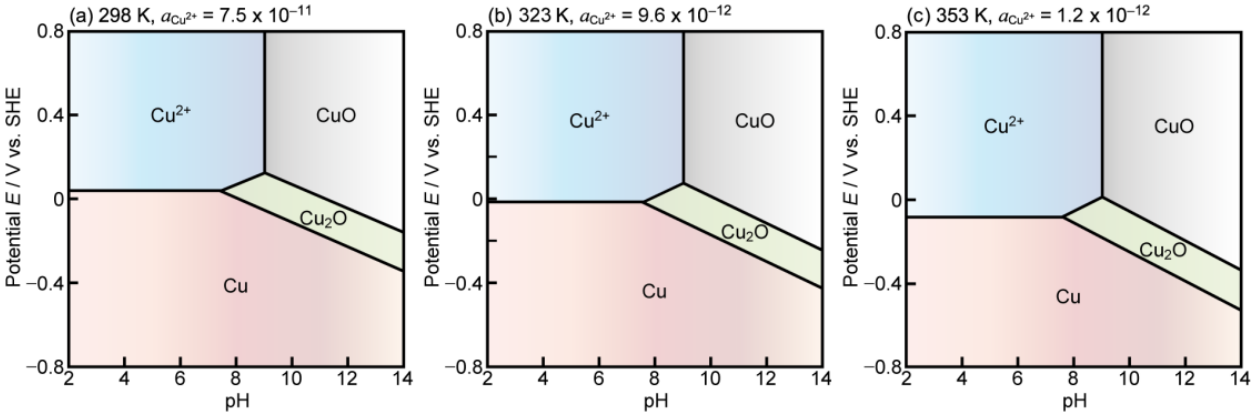

Figure 4 Pourbaix diagram of CuO-H2O system. Increase in temperature (left to right,) results in dissolution at lower potential (Yagi, 2011)

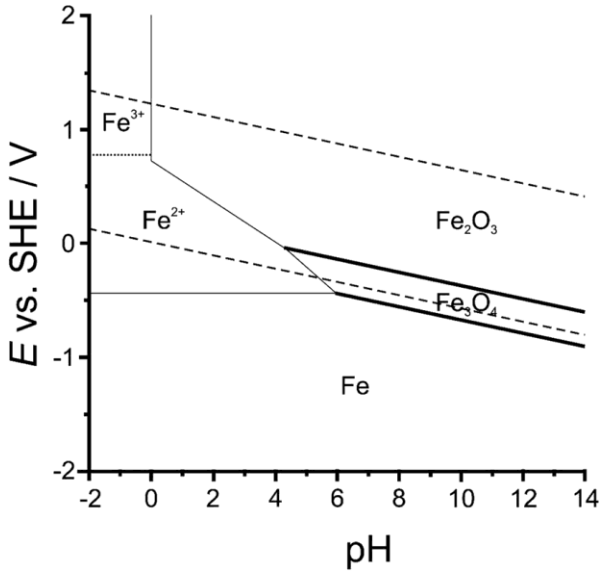

Figure 5 Pourbaix diagram of Fe-H2O system (Perry et al., 2020)

The lines of the Pourbaix diagrams don't indicate a clear-cut change from one state to another. A better way to see it is that they indicate a change in probability of a given state of the metal being found. In other words, the further from the line, the higher the chance that the state indicated in that region is found under the given parameters. So, for example, it's not uncommon to find, with parameters that indicate an iron

oxide region, some traces of ferrous ions, with their concentration increasing the closer the conditions are to the Pourbaix line.

Totally horizontal lines in a Pourbaix diagram indicate that a reaction is solely dependent on redox potential, and not on pH. This is in contrast with vertical lines, which only depend on the pH. Commonly depicted with dotted lines is the region of water stability, above or below which it becomes $2H_2O$ and H_2, respectively. A passivation layer is a protective coating of oxide that protects a metal from further decomposition via corrosion. In iron, its Fe_2O_3. But it generally happens in every reactive metal.

1.3 Copper cementation

Cementation techniques of leached copper have been said to exist since the 10th century, with their origins in China. By the 13th, they reached Europe, where copper sulfide was roasted, leached in water, and the copper precipitated by addition of iron. Other techniques cemented copper from mine water, or exposed copper-rich pyrite ores to rain and air. The small amounts of sulfuric acid generated by the rainwater and pyrites was enough to dissolve some of the copper and create a copper sulfate solution. It was collected and the copper was precipitated with scrap iron (Habashi, 2006).

Presently, the chemical reactions are the same, only with better understandings of the chemistry and better parameter control. To successfully realize cementation, a sacrificial metal with lower electrode potential E^0) will be dissolved into solution, while the ionic metal with higher electrode potential will cement. In this case, the transition $Cu^{2+} + 2e = Cu^0$ has an $E^0 = + 0.34V$, while $Fe^{2+} + 2e = Fe^0$ has an $E^0 = - 0.44V$. Furthermore, the rate and extent of the reaction is, in part, determined by pH, temperature, solution agitation, copper concentration, and the reducing agent.

In an acidic media, such as when using H_2SO_4, copper cementation occurs according to the following reactions:

$$CuSO4 + Fe \rightarrow FeSO4 + Cu \quad (1.21)$$

However, simultaneously, the following unproductive (regarding copper cementation) reactions also occur:

$$H2SO4 + Fe \rightarrow H2 + FeSO4 \quad (1.22)$$

$$Fe2(SO4)3 + Fe \rightarrow 3FeSO4 \quad (1.23)$$

$$Fe2(SO4)3 + Cu \rightarrow CuSO4 + 2FeSO4 \quad (1.24)$$

$$\mathrm{Cu + 1/2O2 + H2SO4 \rightarrow CuSO4 + H2O} \quad (1.25)$$

$$\mathrm{2FeSO4 + 1/2O2 + H2SO4 \rightarrow Fe2(SO4)3 + H2O} \quad (1.26)$$

To keep in mind that in kinetic equilibrium, copper transforms into cupric (cu2+) and cuprous (cu+) ions and vice versa. The presence of these ions, and the instability of the cuprous ones, leads to a disproportionation reaction:

$$2Cu^{+}\ (aq)\ \rightarrow Cu\ (s) + \ Cu^{2+}(aq) \tag{1.27}$$

Were the conditions to be neutral, hydrolyzation of the copper would take place, creating dark red crystals of copper oxide (Shishkin et al., 2018). As reported by Shishkin et al., the copper cementation should only stop once the concentration of copper ions decreases below a threshold that causes the electrode potential of copper to be the same as that of iron. When they equalize, the system is at equilibrium, which should happen when cupric ion concentration in solution (at 25°C) has a ratio of:

$$\frac{Cu^{2+}}{Fe^{2+}} = 1.3 \times 10^{-27} \tag{1.28}$$

Such a high value means that in theory, the reaction reaches equilibrium when virtually of the copper is cemented. However, kinetic limitations prevent the theoretical limit from being reached. Shishkin identifies three stages required for copper cementation where kinetic limitations occur: Ion delivery to cathode surface and ion removal from anode surface through a diffusion layer, the discharge of copper ions to the cathode sections, and the ionization of iron ions on the anodic sites.

Furthermore, the same author describes the process of cementation throughout the reaction. In a 10 minutes cementation experiment, with and without cavitation enhancing, the first 5 minutes correspond to a high rate of copper cementation on the iron anode (in powder form), as the cupric ions have full access to the iron's surface. After 7 minutes, the variables of the system equalized, and steady state was achieved. As more ions deposited, fewer Fe-Cu2+ exchanges took place and cementation decreased, both due to scarcity of cupric ions and access restrictions to the iron's surface. Overall, using a cavitation regime during the reaction increased final copper extraction by 30%. This is theorized to be due to the cavitation reducing the iron powder size from 150μm to 10-30μm, which increases the surface area of the iron. Furthermore, it removes already cemented copper from the iron's surface, creating room for cupric ions to diffuse to (Shishkin et al., 2018).

1.3.1 Kinetics of leaching – Chemical vs Diffusion control

When preparing a chemical reaction, its outcome can be partially simulated with thermodynamic data. Namely, the direction of the reaction, either for the product or for the reactant. However, the speed or intensity of this reaction cannot be predicted in the same way. That is entirely up to the kinetics of the reaction.

It is when predicting the kinetics that one comes across its limiting factors. As described by (Shamsuddin, 2016), there are four defining steps.

1- The transfer of the gaseous reactant from the atmosphere into the liquid solution.
2- Transport of the previously gaseous reactant through the liquid and into the solid-liquid interface.
3- The chemical or electrochemical reaction at the interface of the reactants
4- Transport of product from the previous interface to the solution's bulk

The slowest of these processes is the limiting one, on which the rate of the reaction depends. And it generally is step 2 or 4. Sometimes more than one can be the limiting one. Nonetheless, it is important to speak about what influences them.

In step one the dissolution of oxygen into the solution is the most common configuration. This dissolution depends on the ratio of the concentration of oxygen in the atmosphere over the partial pressure of oxygen in equilibrium in the liquid solution. With increased temperature, the dissolution or solubility of oxygen reduces, and therefore its concentration in the medium. Higher concentration of solute can have the same effect.

Step two is influenced by the ability of the reactant to diffuse through the medium and into the interfaces. Fick's first law of diffusion states that the rate of transport of the reactant is:

$$-\frac{dn}{dt} = -DA\frac{dc}{dx} \tag{1.29}$$

with dn being number of moles of reactant transferring in time dt trough an area of the metal reactant of cross section A. D is the diffusion coefficient and dx is the diffusion distance. If c is the concentration, dc/dx represents the concentration gradient from the air-liquid interface to the solid-liquid interface. Another way to represent this law is by establishing that the diffusion gradient is the difference of c and ci (the concentrations at the bulk and at the solid-liquid interface, respectively,) over δ, (the thickness of that interface).

$$\frac{dn}{dt} = DA\frac{c - ci}{\delta} \tag{1.30}$$

When the reaction achieves completion, no more reactants exist at the solid interface, as all the metal leached. At this point, ci = 0.

Now it is easy to interpret this equation. The rate of diffusion is directly proportional to the concentration of reactant in the bulk and inversely proportional to delta, the thickness of the solid-liquid interface. By

decreasing the boundary layer and increasing the cross-sectional area of the metal, rate of diffusion will increase. This can be achieved with increased stirring, and finer comminution, respectively.

Similarly, step 4, responsible from taking the product way from the solid-liquid interface, is a diffusion process. The difference from the previous is that at the initial moments, c, bulk concentration of product, is zero. By keeping c as low as possible, this rate of diffusion is increased. It's therefore best to keep renewing the stock solution. Now, this is true for soluble products, like Fe(II) species. If the product is solid, such as cemented solid copper, other measures need to be taken to ensure that this is not a step that limits leaching rate.

In this work the step 3, the reaction itself, is only a chemical reaction. Electrochemical ones behave according to a different process which is not in the scope of this work. If this step is the slowest, the process is named as chemically controlled. Any of the others, 1, 2, or 4, and the process is diffusion controlled.

In a **diffusion controlled** one, it is the mechanics of movement of the species going into and out of the surface of the metal that restricts the evolution of the reaction. Diffusion controlled processes depend strongly on the agitation of the vessel, and only slightly on the temperature, when compared to chemical controlled reactions. The Stokes – Einstein equation according to diffusion coefficient helps to visualize this by

$$D = \frac{RT}{N}\frac{1}{2\pi r\eta} \tag{1.31}$$

Here, R is the gas constant, T the temperature, N the Avogadro's number, the radius of the particles to which the leach concerns, and η being the viscosity. As it's seen, there is a direct proportionality of the change in temperature and the change in diffusion coefficient of the solution. The chemical rate constant (k), however, increases exponentially with temperature increase, as it's seen in the Arrhenius equation:

$$k = Ae^{-Ea/RT} \tag{1.32}$$

Chemically controlled processes, therefore, depend exponentially on temperature. In the Arrhenius eq., A is a constant for each chemical reaction, called the frequency factor. Ea is the activation energy, R is the gas constant, and T the temperature in Kelvin. Shamsuddin also described diffusion-controlled processes as having the least activation energy at between 1 and 3 kcal mol^{-1}, chemically controlled ones have the highest (in solid-liquid systems) at over 30 kcal mol^{-1}, and intermediate controlled ones at between 5 and 8 kcal mol^{-1}.

1.3.2 Calculating activation energy

Taking the Arrhenius equation and applying the logarithm of natural base to each side the following expression is obtained:

$$\ln(k) = \ln(A) - \frac{Ea}{RT} \tag{1.33}$$

Highlighting 1/T allows to plot the following equation with Y being ln(K) and X being 1/T. The slope of the graph will be Ea/R and the interception point with the vertical axis (b) will be ln(A).

$$\ln(k) = \ln(A) - \left(\frac{Ea}{R}\right)\frac{1}{T} \tag{1.34}$$

The steeper the slope, which should be negative, the highest the Ea. The lesser the angle of a slope, the lower is the activation energy. Steeper slope also indicates higher change caused by temperature, whereas a straight line with no slope means the reaction is independent from temperature.

1.3.3 Reaction order

The order of a reaction states the importance of a reactant on the evolution of the reaction. It must be calculated experimentally, usually by varying the concentrations of each reactant and measuring the impact on the reaction's rate (r). This is done with the rate law:

$$Rate = k[X]^n \tag{1.35}$$

Where n can be 0, 1, or 2 (zero, first, and second order reaction). If it's a zero-order reaction, the [X] term, reactant concentration, will be zero, and therefore rate only depends on k (M/s). In a first order, there is a linear evolution of the reaction rate according to one of the reactants concentrations, and k is measured in s^{-1}. In a second order one, k is measured in Ms^{-1} and the rate increases exponentially with certain reactants concentration.

In this work, the concentration of the reactants is not one of studied parameters, so reaction order cannot be confirmed experimentally. However, the literature reports copper cementation, and specifically the one using iron as sacrificial metal, as a first order reaction and as a diffusion-controlled process (Awaad et al., 2022).

1.3.4 Reaction parameters

A cementation experiment using iron powder as sacrificial metal (99,4% Fe) to extract copper from etching solutions of electronic processes was consulted (Fouad & Abdel Basir, 2005). The authors produced copper

sulphate crystals ($CuSO_4.5H_2O$) from the etching solution, and used concentrated sulfuric acid used to lower the pH. It was found that an increase in temperature up to 80°C leads to lowers yields and purity, compared to experiments at room temperature. The authors propose that the higher temperatures cause the oxidation of ferrous sulphate ($FeSO_4$) which in turn starts the reaction:

$$3CuSO_4 \cdot 5H2O + 2Fe \rightarrow Fe2(SO_4)3 \cdot 5H2O + 3Cu \quad (1.36)$$

The ferric sulphate salt produced reduces the purity of the copper, by settling along with cemented copper particles. Additionally, it promotes the re-dissolution of cemented copper according to eq. (1.24).

In the same article, pH was varied from 0.5 to 3.5. It was found that the optimal for both copper yield and purity is at a pH between 2 and 3 for [Cu] = 10 g/l, and optimal at pH 2 for [Cu] = 50 g/l. The very acidic conditions (<2 pH) prevent iron hydrolysis.

Another crucial parameter is the amount of sacrificial metal required. This can be calculated using eq. (1.36). The stoichiometric value is 0.879 g Fe/ g Cu, verified by Fouad & Abdel. This calculation is done by looking at the stoichiometric coefficient of the reactants, in this case 1 mole $CuSO_4$: 1 mol Fe. Dividing the molar mass of Fe by that of Cu, 55,845 g/mol and 63.546 g/mol, respectively, yields the stoichiometric ratio of 0.879 g Fe / g Cu.

The authors experimented with adding 1, 2, 3, and 4 times the stoichiometric amount (X) of Fe. Both yield and purity were highest at X=1 (0.879 g Fe/ g Cu) , with a marginal decrease to X=2 (1.758 g Fe/ g Cu) (at [Cu]=10 g/l and pH=1.5 and T=25°C).

Regarding initial copper concentration in the stock solution, the authors used 10, 20, and 50 g/l of Cu, at 25°C, pH 2 and iron stoichiometry 1X. Despite the purity of the copper remaining high throughout the assays, yields decreased from 90% to 70%. Higher copper concentrations resulted in faster reaction rate. The faster cementation resulted in rough copper texture, and the slow cementation resulted in a smooth one.

1.3.5 Copper production

Until 1980 copper production was mostly made via cementation. The Kennecott design (figure 6) from (Habashi, 2006) places scrap iron, cheap and available, on top of a perforated bed. A copper rich solution is streamed at high velocity through the iron. The copper that cements on the metal is quickly removed by the kinetic force of the stream, which carry the copper particles into a copper settling and collection zone, where the stream's velocity is slow, and gravity is able to separate solids and liquids. This design can be profitable, but it has some drawbacks. Namely, due to parasitic reactions, total copper recovery is not achieved, and 2-3 kg of iron must be used per kg of copper, which is far from the stoichiometric

requirements. Hence the need for cheap iron to be used. The deposited copper only has 80 to 90 % purity, which means it requires further refining (Habashi, 2006). Nowadays almost 20% of copper is produced via electrowinning. This process is still used, although in very specific cases, such as on mine tailings and with cheap scrap iron, such as food cans. Some companies report that, recently, up to 300,000 tons of scrap iron was consumed annually in copper cementation near mines (Michaud, 2017)

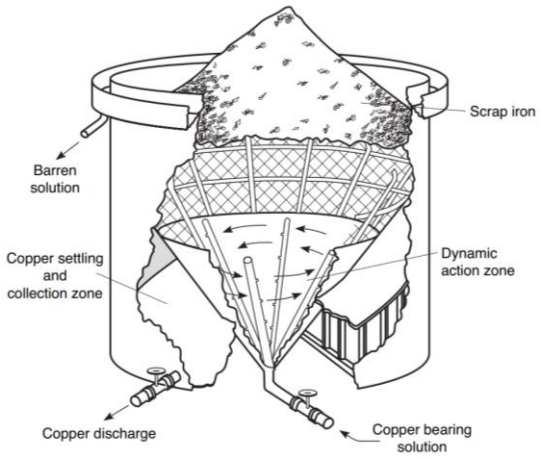

Figure 6 Copper cementation process setup, used for copper production (Habashi, 2006)

1.4 Objectives

This master thesis project aims to characterize a new US setup, and to investigate the possible intensification of the copper cementation reaction caused by US. The eventual intensification can be a consequence of ultrasound induced mechanical effects, of the sonochemistry taking place, or of both processes simultaneously, and this will be addressed.

To obtain best results, a set of silent assays will be preliminarily performed to determine the best value for the following reaction variables: temperature (40-60°C), agitation (200-500 RPM), and pH (2.0-2.5). Maximum copper recovery (%), time required to achieve it, and precipitant metal consumption will be the parameters evaluated to determine the success of each scenario. The best values will then be used in the sonicated assays. The US are expected to improve the reaction characteristics, as it's predicted that the passivation layer (a well-known reaction limiting structure) will be destroyed in the process.

To obtain reproducible and useful results for further work, the characterization of the transducer-reactor setup will be made with calorimetry characterization, by measuring the US induced thermal change in a thermally insulated vessel. Activation energy calculation and discussion will also take place, along with a preliminary evaluation of the optical aspects of the cemented copper, and US induced radical formation will also be studied with iron titration.

Some enhancement of the reaction is expected to happen. To which degree and, essentially, if it's economically and environmentally viable, are challenging questions which will be addressed. Entrepreneurial aspects of this technology will be explored regarding the economic and technological viability, while considering the challenges faced by an eventual market entry.

This work will prepare the ground for future works which should encompass a more in-depth study of the resonance frequency influence on the process parameters, and of the cementation's energetic consumptions.

Chapter 2

2. Methodology

2.1 Safety and good practices regard

A few fundamental rules were followed during the totality of the experiments made. In this section They are briefly mentioned. Water is never placed onto acid, acid always onto water. When handling acids, gloves, protection glasses and lab coat are mandatory. When working around an active ultrasonic source, earplugs and/or sound blocking headphones are used.

When handling the scales, care was taken to reduce the airflow in the room, either by closing the doors either by staying still for a few seconds and breathing away from the measuring device.

When preparing liquid or solid samples, making dilutions, or having filled beakers in the work area, care was taken to identify everything with date, personal ID identifiable by the laboratory's staff, and any hazard warnings if required.

When pipetting (with rubber pipette balloons) solutions into another container, the pipette's tip was gently pushed at a ~45° angle against the container's wall for approx. 15 seconds. This is to ensure complete transfer of the liquids.

2.2 ICP-MS analysis

2.2.1 Sample preparation/procedure

When dealing with small sample volumes of uncertain element concentrations, such as in the 5ml samples taken throughout the experiment, dilutions need to be made. To promote accuracy, two dilutions are usually made, by a factor of 20 and 1000. This is to give the ICP computer two windows of concentration ranges of any element.

In a 20 ml volumetric flask are put a few ml of deionized water (diH2O), followed by 400 µl of nitric acid (HNO_3). To this, 1 ml of sample is added. Lastly, diH2O is added until the solution's meniscus is at the 20 ml mark. This way, the sample was diluted by a factor of 20x.

In a 50 ml volumetric flask, a few ml of diH2O are placed, followed by 1ml of the previously diluted solution, well homogenized. The flask is filled until the 50 ml mark with diH2O. The sample was now

diluted by a factor of 1000x.Due to the successive steps taken, which involve minute volumes being added, each measuring uncertainty plus user error will be propagated and can be significant

2.2.2 Working principle

Inductively coupled plasma mass spectrometry (ICP-MS) is a technique which allows to determine the concentration of elements in liquid, solid, and gaseous samples. It's a versatile tool, used in many fields. Through its ionic source that reaches high temperatures (in the range of 5000°C), the equipment atomizes any substance, breaking every molecular bond of every molecule before they reach the detecting region. Despite its versatility, there are limits to some characteristics of the samples. Namely, salt concentration limits, as they can potentially obstruct the detectors or cause contamination of the machine. This can be prevented by volatilizing these solid components into gaseous ones. One way to do it is through nitric acid (HNO_3) addition, which incentivizes decomposition of the sample. In the case of liquid sampling, a nebulizer is used to create a small pray of liquid. From the sample tube to the detectors. (Ammann, 2007).

2.3 Iron titration

2.3.2 Sample preparation/procedure

In a 100 ml erlenmeyer, 20 ml of acid solution is added with a graduated cylinder, followed by 1 ml of the liquid sample, added with a micropipette. The walls of the erlenmeyer were rinsed with around 20 ml of diH2O, followed by 4 to 5 drops of indicator liquid. Then, the titration burette is filled with the potassium dichromate solution ($K_2Cr_2O_7$). Then, this liquid is titrated drop by drop until the sample solution permanently turns from transparent to a purple color (see fig. 7). This is to be done patiently, as one drop is the difference between a fully transparent and a fully opaque solution. Additionally, the erlenmeyer should be stirred either manually, after each drop of agent falls, or with a magnetic stirrer at 350 rpm, as long as there is no splashing. For each sample, three titrations were made, and the average was used as the volume of dichromate solution.

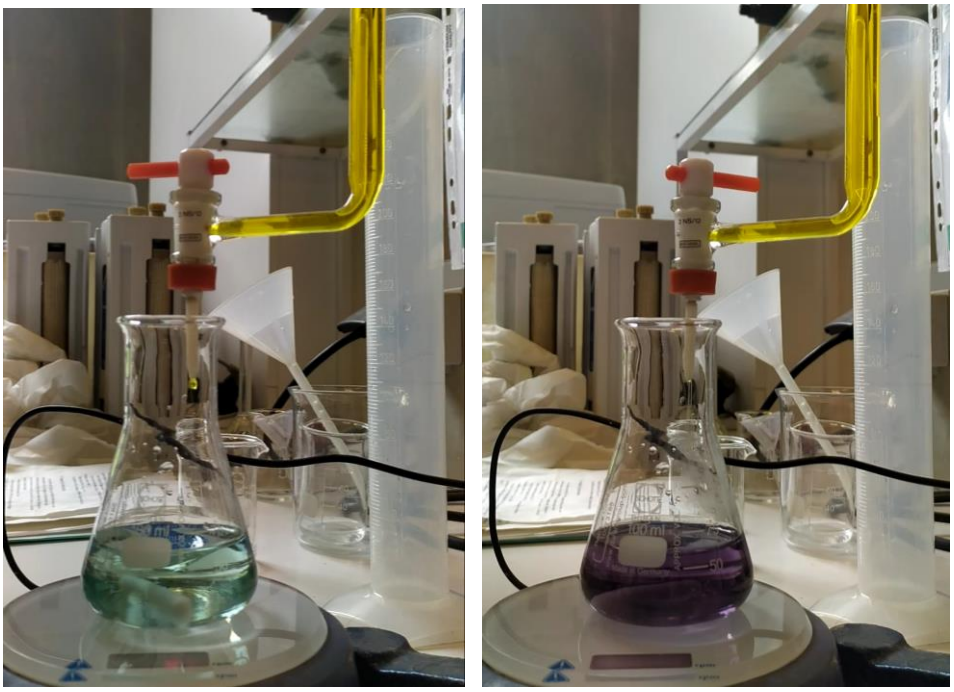

Figure 7 Left, solution is one titrating agent's drop away from equilibrium; Right, after equilibrium was reached

When the sample to be titrated is expected to have a high ferric ion concentration, the procedure can become more complex by requiring the burette to be filled several times for each sample. This costs time and too much dichromate solution to be used. Dilutions by a factor of 10x, 20x, and 100x were made for the different samples analyzed. To dilute by any of the factors, “dilution factor -1” g of diH2O are measured, followed by the addition of 1 ml of sample. To exemplify, in the 20 x dilution, 19.000 ± 0.006 g of diH2O were weighed, in which 1 ml of sample was diluted.

2.3.3 Working principle

This technique is used to quantitively measure the Fe^{2+} (ferrous ions) concentration in a liquid sample. A standard solution is titrated by a titrating agent. The titration is done by measuring the amount of agent required to achieve a balance between the analyte and the titrating agent. This balance is revealed by adding an indicator to the analyte beforehand, which causes a permanent and perceptible change in color when that chemical balance is reached. Additionally, an acidic buffer solution is also added beforehand to maintain a constant pH in the solutions. By performing the titration with a standard solution of known concentration (using eq. (2.1) to determine c), the sensitivity of the titrating agent to ferrous ions is calculated, as well as the agent’s concentration or molarity (eq. (2.2)). By knowing the volume of the titrating agent required for a sample, $V_{Fe^{2+}}$, it's then possible to calculate the concentration of ferrous ions in solution (eq. (2.3)).

$$c_{Mohr} = \frac{m_{Mohr}}{M_{Mohr}} \tag{2.1}$$

$$c_{Cr2O7^{2-}} = \frac{c_{Mohr} \times V_{Mohr}}{6 \times V_{Cr2O7^{2-}}} \tag{2.2}$$

$$c_{Fe^{2+}} = \frac{6 \times (c_{Cr2O7^{2-}} \times V_{Cr2O7^{2-}})}{V_{Fe^{2+}}} \tag{2.3}$$

$$Fe(SO_4)_2(NH_4)_2.H_2O \tag{2.4}$$

$$K_2Cr_2O_7 \tag{2.5}$$

$$C_{24}H_{20}BaN_2O_6S_2 \tag{2.6}$$

The standard solution used is Mohr's salt, eq. (2.4). The titrating agent is potassium chromate, eq (2.5). The indicator used is barium diphenylamine sulfonate eq (2.6). The acid solution buffer is made of sulfuric and phosphoric acid.

After having the Fe^{2+} concentration calculated, the Fe^{3+} concentration is easy to determine by using ICP analysis. It gives a total iron concentration of the sample, to which the Fe^{2+} is subtracted, leaving only the ferric ions concentration.

2.4 Resonance frequency determination

2.4.1 Working principle

The resonance frequency (R.F.) of a material is generally determined as a frequency or region of frequencies where the body in question more efficiently or optimally translates the energy input (in the form of a periodically acting force, such as sound waves) into the amplitude component of its vibration. Some observable examples of this phenomena are when a human produces a soundwave that shatters a wine glass, or when strong winds cause bridges without energy dampeners to oscillate violently and collapse. Resonances are seen anywhere from the atomic scale to the galactic one, and are not limited to acoustic waves, as mechanical, electromagnetic, and acoustic are just some of the examples.

It's therefore straightforward to understand that the study of any phenomena that is influenced by vibrational effects should consider the resonance frequency of the given setup. Knowing the impedance (Z) of the system is one way to know the R.F, as at that moment Z=0. The transmission of U.S. waves is inversely proportional to Z. One way to determine this frequency is by placing a setup in a sound chamber and striking it at several values of wave frequency. Special microphones measure the acoustic resistance (R) and acoustic reactance response (X), which are measured in acoustic ohms.

$$Z = R + iX \tag{2.7}$$

In the equation above, R is the real portion and X is the imaginary portion of acoustic impedance, Z (Ren & Jacobsen, 1993). When measured empirically, the resonance frequency is when Z=0, and therefore when R + X = 0.

2.4.1 Measurement setup

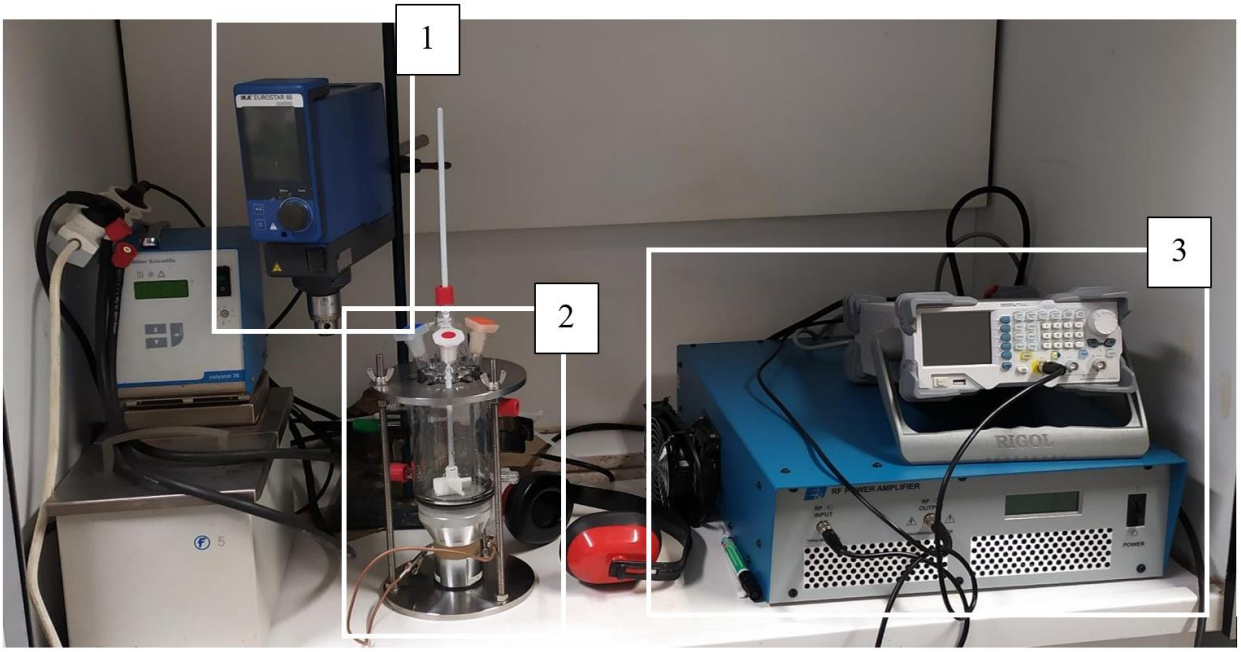

Figure 8 Complete setup for US assays and res freq. determination

To quantify the influence of the setup on the transducer's resonance frequency, the tests were performed firstly on just the transducer (coupled with the borosilicate glass), and then on the transducer and setup. Two transducers were tested, 1 (named "UHU" in the results section) and 2 (names "Other" in the results section). The setup connected to the transducer was exactly the one used during assays, and it consisted of the stirrer, element 1 on fig. 8, and wave generator and power supply, element 3.

2.5 Characterization of the vessel-transducer system – Calorimetry

As was briefly seen in the introduction, there are several methods for characterizing an ultrasonic system. For feasibility, the mechanical approach was taken, instead the chemical. With calorimetry, U.S. will be supplied to the reactor and its medium, and the change in temperature will be measured, along with the power of the supplied sonic waves. This information is then converted into calorimetric power. This metric will serve as the basis of comparison against other setup configurations, parameters, and works in the literature. One of the key factors of this method is the temperature control. All the heat that is generated in the system should be contained and measured, with no loss of matter or heat to the environment.

Insulation: Insulating strips (one side aluminium foil and the other polystyrene) of 2.5 mm thickness were used. They covered the full circumference and height of the vessel. In total, three layers were used. Attention was given to tightly wrap around the body of the vessel, and to minimize the areas of the vessel without insulation (four entrances used for access to the jacketed portion of the vessel). For tightly wrapping, each section of insulation that was successively longer by 2x the thickness of the strip. To reduce the area without insulation, the circles made for the entrances were slitted. Each layer was locked with duct tape. As the goal of this step is to contain the heat of the system within itself, and ideally the matter as well, like an adiabatic system, the aluminium face of the strips is always facing inwards to the reactor. This is because the high emissivity of al makes it a great reflector of heat (Adibekyan et al., 2021). The polystyrene face on the other hand, is a great heat insulator due to the many air bubbles within it. This will trap any heat that is absorbed by the al foil.

Of the five vessel "necks", three of them were capped. Of the uncapped, one was used for the stirrer blade, and the other for the thermal probe. These two openings allow for some water vapor to escape, however, at the experimental temperatures achieved, this was considered negligible. The jacketed portion, or double walled section of the vessel was dried, and the entrances covered with parafilm. This ensures a cushion of air between the two walls of the vessel, which slows heat transfer.

Transducer: A bolt clamped Langevin (BLT) piezoelectric transducer was used. It was 12 cm high, with a top face of 7 cm in diameter. A cylinder of borosilicate glass was glued to the top face, to protect the transducer from the environment and chemical reactions. Fast hardening epoxy was used as glue for both transducers. Both glass and transducer surfaces were cleaned thoroughly with norvanol. An equal amount of resin and hardening were mixed with the available spatula. Mixing took approx. 1 minute. The mixture was spread so that the total surface of the glass was coated with it, which took approx. another minute. The glass was firmly pressed against the transducer, and air bubbles squeezed out. The transducer rested on top of the glass to apply pressure. Extra weight was used to guarantee a strong bond. Bonding occurred for 20 minutes. Transducer 2 had more epoxy applied than necessary, which might have decreased its performance.

Supplying and modelling the energy to the transducer are a RIGOL DG1032 Z 2 channel wave generator and an Electronics & Innovation model 2100L RF power amplifier.

Frame 2: Two faces, connected by three rods, all made of 360 type steel were used. Between the two faces, cylindrical in shape and with 15mm thickness, are the components of the experiment. Ordered from bottom to top, these are: a PDM circular pad 3mm thickness, the transducer w/ glass, a gasket, the vessel body, another gasket, the vessel lid, and a final gasket. The rods that cross the metallic faces are threaded, so wing

nuts were used to tighten the metallic faces and compress the transducer-gasket-vessel system. Through the top central neck of the lid is the stirrer blade, attached to an IKA Eurostar 60 control device. Its weight is 3668.6g.

Frame 1: The same as frame 2, but with the faces' thickness reduced by half. This frame was used with transducer 1.

Temperature control: A fisher scientific polystat 36 was connected to the jacketed part of the vessel. This equipment is only capable of heating, and not cooling, and was therefore used to maintain the reaction system at a temperature above room temperature. A 12V fan was pointed to the transducer at 10 cm distance, to keep it cool, as a significant increase in temperature can decrease its efficiency.

Measurements: The temperature was taken with a TFK 325 temperature probe from WTW. The forward and reverse power measurements were taken from the on-board monitor on the power amplifier.

Calorimetry procedure 1: Frame 1 was mounted. The stirrer was placed at a specific height, which was marked in the stirrer's rod to ensure repeatability. A joe's flask was used to measure 250 ml of deionized water, which as put in the vessel, after it was made watertight by tightening the frame. The thermal probe was fixed in place with clamps. Transducer 1 had was charge neutralized by connecting both contacts with crocodiles. Wave generator was connected to the power amplifier which was connected to the transducer. Red crocodile (positive) connected to the highest contact on the transducer, and black crocodile (negative) to the lowest. Stirrer was set at 300 RPM. The frequency and Vpp were set in the wave generator. The channel output was turned on at the same time as a 10-minute timer. Each set of freq. and Vpp parameters was repeated 3 times.

Procedure 2: The same steps as procedure 1 but using frame 2 and transducer 2.

2.6 Control reaction – Cementation of copper on steel balls

Description of procedure and explanations

1. The water heater is turned on and heated to 40 or 60°C (fisher scientific polystat 36)
   1.1. (Care is taken to guarantee a proper liquid flow to and from the vessel, by decluttering the table and untangling the tubage.)

2. Around 19.67 g of copper sulfate are dissolved in 1000 ml of dH2O, with stirring at ~400 RPM, and ambient temperature. pH meter is placed in the solution's container. H2SO4 is added with the micropipette until pH of 2.00 or 2.50 is reached. This is the stock solution used for 3 tests.
   2.1. Copper (II) sulfate pentahydrate (CuO4S.5H2O) from AnalaR NORMAPUR was used, it has iron

concentration of 11ppm; sulfuric acid 95-97% from EMSURE; Ø60mm 4 bladed stirrer;
2.2. Due to the 20 µl accurate volume measurement limit of the pipette, this is the minimal addition of acid that can accurately be made.

3. The vessel is assembled: metal base, PDM cushioning, transducer & borosilicate glass, double jacketed glass reactor, (Ø40mm 4 bladed stirrer is now placed), gasket, reactor's lid, gasket, metal top. The guiding beams cross both metal bases, and are tightened at the top, firmly. The stirrer is connected to its IKA Eurostar 60 control machine.
   3.1. (The reactor's jacket design allows for the heater's water to heat the solution to the desired temperature)

4. Precisely 250 ml of stock solution are placed in the vessel, along with a thermal probe, until the solution reaches the desired temperature for the test, 40 or 60 °C
   4.1. (While this goes, IDing of the sample vials is done, weighing of the beads and other material needed for later stages, and calibration of the measuring equipment)

5. Around 2.22 g of steel beads (68 units) are weighed, then washed in acetone to remove protective oil layer, dried, and re-weighed.
   5.1. (Beads are not washed more than 2 days before usage, to prevent the steel from oxidizing. The beads have 2 mm diameter, and are mostly made of iron…)

6. The stirrer is turned on to 200 or 500 RPM. The beads are introduced in the vessel and a timer is immediately started. At 5, 30, 60, 90 and 120 minutes, the stirrer is stopped, a 5 ml sample is taken, the pH is measured, H2SO4 is added, or not, and 5 ml of stock solution are added.

7. The PLS is filtered, along with the wash solution. A 583/3 filter is used, as well as acid (pH of 2 or 2.5) wash solution. PLS volume and weight are taken, along with wash solution's volume. The filter and solid residue are placed in an oven (@65°C overnight), and then weighed, when cooled. A sample of PLS and stock solution are sent to be analyzed by ICP (great for detection of metallic elements at low concentrations in liquid samples).

The reactor, stirrer, and insulators are washed, and re-assembled.

2.7 U.S. assisted reaction – Cementation of copper on steel balls

5-6*. The US assisted procedure is identical to the control one in its totality, except for an extra step. Between step 5 and 6 from the previous section, both the wave generator and power supply are turned on. A conducting wire is used to neutralize the charges in the transducer from previous utilizations,

by connecting its positive and negative poles. After charged neutralized, the “crocodile” type connectors of the power supply are connected to the transducer. The parameters required for the specific assay are dialed in.

5-6.1*. When performing temperature or pH measurements, both stirring, and US were stopped. Typically, these measurements took less than 1 minute, so it wasn’t considered detrimental to the accuracy of the results. Were this step to be ignored and the measuring equipment would be at risk of being damaged.

2.8 Calibration of the measuring equipment

1. pH meter – Calibrated every day, first with a reference sample of pH 7, then one with pH 2.
2. Eh meter – Drift measurements are done every other day, with standard samples of 640, 470, and 220 mV Ag/AgCl.

3 Thermal probe- They do not require calibration.

Chapter 3

3. Results and discussion

3.1 Calorimetry

For this characterization, Vpp and frequency were varied. Three tests were performed for each set of parameters. Vpp varied from either 1, 1.5, or 1.9V, and frequency from 20, 40, and 60 kHz. In the first set of experiments, frame 2, twice as thick as frame 1, was used to hold the transducer-vessel system. The initial temperature of the liquid medium was not controlled.

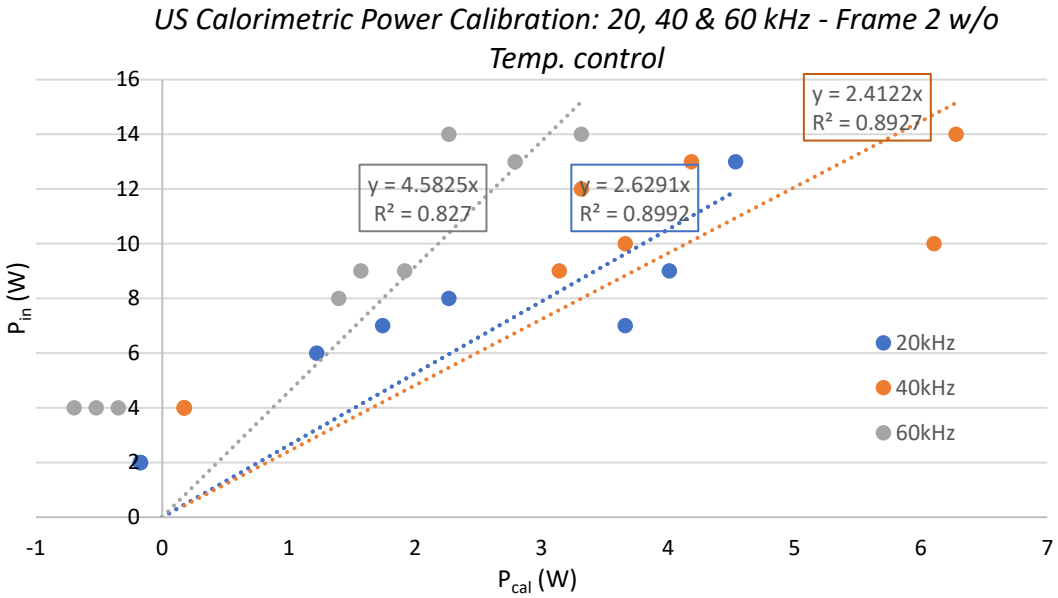

Figure 9 Calorimetric data at 20, 40, and 60 kHz. Frame 2 was used, and the initial temperature of the water in the vessel was not regulated. Significant dispersion between results is observed.

In the second set of experiments, the same frame 2 was used, but this time with the initial temperature of the liquid medium being kept below 26°C.

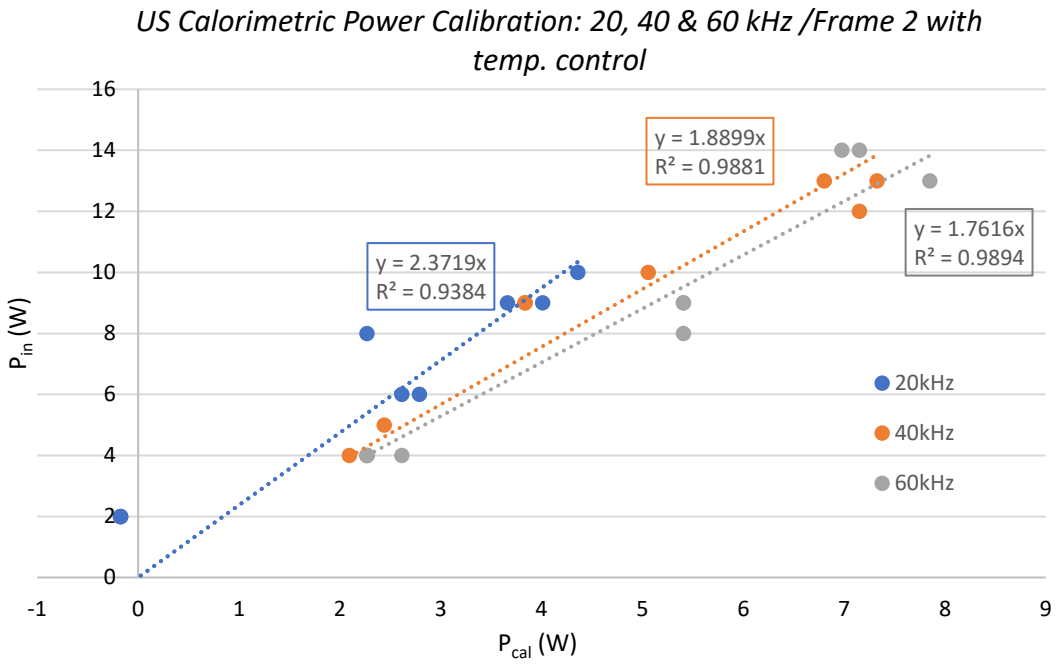

Figure 10 Calorimetric data at 20, 40, and 60 kHz. Frame 2 was used and the initial temperature of the water in the vessel was regulated.

For the last set of results, frame 1, thinner and lighter, was used. The results are presented below.

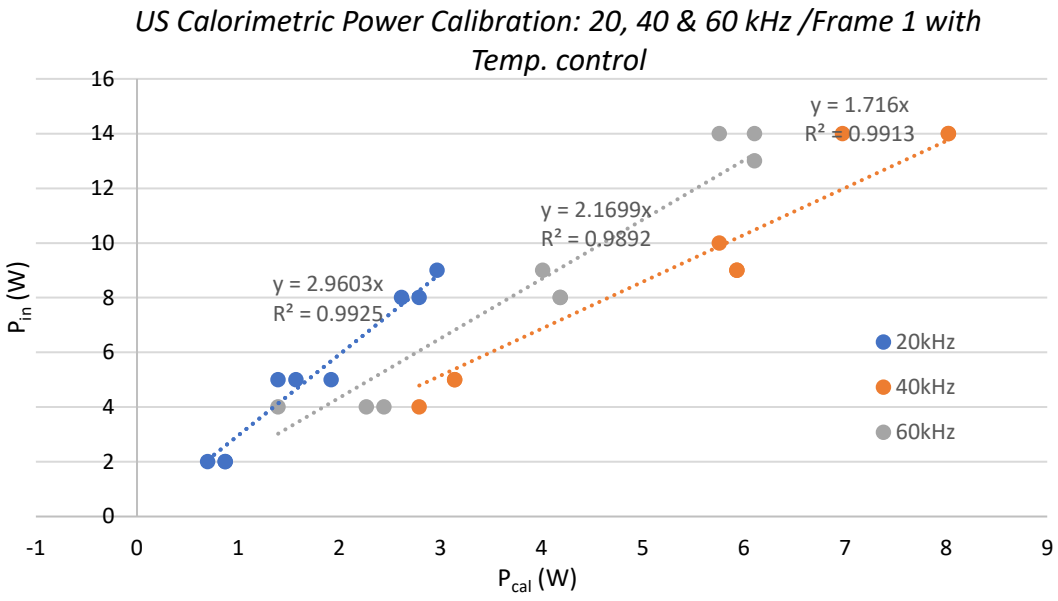

Figure 11 Calorimetric data at 20, 40, and 60 kHz. Frame 1 was used and the initial temperature of the water in the vessel was regulated

3.1.1 Discussion on calorimetry results

In the first set of results, it quickly became apparent that there was a significant discrepancy between values obtained for the same parameters. The only system variable within each subset of parameters was T_0, the initial temperature of the liquid medium. At first glance this does not seem like an influencing factor, which (Kimura et al., 1996) experimentally verified. The specific heat capacity of liquid water is 4179 J/(kg K), and as this value is constant, it should not influence Pcal whether T_0 is 22 or 30°C. Additionally, the duration of each test was small, at 10 minutes so evaporation can be considered negligeable.

The data was analyzed with bivariate correlations and linear regression coefficients in SPSS. In the model 1, "Uncontrolled temperature" 81 results were used to study the influence of the variables Input power (T_In) and initial temperature (T_T) on the outcome variable calorimetric power (T_Cal). In this model, only the results in which T_0 wasn't controlled to be <26°C were used. The table on the left shows that the variable Input power strongly correlates (Pearson = 0.82) with the outcome variable, in a positive direction (because Pearson correlation is positive and between 0.7 and 0.9) (Mukaka, 2012). This is to be expected, as higher supplied power correlates strongly and positively with calorimetric power. The initial temperature variable (P = -0.15) has correlation, albeit low, (Pearson between 0 and -0.5) on the outcome variable, with negative correlation. This means that to a small extent, the evolution of the outcome variable is inversely correlated to the initial temperature.

Correlations

		Uncont. T_Cal	Uncont. T_T	Uncont. T_In
Pearson Correlation	T_Cal	1.000	-.152	.823
	T_T	-	1.000	.308
	T_In	-	-	1.000

Coefficients[a]

Model		Unstandardized Coefficients B	Unstandardized Coefficients Std. Error	Standardized Coefficients Beta	Sig.
1	T_T	-.233	.042	-.448	.000
	T_In	.482	.041	.960	.000

Figure 12 Statistical data calculated with SPSS software. Left, the correlations, or the degree of influence between variables is seen. Right, the amount of change caused by one variable (B), along with significance (Sig.). Data from unregulated initial temperature and frame 2

Having confirmed the correlation between those variables, the linear regression between them and the outcome variable can be calculated. Firstly, the null hypothesis (H_0) is defined as being:

H_0: The input parameter initial temperature does not influence the output parameter calorimetric power.

As can be seen in the figure above, on the right, for every unit of Input power, the calorimetric power will increase on average 0.482 units ± 0.041. For every unit of initial temperature, the calorimetric power will decrease on average 0.233 units ± 0.042. Both these results are statistically extremely significant, given their sigma (seen as "sig.") of 0.000 (which is higher than 0.05, the standard value to accept a hypothesis). The null hypothesis is rejected, initial temperature has a negative influence on the output.

This is in contrast with literature results which found that thermally determined power was independent of the initial temperature (in the interval of 0 to 40°C) (Kimura et al., 1996). However, Kimura's results haven't been considered relevant for this work, as they used low sonication durations (30 s) and performed the temperature measurements with a cooling apparatus with a large (unspecified) volume of coolant. These differences and the high correlations found in the statistical analysis led to the conclusion that for the used setup, initial water temperature (above 26°C) influences calorimetric measurements.

Correlations

		Tcont.cal	Tcont.T	Tcont.in
Pearson Correlation	Tcont.cal	1.000	.449	.939
	Tcont.T	-	1.000	.361
	Tcont.in	-	-	1.000

Coefficients[a]

Model		Unstandardized Coefficients B	Unstandardized Coefficients Std. Error	Standardized Coefficients Beta	Sig.
2	Tcont.T	.353	.143	.126	.017
	Tcont.in	.470	.027	.894	.000

a. Dependent Variable: Tcont.cal

Figure 13 Left, the correlations, or the degree of influence between variables is seen. Right, the amount of change caused by one variable (B), along with significance (Sig.). Data from regulated initial temperature and frame 1

In a second model, T_0 was controlled to be below 26°C. This time, input power is very, and positively, correlated with the outcome variable, better than achieved previously. T_0 was shown to correlate positively with Pcal, instead of the negative correlation seen previously. But in this case, it was likely due to the protocol used. Unheated water was used for the lower power input measurements, which resulted in final temperatures not far from the initial ones. If final T was below 26°C, the same water was used for the following measurement at higher power. This reduced time and simplified the calorimetric study but resulted in the positive correlation between initial temperature and input power.

The null hypothesis remains the same as previously.

Results show a similar evolution of calorimetric power with input power, at 0.470 increase in Pcal for every unit of increase in Pin. A unit change of initial T causes an increase of 0.35 units in Pcal, however, the statistical significance of this effect is 100 times lower, at a P-value of 0.017. Therefore, the calorimetry conversion factors were defined with sets of values in which T_0 is controlled. For further work, it's recommended that the calorimetric characterization be made with:

- A controlled initial temperature, ideally keeping it equal throughout the measurements.
- Recording the temperature change throughout each measurement and not just initial and final temperature.
- Accounting for equipment heating, such as transducer and vessel.
- Reducing the experiment time to 5 or less minutes, to reduce the impact of heat losses to the environment.

- Performing the measurement also at resonance frequency.

During the U.S. experiments the power amplifier only displays input power. This value needs to be converted to the expected calorimetric power. For different frequencies and setups, different conversion factors need to be used. In this case, to obtain Pcal, Pin must be divided by the following factors.

Table 1 Calculated conversion factors for the characterization of the ultrasonic setup with regulated initial temperature

	Frame 2			**Frame 1**		
Frequency	20	40	60	20	40	60
1/Factor	2.372	1.890	2.129	2.960	1.716	2.170
R^2	0.938	0.988	0.996	0.993	0.991	0.989

$$Calorimetric\ power\ (Pcal) = \frac{Power\ input\ (Pin)}{Conversion\ factor\ (F)} \tag{3.1}$$

These conversion factors were calculated using a linear regression and defining the interception at zero. The R^2 gives us the fraction of the discrepancy between regression and the actual values which is explained by the model. In this case, the R^2 is particularly high for all scenarios except frame 2 at 20 kHz.

3.2 Iron titration

Here the evolution of the amount of ferrous iron in the vessel is plotted, for assays 90 (silent) and 91 (sonicated). As a reminder, 2.218 g of steel balls were used in assay 91. Assuming 98% of iron in them, only 2.173 g of iron was in the vessel. At 181 minutes there is an inconsistency in the data, due to excess iron, which is addressed in the discussion.

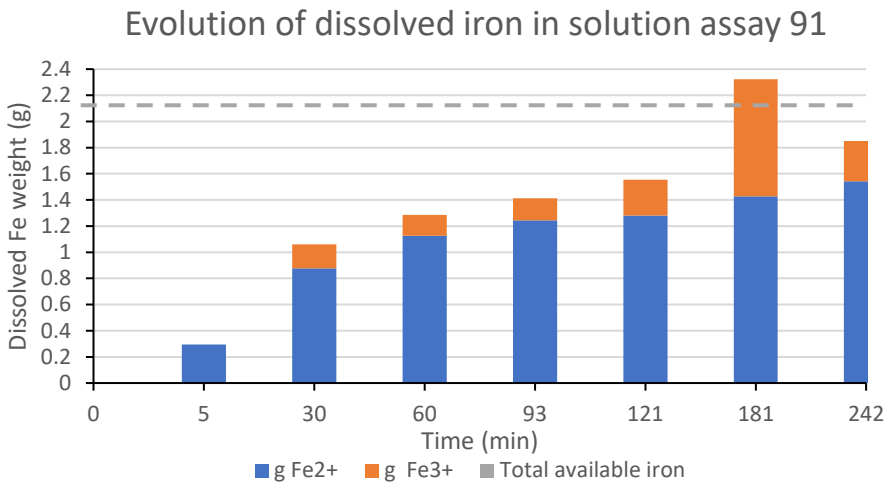

Figure 14 Assay 91's evolution of ferrous and ferric ions in solution, along with a dashed line showing the physical limit, indicating an error.

For assay 90, the physical limit of iron content is also 2.173. The dissolved iron in solution does not get close to this limit.

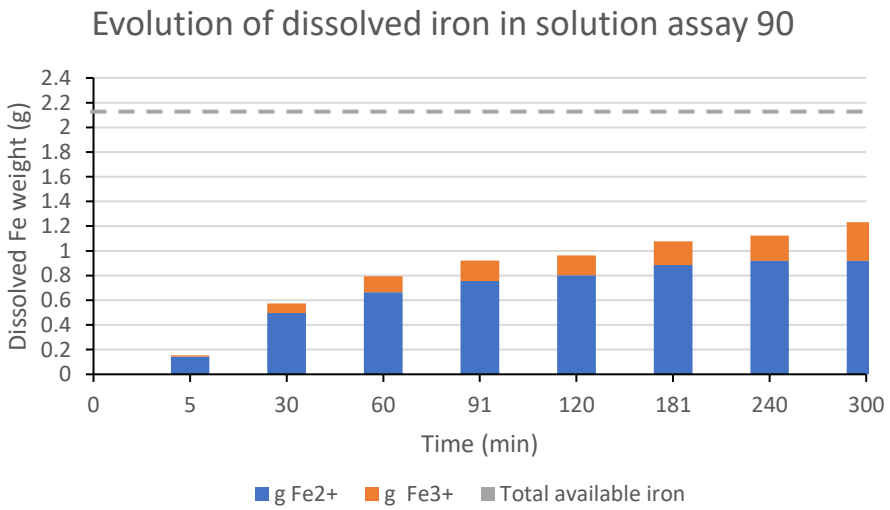

Figure 15 Assay 90's evolution of ferrous and ferric ions in solution, along with a dashed line showing the physical limit, well above the total iron obtained.

By plotting a ratio of ferric ions over total dissolved iron the amount of produced radical can be easily understood. Assay 91 oscillated significantly at the 180-minute measurement, but again, this is due to an error. Assay 90 slowly increased its ratio, or its dissolved ferric ion content for 1h30, after which it stabilized at 18% of ferric ions in solution, until the last measurement where there was an increase of almost 40%.

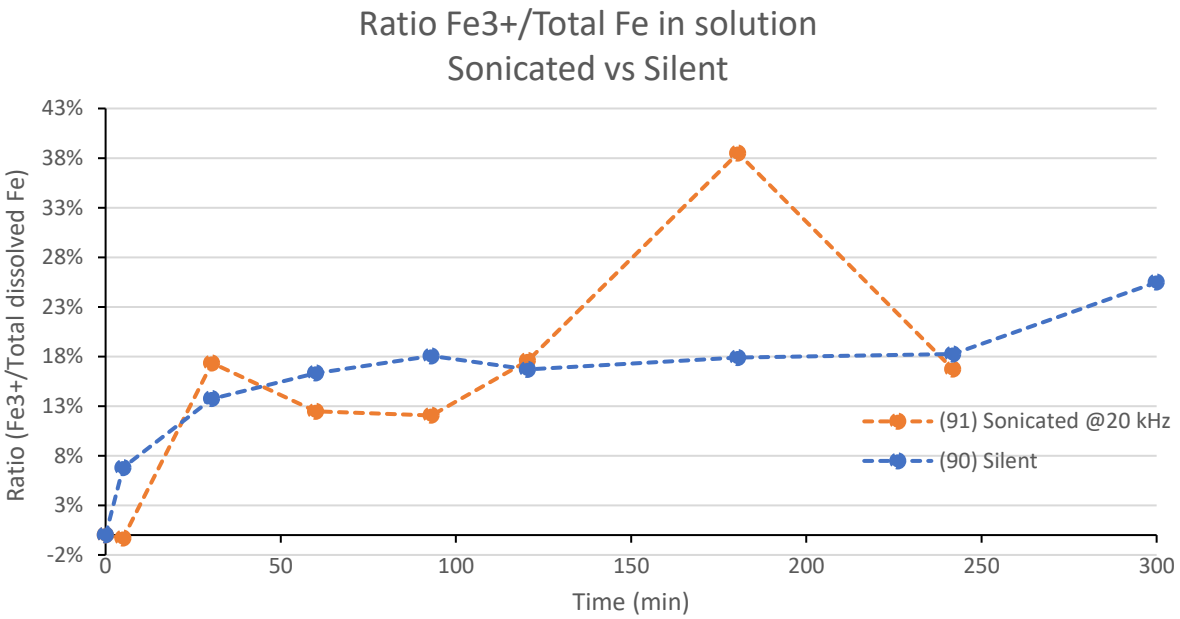

Figure 16 Evolution of the Fe^{3+} ion concentration in solution in silent and sonicated conditions

Due to the differential evolution of the ferric ion concentration, the slope was calculated for the first 30 minutes, and for that point onwards. Growth in the first 30 min (assay 90) is very significant, but it stabilizes shortly after. For the sonicated assay (91), growth is 8 to 30 times faster during the first 30 minutes, depending on whether sample 181 min is considered or not, respectively.

Table 2 Different growth rates of Fe3+ concentration, for assays 90 & 91

	slope (% / 10min)		
Assay	first 30 min	after 30 min	after 30 min*
91	6.1	0.7	0.2
90	3.9	0.3	-

*sample @ 181 min not considered

3.2.1 Iron titration

Data plotted in fig. 14 shows a fast increase of Fe^{2+} until the 60-minute mark, after which it continues to increase but slower, and looking at copper cementation data, that time corresponds to near maximum copper recovery. Following eq. (1.21) this makes sense, one mole of Fe^{2+} is produced for every mole of cemented copper. However, when after maximum copper recovery is achieved, Fe^{2+} continues to increase. This is to be expected if equations (1.22) and (1.23) are considered. Both sulfuric acid and ferric ions, when in contact with solid iron, will generate Fe^{2+}. Because the amount of iron given to the system is higher than the

stoichiometric amount, these secondary reactions can still occur with the excess iron. As seen previously, US can lead to increased radical formation. This can explain why on assay 91 (sonicated), [Fe^{3+}] growth was 2.5 to 3.3 times that of the growth of assay 90.

Even after plateauing the main copper cementation reaction, the system had enough resources to continue secondary reactions. This might have been observed empirically. As by the end of the assay, when stirring was stopped, gas bubbles were leaving the copper shells (with the steel balls still trapped inside). This could have been hydrogen gas, which is a product in eq. (1.22), and indicates the production of ferrous ions.

These observations make it clear that in any economically restrictive environment (industry), care should be taken to limit the amount of sacrificial metal to the absolute necessary. Otherwise, more resources than necessary will be spent, such as the acids and sacrificial metals involved.

In the titration of assay 91, the sample taken at min 181 shows a mistake. This can be said with confidence, as the sum of Fe^{2+} and Fe^{3+} adds to 2.32 g of iron, and only 2.17 g of it were introduced in the reactor.

- The titration itself appears to be correct, as it follows the same growth pattern as the other samples, and each titration was performed 3 times. No inconsistencies are found in the data of this sample. Despite unlikely, this was probably the cause of the mistake. For future work, the iron titration should be performed with more care.
- Sample dilution for ICP analysis could have been performed incorrectly, but the copper values of the same sample, which are analyzed simultaneously, show no discrepancy.
- Sample contamination could have occurred, but the dilutions and sample handling were performed simultaneously for all samples, and the protocol with which it was made leaves few chances for an individual sample to be contaminated and not the surrounding ones.

In figure 15, Assay 90 showed a fast increase in Fe^{2+} concentration until the 60 minutes mark. By this point, Fe^{2+} in solution is half of the achieved in assay 91. As seen in the copper recovery graph of figure 39, assay 90 reached plateau at 240 min. It can be said that no more copper cementation occurred. This is supported by the fact that at that same 240 min mark, the amount of Fe^{2+} also plateaued. In the hour that followed plateau Fe^{3+} concentration increased by over 50%, and copper recovery decreased by 3%. In the hour before plateauing, it only increased by 6%. This evidently shows that after maximum recovery is reached, the process becomes counterproductive.

The plateau in ferrous ions is an indicator of the end of copper cementation as explained previously. But "predatory" equations such as eq. (1.24) consume solid copper and produce ferrous ions. Why is no increase in its concentration seen in the silent assay? A few theories can be formed.

- The reactions balance out. While eq (1.24) produces Fe^{2+}, eq. (1.26) consumes it.
- Not enough sulfuric acid ions are present in solution to oxidize iron and produce Fe^{2+}
- No more solid iron is accessible to oxidizing species, preventing the reaction from occurring

3.3 Resonance frequency determination

The resonance frequency tests were performed in KU Leuven by Ir. Mohamed Aâtach in the 15th of June.

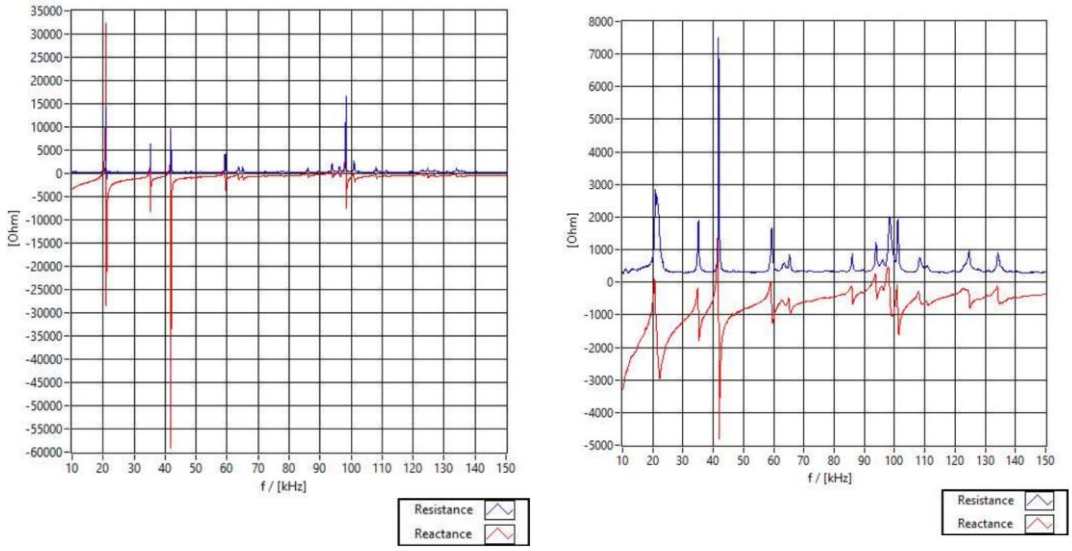

Figure 17 Left, resistance and reactance measurements of transducer 1 alone; Right, same measurements for the setup transducer 1 and frame 1

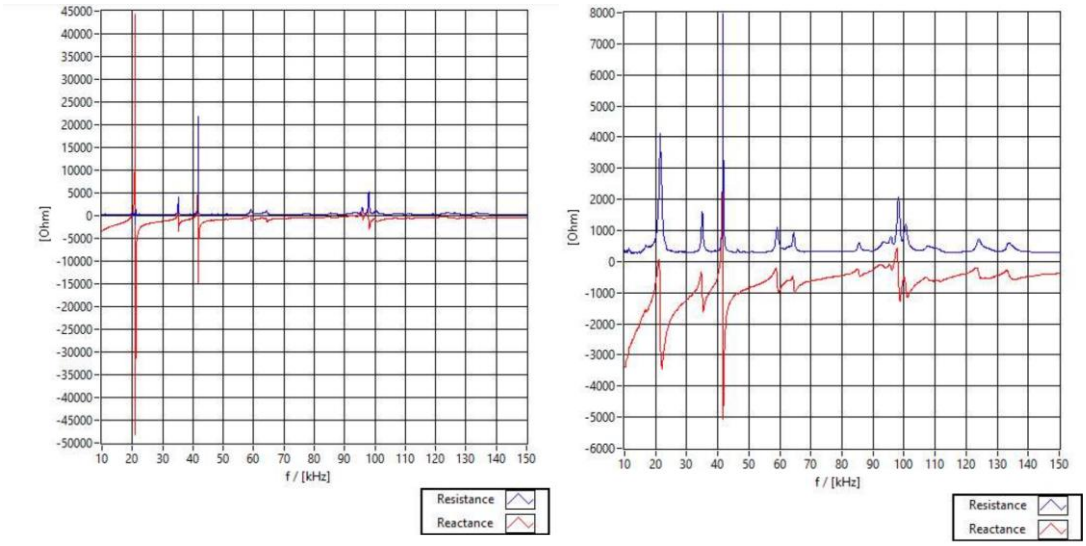

Figure 18 Left, resistance and reactance measurements of transducer 2 alone; Right, same measurements for the setup transducer 2 and frame 2

Table 3 Determined resonance frequencies in transducer and reactor

	Freq (kHz) at intersection of R and X				
Trans. 2	20.0	41.0	-	97.3	
Setup 2	-	41.1	-	-	
Trans. 1	20.0	41.2	59.1	97.3	35.0 & 93.5
Setup 1	-	41.3	-	-	

3.3.1 Discussion on resonance frequency (RF) determination results

After assembling the transducer and its borosilicate glass protection for the first time, possibly too much epoxy was used, and eventually, even the wrong type of epoxy. These assumptions came from the low power input observed in initial trials. The results of the RF determination indicate that transducer 2 was impaired in terms of its ability to resonate. Despite both transducer 1 and 2 being similar, t2 did not resonate at the supposed ~60 kHz mark. This is understood visually, as there is no intersection between the resistance and reactance lines in fig. 18, left, at those frequencies. This is further cemented by the data analysis performed with the raw data, which did not yield results indicative of resonance.

It has been reported from comprehensive studies that epoxy has damping coefficients 50 times greater than borosilicate glass (Ono, 2020). By applying too much of the epoxy, part of the ultrasonic energy appears to be absorbed by it, especially in the 60 kHz range. Due to its impact on the behaviors at play, it's suggested that further studies try to optimize the thickness and kind of epoxy. This could be done by studying a range of increasing weights of applied epoxy. Another recommendation is to experiment with different glues, especially ones with the lowest possible attenuation factor.

The most relevant aspect of this measurement was to assess influence of the complete setup on the resonance frequencies of the reactor. Its effects are clear. A significant amount of energy is absorbed by the setup. Both with transducer 1 and 2, no resonance is reached at the previous resonance frequencies of 20, 59, 97, and 35 kHz. Only at 41.3 kHz the impedance of the reactor reaches 0. This information is of great importance to maximize the efficiency of the ultrasonic device as well as its effects. Due to availability of KU Leuven during adverse times, this information was collected only after some sonicated tests had been made. Nevertheless, the importance of experimenting with lower frequencies remains, due to its strengthening of cavitation effects. During assays at the RF, the effects of the ultrasounds were significantly intensified. It was easily observed in the power supply. If previously 1.9 V were needed to supply 14 W of input power at 20 kHz, at resonance 1 V or less was enough to achieve the same. Cavitation noises and visual effects were also extremely noticeable during experimentation.

For further studies, the resonance frequencies of the reactor with a complete setup should be acknowledged beforehand. This should leave room to tweak the setup in case there are problems achieving resonance.

3.4 Silent copper recovery

As mentioned before, the first experimental step of this work consisted in the silent assays for copper recovery. They were done to obtain a baseline on the system's behavior. Additionally, they were of great importance to better understand the effects of each parameter on the reactions at place. The results of those assays are now presented.

3.4.1 pH effects at low temperature & low RPM (40°C & 200 RPM):

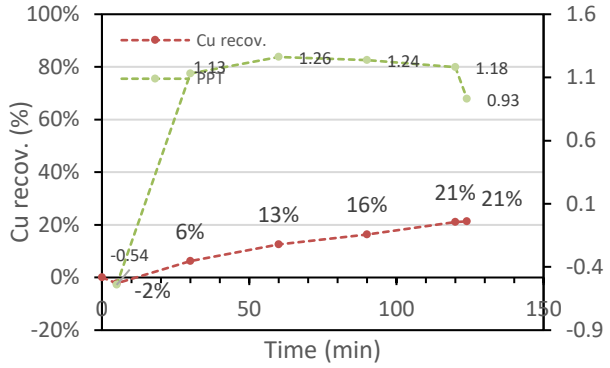

Figure 19 Copper recovery and PPT evolution of assay 3. pH 2.5, 40°C and 200 RPM

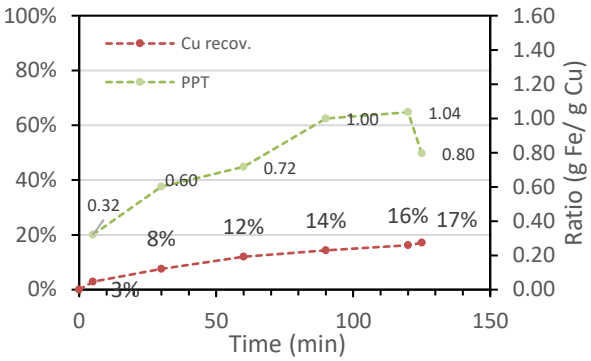

Figure 20 Copper recovery and PPT evolution of assay 8. pH 2.0, 40°C and 200 RPM

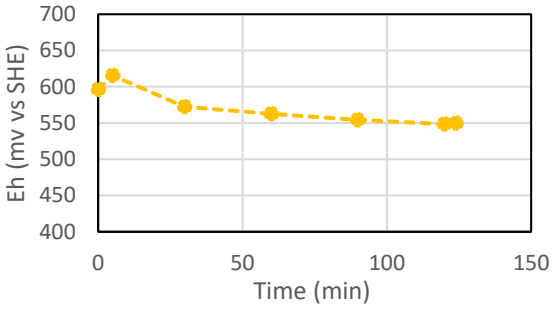

Figure 21 Eh evolution of assay 03

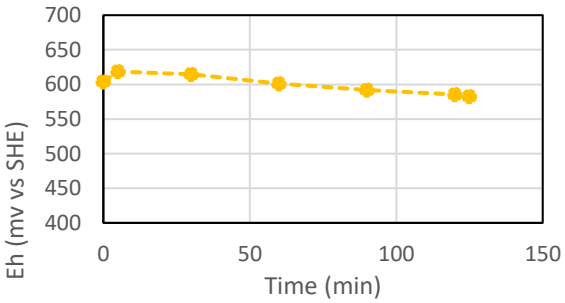

Figure 22 Eh evolution of assay 8

Table 4 Experimental results low temperature low RPM

	Reaction parameters		Precipitation factor	
Assay	Fe leaching	Cu recovery	Obtained	Theoretical
03	11%	21%	1.18	0.88
08	9%	16%	1.04	

3.4.1.1 Discussion on pH effects at low temperature & low RPM (40°C & 200 RPM):

The goal of this and the following discussions is to better understand how a parameter predicts the behavior of the system and find a coherent model that applies to all the performed assays. To compare between them, valuable key indicators need to be selected for comparison. The most relevant ones should be simple to convey and calculate and be compatible with the indicators currently used in the literature. In this work, the following were used to arrive at different conclusions.

- Copper recovery
- Rate of copper recovery
- Precipitant factor
- Copper recovery per calorimetric power, volume, and duration of cementation

When T and RPM are low, having a "high" pH of 2.5 showed an increase in Cu recovery, at the cost of increasing iron consumption, and hence the increase in precipitant factor (PPT), that stabilized at ~1.2. This is almost 40% higher than the stoichiometric ratio. This increase is likely due to the unproductive reactions caused by Fe(III) ions, which conduct the reactions seen in eq 3 and 4, along with oxygen which likely promoted the re-dissolution of cemented copper as well as producing Fe(III) ions according to eq 5 and 6, respectively. According to these assumptions, the presence of an oxygen rich atmosphere is likely to contribute to the increase of precipitant factor. Despite the interest in a possible work carried out under an inert atmosphere, this is also likely too costly and complex to be economically feasible in an industrial setup. In assay 3, in which the previous parameters were used, at the 5-minute measurement, a precipitant factor (PPT) of -0.5 is recorded. This is impossible, but is due to a dilution error, which wrongly increased the copper concentration of the sample taken at 5 minutes to 5.2 g/l, whereas the initial sample's concentration is only 5 g/l of copper, resulting in a negative PPT.

When the pH was reduced to 2, copper recovery remained similar, but precipitant factor decreased significantly and stabilized at around 1.04. A lower factor is great as it indicates that fewer secondary or unproductive reactions are happening. A 20% reduction in precipitant factor translates to 20% reduction in the expended metal and therefore 20% reduction in cost of buying the precipitant metal. In the specific case of assay 8 an odd behavior is found. The precipitant factor is below 0.88, the theoretical minimum, for the first 3 measurements, or for the first hour of the experiment. As it's not possible to produce 1 g of Cu with less than 0.88 g of Fe, and as there are no secondary reactions that could re-cement dissolved iron, which would interfere with the PPT, it's assumed that these errors are due to uncertainties. By simulating an initial or stock solution of assay 8 which had 2% less copper concentration, all PPTs would have values equal or higher than 0.88 . A 2% variation is considered small enough to be common. It is particularly impactful on

the initial samples taken because the quantities involved were very small, where decimals of g/l often make the difference.

The lowest measured Ea value was measured in the first 5 minutes of low RPM and pH parameters. In these conditions, the reaction is almost completely controlled by the diffusion mechanics. At 30 minutes the slope is the steepest, meaning it was the point where temperature was having the highest influence, and somewhere between 60 and 90 minutes, the slope inverts. This is a strange phenomenon, which might indicate that the reaction has already achieved maximum recovery. This is verified by the copper recovery plots. What can also be seen is that the interception of the vertical axis (ln A), on average, keeps decreasing. This is related to the frequency factor (A). As time passes, less collisions between reactant particles happen.

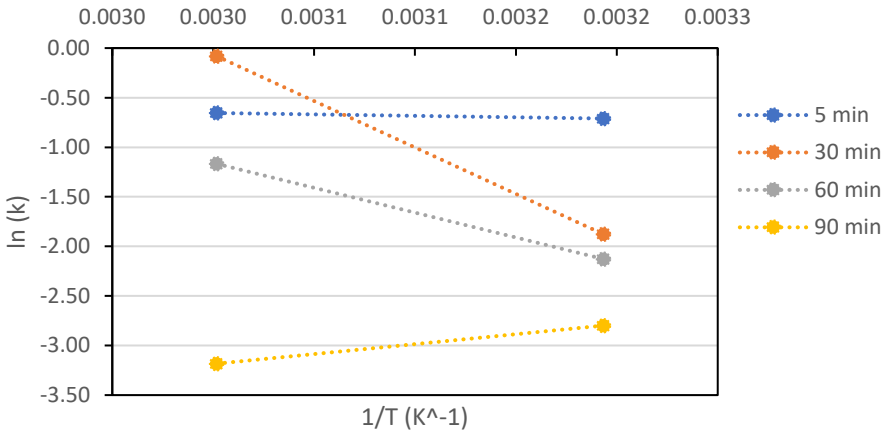

Figure 23 Activation energy of copper cementation at 200 RPM and pH 2, measurements taken at 40 and 60°C

3.4.2 pH effects at high temperature & low RPM (60°C & 200 RPM)

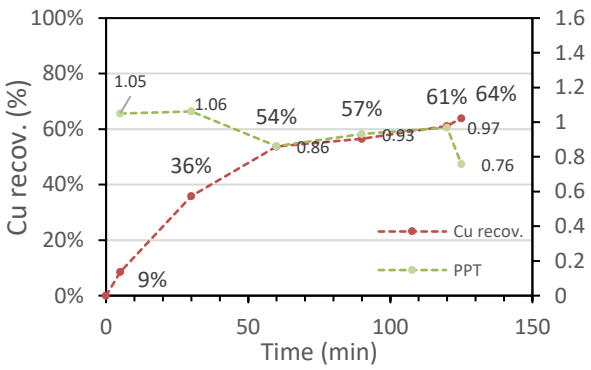

Figure 24 Copper recovery and PPT evolution of assay 13. pH 2.5, 60°C and 200 RPM

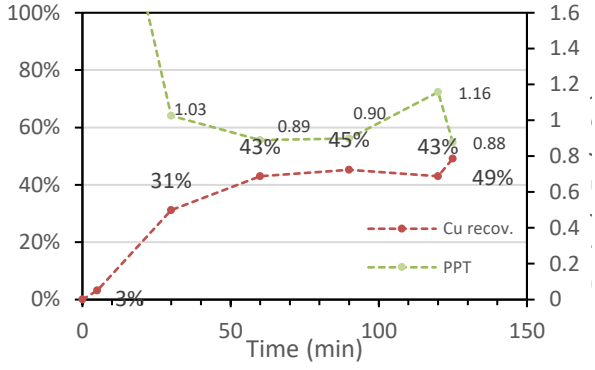

Figure 25 Copper recovery and PPT evolution of assay 19. pH 2.0, 60°C and 200 RPM

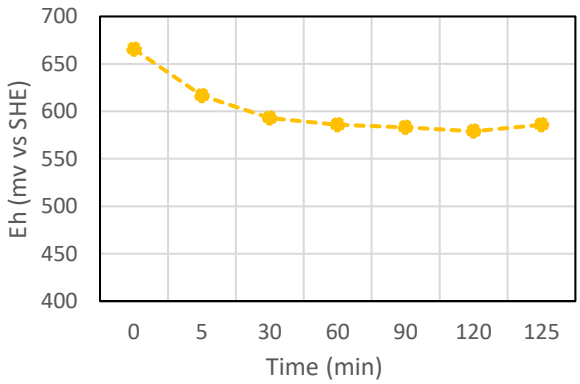

Figure 26 Eh evolution of assay 13

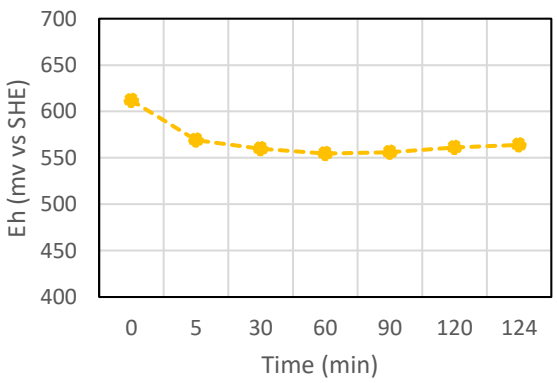

Figure 27 Eh evolution of assay 19

Table 5 Experimental results high temperature low RPM

	Reaction parameters		Precipitation factor	
	Fe leaching	Cu recovery	Obtained	Theoretical
Assay 13	30%	61%	0.97	0.88
Assay 19	27%	43%	1.16	

3.4.2.1 Discussion on pH effects at low temperature & low RPM (40°C & 200 RPM):

Looking into assays at high temperature and low RPM, one could expect similar results, like previously, when manipulating the pH. This is not the case. With the pH at 2.5 (Assay 13), copper recovery was at 61% after two hours, without signs of plateauing, and with a precipitant factor of 0.97. At the lower pH of 2 (assay 19), recovery peaked at 45% after which it plateaued. Precipitant factors were similar between the

two. However, comparing with the previous scenario at low temperature, an extra 20 to 40% of copper was recovered.

From scenario 1 to 2 the temperature increased from 40°C to 60°C, or by 50% . Considering that the copper recovery increased by 200% (high pH assays) and ~250% (low pH assays), there seems to be a moderate impact of temperature on the cementation. This could indicate an intermediate or mixed controlled process, but this theory will be further cemented deeper in this discussion.

3.4.3 pH effects at low temperature & high RPM (40°C & 500 RPM)

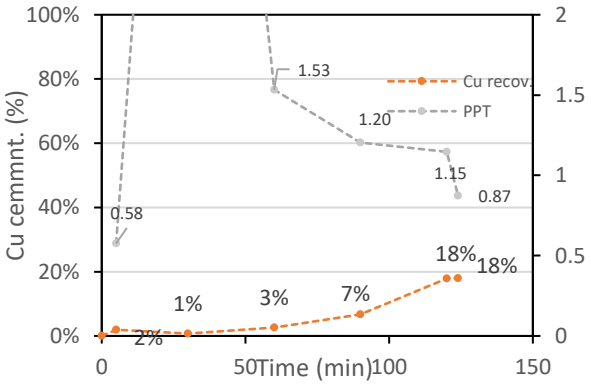

Figure 28 Copper recovery and PPT evolution of assay 05. pH 2.5, 40°C and 500 RPM

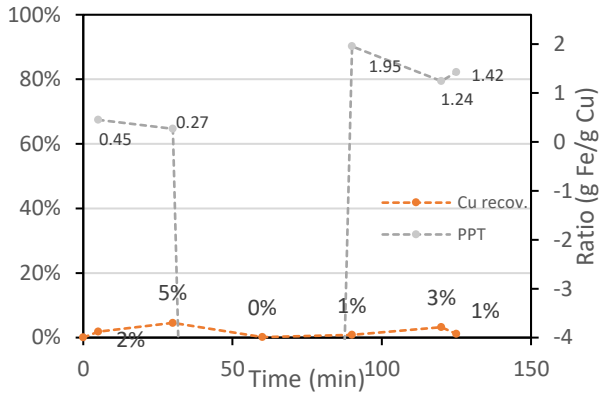

Figure 29 Copper recovery and PPT evolution of assay 10. pH 2.0, 40°C and 500 RPM

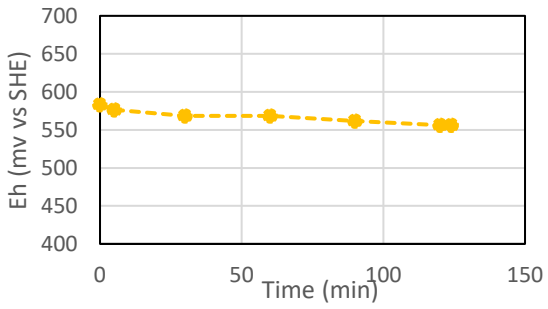

Figure 30 Eh evolution of assay 05

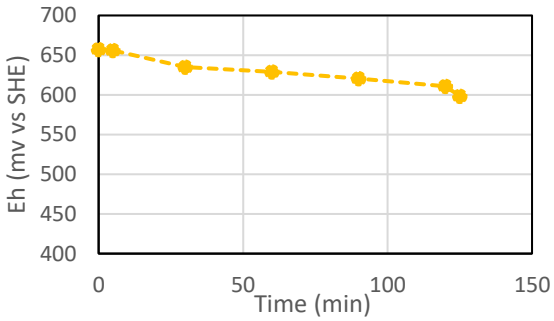

Figure 31 Eh evolution of assay 10

Table 6 Experimental results at low temperature and high RPM

	Reaction parameters		Precipitation factor	
	Fe leaching	Cu recovery	Obtained	Theoretical
Assay 05	9%	18%	1.15	0.88

Assay 10	1%	3%	1.24

3.4.3.1 Discussion on pH effects at low temperature & low RPM (40°C & 200 RPM):

For this third scenario assays 5 and 10 are compared. The new variable introduced, high RPM, appears to have had detrimental effects on the process, when compared with low RPM scenario of section 3.4.1. Assay 5 had ~20% decrease in copper recovered compared that scenario's assay. Here, PPT was very irregular but once again it was likely due to the small concentrations being measured. When these concentrations increased, PPT stabilized at the same ~1.2 seen in assay 3.

For assay 10, whose pH was set to 2, there was an almost negligeable recovery of copper. Why would an increase in RPM inhibit this process? One hypothesis is that more oxygen was introduced in the reactor due to the high RPM. Then, due to the temperature and pH conditions, mostly side reactions took place, such as hydrogen production, iron dissolution into Fe(II), and conversion to Fe(III).

3.4.1 pH effects at high temperature & high RPM (60°C & 500 RPM)

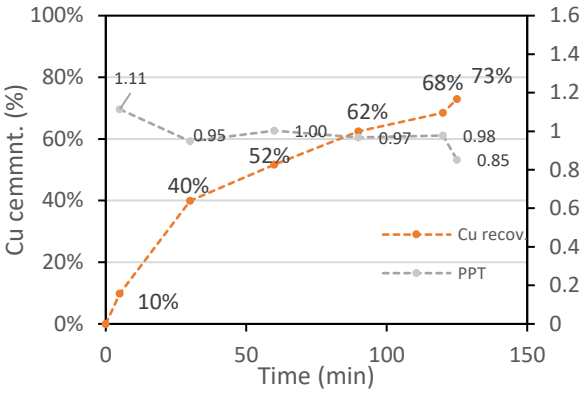

Figure 32 Copper recovery and PPT evolution of assay 16. pH 2.5, 60°C and 500 RPM

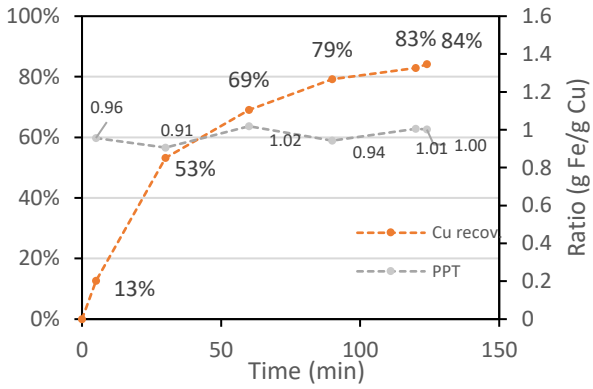

Figure 33 Copper recovery and PPT evolution of assay 22. pH 2.0, 60°C and 500 RPM

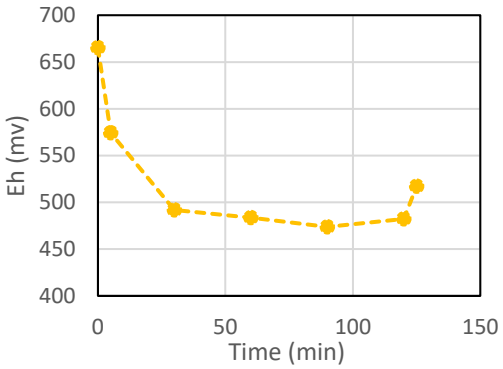

Figure 34 Eh evolution of assay 16

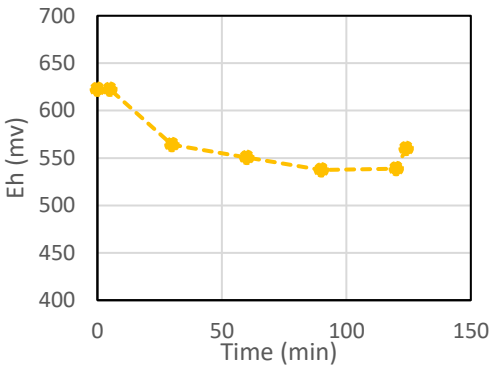

Figure 35 Eh evolution of assay 22

Table 7 Experimental results at high temperature and high RPM

	Reaction parameters		Precipitation factor	
	Fe leaching	Cu recovery	Obtained	Theoretical
Assay 16	38%	68%	0.98	0.88
Assay 22	53%	83%	1.01	

3.4.1.1 Discussion on pH effects at low temperature & low RPM (40°C & 200 RPM):

For this scenario once again, the temperature was increased by 50%. Comparing to scenario 3, where the parameters are the same, except for temperature, a sharp increase in recovery of copper is seen. Assay 16 showed an increase of copper recovery of 280%, at the two-hour measurement, compared to assay 5 (both

at the same pH, 2.5). This is again a sign of mixed controlled processes, despite several works stating that copper cementation into iron is a diffusion controlled one.

Looking at the copper recovery, assay 22 showed the best results after two hours (83%), along with one of the best precipitant factors (1.01).

From the kinetics of leaching chapter, the approximate activation energies of chemically and diffusion-controlled processes are known. In the first 90 minutes, the reaction averaged 16 kcal/mol, which lays between chemical and intermediate controlled ones.

Table 8 Calculated Ea (Kcal/mol) for every non-sonicated scenario. A comparative scale is presented, to help identify which controlling category each scenario falls into

Parameter	**low pH**		**High pH**		**Diffusion**	**Intermediate**	**Chemical**
	5 min	Average	5 min	Average	Kcal/mol		
High RPM	20	24	17	10	1-3	5-8	>30
low RPM	1	6	12	6			

This table showcases the complex nature of the cementation reactions. At low RPM, all the assays had energy activations, on average, close to those of the diffusion-controlled reactions or on the intermediate range, while at high RPM, it was much closer to the chemical-controlled ones.

A particularity of low RPM assays is that in all of them, the metal beads formed clumps, as can be seen in the figures below. These structures and the lack of collisions between the beads (which can be deduced from the filtering paper with no fine particles, and the absence of exposed iron on the beads) that would break apart pieces of copper reduced the availability of iron to such a degree that the diffusion of the cupric ions into the solid-liquid interface became the limiting factor. So, its inhibition to cement copper reduced the activation energy, otherwise known as sensitivity of the reaction to temperature. No matter the increase in temperature, not enough cupric ions were reaching the solid iron. The assays in which the reaction was most effective (low pH, high RPM) were the one with the highest Ea at 24 kcal mol^{-1}. This is considerably higher than the 5 kcal reported in Shamsuddin. The second most effective (high pH and RPM) had the second highest sensitivity to temperature.

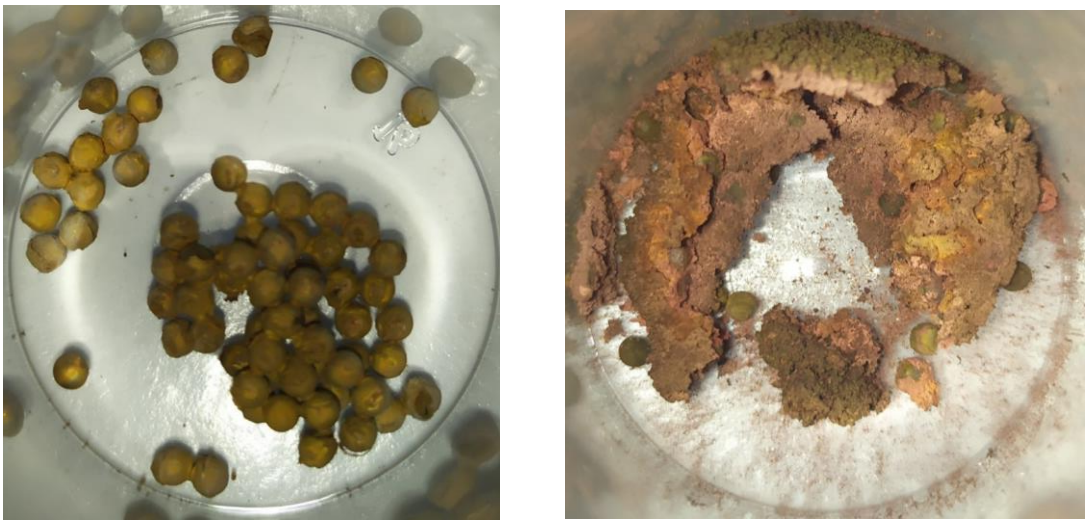

Figure 36 Left, solid residue from assay 8 obtained after filtration (fine residue was separated). The beads are strongly stuck together in the shape formed at the bottom of the reactor; Right, solid residue from assay 93

As was reported in the literature, there is a maximum agitation rate beyond which air bubbles and other phenomena form in the solution, preventing reactions from taking place effectively. This has been reported by some authors as being ~2500 RPM (Shamsuddin, 2016), but this will vary considerably with all other parameters (viscosity, blade type, vessel type, volume of solution). If a following work takes place, the Ea measurements should be performed at that maximum agitation rate. Then, the temperature should be increased, and tests done at multiple different temperatures, to increase the reliability of the Ea measurement. This is recommended as in this work the measurement was obtained solely from two data points, at different time intervals of the experiment, as seen in figure 37. Then, the influence of temperature could be calculated based on multiple data points.

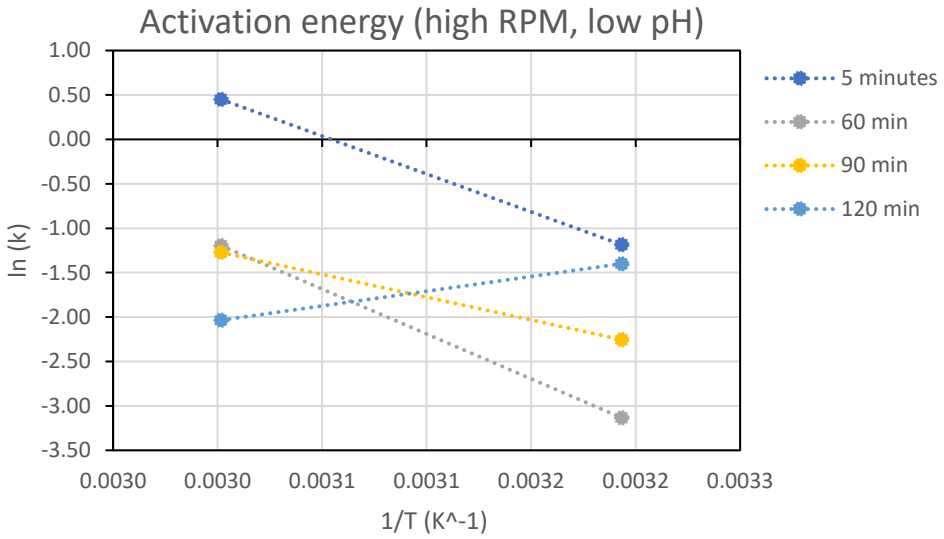

Figure 37 Activation energy of copper cementation at 500 RPM and pH 2, measurements taken at 40 and 60°C

Other indicators are important to determine the performance of this process. However, due to time, cost, and to not over-broaden the discussion of this work, these were not performed. They are, however, recommended for further studies on this topic. Namely:

- Imaging analysis, specifically with SEM, and XRF or SEM-EDS analysis of the deposited metal. The former would provide a qualitative approach that would determine very important parameters such as particle size, porosity, and roughness. The two latter, quantitative, would be paramount to determine the purity of the copper. As there is mostly only copper and iron on the solid residue, EDS should be good enough. This could answer several questions regarding what could be done with the recovered metal.
- Determination of the optimal rotation speed for the specific setup

3.5 US assisted copper recovery

With the influence of the parameters at hand having been studied, the ultrasonic assays could now begin. However, relevancy was found on the pursue of each assay reaching a copper recovery plateau. The reasoning being that this would be beneficial to assess the effects of US on the time required to achieve maximum efficiency. To that end, one silent assay was performed for 5 hours (this value was determined by paying attention to pH evolution and to the solution's color). The most efficient parameters, found previously, were selected. An ultrasonic test at 20 kHz then performed. This frequency was selected as cavitation phenomena occur more intensely at lower frequencies. The two following assays were performed at lower RPM. The first of these was done to understand if extra kinetic energy from the stirring at 500

RPM was the source of the increase in efficiency rather than the ultrasounds themselves. The second, done at the RF of the system, was performed to understand the effects that it could have on the reaction.

Table 9 Compilation of pH, temperature, stirring, US freq, and time parameters used in the sonicaated assays

Assay	pH	Temp	RPM	Freq	Duration
90	2	60	500	-	5h
91				20	4h
92			200	20	3h
93				40.5	3h

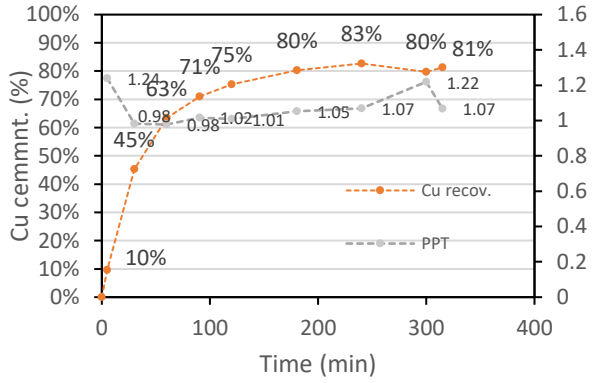

Figure 38 Copper recovery and PPT evolution of assay 90. pH 2.0, 60°C and 500 RPM

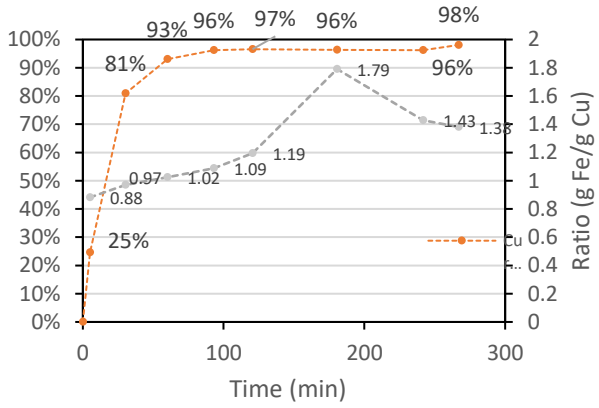

Figure 39 Cu recov. and PPT evolution of assay 91, pH 2.0, 60°C, 500 RPM, 20 kHz and Pcal=4.7±0.3W

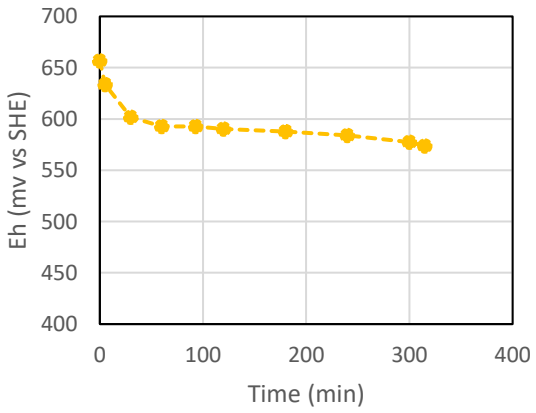

Figure 40 Eh evolution of assay 90

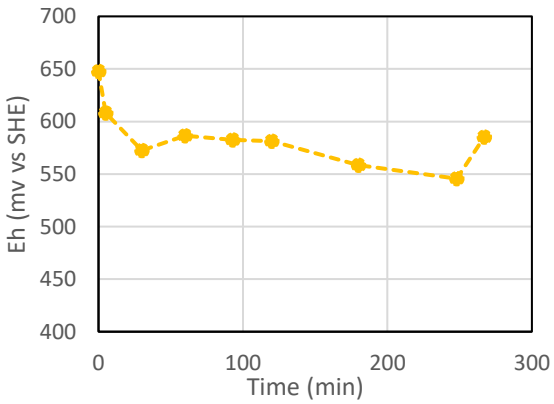

Figure 41 Eh evolution of assay 91

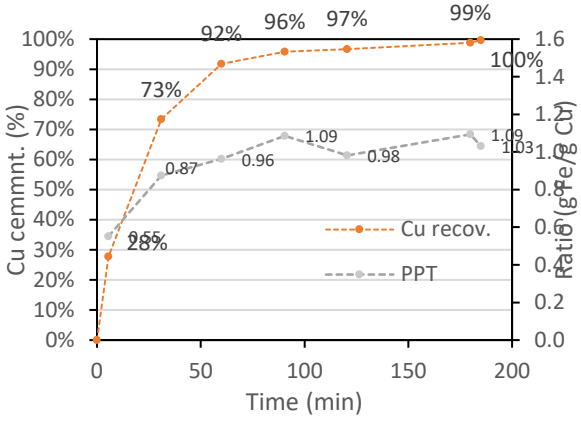

Figure 42 Cu recov. and PPT evolution of assay 92, pH 2.0, 60°C, 200 RPM, 20 kHz and Pcal=4.7±0.3W

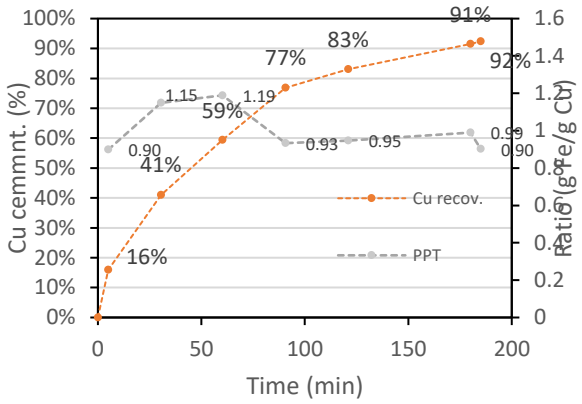

Figure 43 Cu recov. and PPT evolution of assay 93, pH 2.0, 60°C, 200 RPM, 40 kHz and Pcal=4.7±0.3W

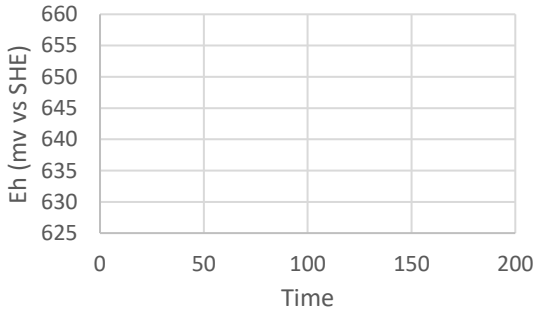

Assay 92 - Data non-available due to user error

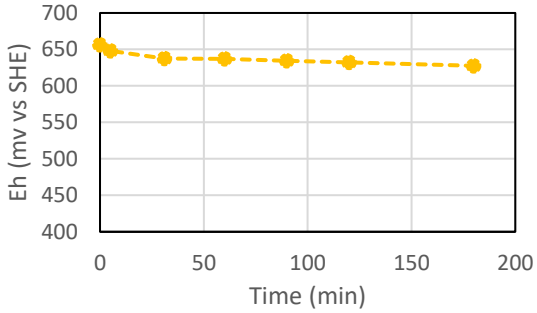

Figure 44 Eh evolution of assay 93

Table 10 Compilation of experimental results obtained with US intensification

	Reaction parameters		**Precipitant factor**	
Assay	Fe leaching	Cu recovery	Obtained	Theoretical
90 – Silent 500 rpm	55%	80	1.22	0.88
91 – 20 kHz 500 rpm	93%	96%	1.43	
92 – 20 kHz 200 rpm	98%	99%	1.1	
93 – 40 kHz 200 rpm	55 %	92%	0.99	

3.5.1 Influence of the cavitation effects

The best parameters found for silent copper recovery were in assay 22 using pH 2, 500 RPM, and 60ºC. However, in the two hours of the silent tests, maximum recovery, or plateau, wasn't reached for this assay. Therefore, those same parameters were used again, in a 5h experiment, assay 90. This time, a plateau was reached after 3 hours, at 83% recovery and a satisfying PPT of 1.07. This is the baseline for the sonicated assay.

The same conditions of assay 90 were applied, but with ultrasonic power being supplied, at 20 kHz, corresponding to a calorimetric input of 4.3 kW. What is observed is a remarkable increase in both the maximum recovery and the time to achieve it. After 1h30, the recovery peaked at 96%, with a PPT of 1.09. After this point, secondary reactions were happening, as the copper recovery remains the same, but iron continues to be consumed. To achieve the same recovery as in the silent assay, the sonicated one required only 30 minutes. Meaning the recovery speed was 6 times faster, while PPT was 10% lower.

Looking at the first 5 minutes, the sonicated reaction was already 2.6 times faster than the silent. And why this happens can theorized simply by looking at the reactor. In figure 45, taken at roughly 5 and 30 minutes into the silent experiment, the steel balls can be seen at the bottom, now brown in color, and slightly larger at 30 minutes, due to a thicker copper coating.

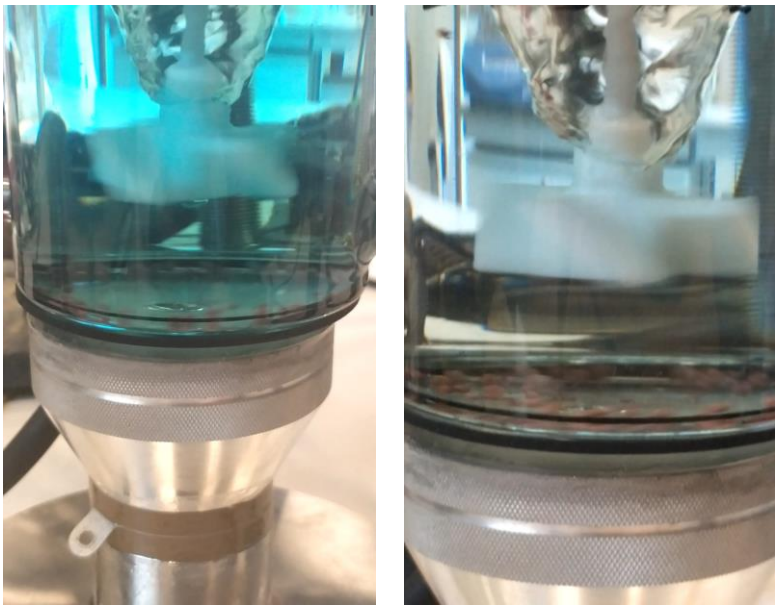

Figure 45 Photos of silent assay 90, taken 5 and 30 minutes into the reaction (left and right image, respectively). Beads can be seen at the bottom of the vessel, brownish in color.

From the Ea calculations made previously it's assumed that the reaction is controlled both from diffusion and chemical processes. And the reason why it is in part diffusion controlled is that the solid layer of copper

that deposits on the steel beads is an obstacle between the cupric ions in solution and the solid sacrificial iron, that is now surrounded by copper. However, looking at the reactor of the sonicated assay, in figure 46, taken at the same time intervals, the difference is clear. At 5 minutes the solution begins to be opaque. This is likely due to the cavitation effects of the ultrasonic energy.

Figure 46 Photos of US assay 91, taken 5 and 30 minutes into the reaction (left and right image, respectively). Copper particles make the solution opaque. On the right, crests and troughs of the modulated wave signal are seen

As seen in Pflieger's and Kiss's work previously, a frequency of 20 kHz was found to stimulate the most intense bubble collapse events, that generate very high pressures, (compared to higher frequencies). As they happen, the recently formed copper shell is damaged and comes off the steel beads. Additionally, in the table of the bead morphology, the shells of assay 22 (whose parameters are the same as in 90 and 91) are very rough and porous. Pflieger also stated that imperfections in the vessel and solid impurities in the liquid act as a nucleation spot for bubbles. As they sit in a solid surface, the bubbles grow asymmetrically and collapse causing jet streams. As copper deposits, it's broken off, exposing solid iron to the cupric ions which more easily diffuse into it. Time passes and the reactor becomes filled with suspended copper particles that make the solution opaque. So opaque that the peaks and throughs of the ultrasonic waves can be discerned in the liquid.

After completion, the solid residue left in the filtration filter formed a uniform film, seeming like paint (as can be seen again in table of bead morphology, although in the picture there, the residue is already dry and therefore flaky and broken). The stirrer, reactor walls, and the different tools used in the filtration, made of plastic and glass, were also coated in this film, which was very hard to remove due to its small size. This was unlike any other assay before.

It's hypothesized that the constant cavitation effects, which likely had, for the most part, nucleation points in the small copper particles surface, kept reducing their size until the micro or nano scale. How long was necessary to reduce them is uncertain. When taking the samples from the vessel and into the sample tubes, filters were used to prevent solid particles from possibly interfering with the chemical analysis. These filters were inspected, and the particles retained in them don't show significant differences in apparent size. This could indicate that the very thin powder might have been produced quickly. Further work should look at this possibility closer.

As seen before, the precipitant factor, or the amount of iron required to cement one gram of copper, was also lower in the sonicated assay. Although not a great amount (~10% lower PPT), the US made the iron usage more efficient, which again is likely due to it being directly exposed to the cupric ions.

Another theory stands on the degassing properties of the ultrasonic energy. It's been established from Shamsuddin and Habashi that the presence of oxygen in the copper cementation is correlated with unwanted reactions and products, and increased iron consumption. Equations (1.25) and (1.26) both have oxygen as a reactant and produce unwanted effects, like promoting the re-dissolution of cemented copper and promoting ferric iron production (Fe^{3+}). Degassing is a common process to remove dissolved gases in liquids, which is often done with ultrasonic energy. This is proposed as a justification for the decreased PPT of the sonicated assay when compared to the silent one in the conditions.

Looking at the titration data, the same conclusion can be reached. The sonicated assay produced more radicals and promoted the formation of ferric ions, which constituted 17% of total iron in solution after only 5 minutes, compared to the silent assay which had 14%. Shortly after, at the 30-minute measurement, Fe^{3+} of the sonicated sample had dropped to 12 % which remained constant until maximum recovery was achieved. After this point, Fe^{3+} increased again. If this process is to be implemented, care will need to be taken to prevent the reaction from reaching the recovery plateau and avoid unwanted iron consumption and byproduct production. The silent assay, in the same time frame, increased its Fe^{3+} concentration to 18% of total dissolved iron, which was then constant throughout the experience.

The lower Fe^{3+} concentration of the sonicated sample is associated to its degassing capabilities, which are probably greater than the "gasification" capabilities of the stirrer, which is constantly agitating the solution.

It can be concluded that for the specific conditions of assay 90 and 91, the applied ultrasounds don't increase ferric iron in the solution, despite the well-known effect that ultrasounds induce radical formation in water (Riesz & Berdahl, 1985).

Some authors (Rooze et al., 2011) noted a decrease in transducer reliability as it increased its temperature. In a heated assay which lasts 4 h of continuous sonification this could certainly be a problem. A powerful computer cooling fan was used to mitigate this effect. It appeared to work well, as the results seen throughout the sonicated experiments were reproducible, and the transducer was touched occasionally without a major difference in temperature being noticed. This is not reliable as a means to confirm its operating temperature, but as the recovery plateau occurred very quickly after 1h30, it's unlikely that there was any interference of temperature during this time. It is not advisable to touch the transducer bare hands as the risk of a mild electrical shock is high. Were the heating of transducer to be a problem, a pulsed sonication working mode would probably be used.

Another effect of the ultrasonic energy was on the Eh potential, which decreased significantly faster than the silent assay. This is possibly unrelated to the US themselves, as in the previous assays the pattern seems to indicate that higher initial copper recovery translates to steeper decline in Eh potential. Somewhat oddly, the RF assay showed the smallest decrease in Eh. Neither the mechanisms behind this decline neither its possible effects that take place between sample taking and chemical analysis were studied or analyzed. Both due to lack of time and due to lack of any real noticeable effects.

3.5.2 Influence of RPM

Having observed and discussed the influence of sonicating on the cementation reaction, one can strive to better optimize and understand the influencing parameters. It has been widely reported in the literature, including Shamsuddin's work that increased stirring, or agitation, is related to increased cementation rates, up to a maximum after which the liquid behavior and interaction with the air stops being helpful. To understand purpose of the high rotation speed of 500 RPM, another sonicated assay was performed, assay 92. Here, all conditions are similar to assay 91: Temperature, pH, ultrasonic frequency and calorimetric input, except for the rotation speed of the stirrer which was reduced to 200 RPM.

What is observed is an almost perfectly identical reproduction of the previously obtained results. Plateau was reached after 1h30min, having 96% of copper recovery , with a PPT of 1.09. These can be very compelling results that the sonicated reaction does not need nearly as much rotation speed as the silent ones. Referring to its influence on silent samples at 60°C, increased RPM resulted in an additional 8-40% of recovery. Now, when sonicated, this is not seen. The functions of the rotation speed, increasing the diffusion rate of the reactant into the iron, and increasing the diffusion rate of the cemented copper out of the boundary

region of the iron-solution, were probably completely replaced by the ultrasounds (until 200 RPM). The sonication had this effect due to the cavitation events and its consequences, which very effectively removed the copper shells. Then, the exposed iron was very easily put in contact with renewing cupric ions with the 200 RPM rotation.

In fact, extraordinarily, the lower rotation speed had a favorable outcome on the reactions taking place. In the 500 RPM assay the PPT was last recorded at 1.43 after 4 hours. No conclusion can be made about if this was a plateau or not, due to the previously discussed error of the 3h measurement, so the worst-case scenario is assumed and the reaction's PPT plateaued. In the 200 RPM assay, PPT clearly maxed at 1.09 after 3 hours. This reinforces the idea that the lower rotation speed is introducing and dissolving less oxygen in the solution. This directly impacts the amount of unwanted side reactions that take place and consume both iron and copper unnecessarily (for the full explanation of this process please refer to equations 4 through 6 and to the previous subchapter "Influence of the cavitation effects").

No discussion can be had about the effects on the redox potential due to laboratory malpractice which resulted in the non-measurement of the samples. Nonetheless, a strong argument can be made about the benefits of utilizing lower rotations speeds. Both for reduction in the energy required by the stirring equipment both for reduction of the precipitant metal utilization, although the latter is true only if the reaction continues beyond copper recovery plateauing, which hypothetically could be used to alter the physical properties of the copper particles.

3.5.3 Influence of resonance frequency

Up to this point only 20 kHz frequencies were used to produce ultrasounds. The voltage applied varied throughout the experiment, but the goal was always to maintain a stable power input (measured during the assays as forward power minus reverse power) of 14 Watts which at 20 kHz correspond to a calorimetric power input of around 4.7 W. To achieve these values voltages had to be in the range of 1850 to 1950 mV.

When the RF region of the setup was known to be around 41.3 kHz, this was chosen as the next frequency to be used. A preliminary test was made with water to test this RF, but true resonance was achieved at 40.5 kHz. This difference from the value obtained in the impedance measurements of KU Leuven is due to the differences in setup configuration. Having 250 ml of water changed slightly the behavior of the setup to ultrasounds. Very quickly it was understood that at resonance, 1900 mV is too high of a voltage. The power readings of the power supply were erratic and unstable, and the power input seemed to be very high, above 40 W (although it's difficult to be sure due to the quickly changing readings). Only by reducing the voltage to 1000 mV was the power input stable at 9-11 W (which at 41 kHZ is equivalent to 4.7-5.7 W of

calorimetric power). As assay 92 demonstrated that the decreased RPM had virtually no impact on the recovery rate and some benefits to the PPT, 200 RPM was also chosen for assay 93.

Throughout the experiment, extra care was taken to keep adjusting the voltage, which had to be slightly increased as time passed. Likely, the change in viscosity altered the RF and the efficiency of the ultrasounds. The suspended particles would have probably absorbed some of the energy to further break apart and reduce in size or they could have made the transmission of the waves more difficult. This would have caused the transducer to require more voltage to deliver the same power to the system.

The results of the assay 93 (at the RF and 200 RPM) weren't as good as the previously sonicated ones. In a plot of ln (1-X) against time, seen below, this is apparent. Recovery rate was much slower than assays 92 and 93. Until the 90 minutes mark, it wasn't better than the silent assay at 500 RPM.

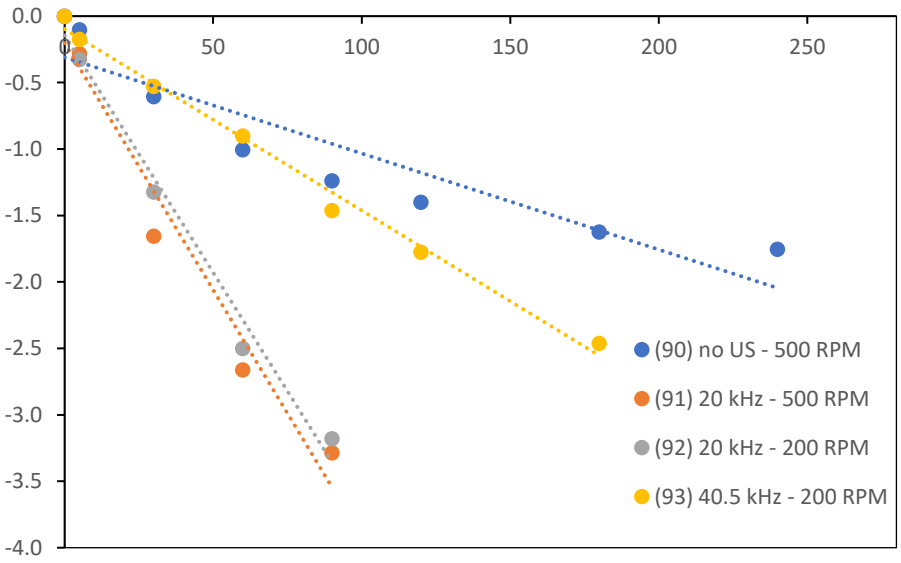

Figure 47 Recovery rates plotted as ln(1-X), with X being recovered fraction. Steeper slope means faster cementation.

This can be interpreted in a few ways:

- Because assay 93 was performed at a lower mechanical agitation than the silent assay, and yet results were similar for the first 1h – 1h30, and knowing from the previous discussion that, in silent conditions, increased RPM was correlated to increased recovery, in assay 93 the ultrasounds replaced the increased agitation which assay 90 had. After that initial time, however, the sonicated sample did achieve better results. After the same 3h time had elapsed, the sonicated one reached 91% recovery over the 80% of the silent.

- The higher frequency of 40.5 kHz might be less suitable to enhance the cementation reaction of copper on iron. The influence of higher frequency on reducing the size of bubbles and therefore reducing the intensity of the cavitation events, as well as favoring stable cavitation has been confirmed previously. This is unlikely to be the major cause as the frequency change was too narrow to influence copper recovery so greatly.
- The calorimetric study was performed for the frequencies of around 20, 40, and 60 kHz. But in none of the frequencies did the equipment behave as it did when RF was achieved in assay 93. Likely, resonance wasn't reached during the calorimetric study. If that is the case, the data obtained is likely unfit, or unrepresentative of the heat power transmittance to the reactor during resonance events. It would mean that perhaps not enough power was being given to the transducer.

Despite the relative bad results of assay 93, interesting remarks can be made. Below, on the right, is a picture of the clump that formed shortly after the reaction started. The cemented copper is acting as a glue that holds all the beads together. This was observed only in low RPM assays, such as in 92 (left) 5 minutes after reaction start, but in assay 93 this effect was the most pronounced.

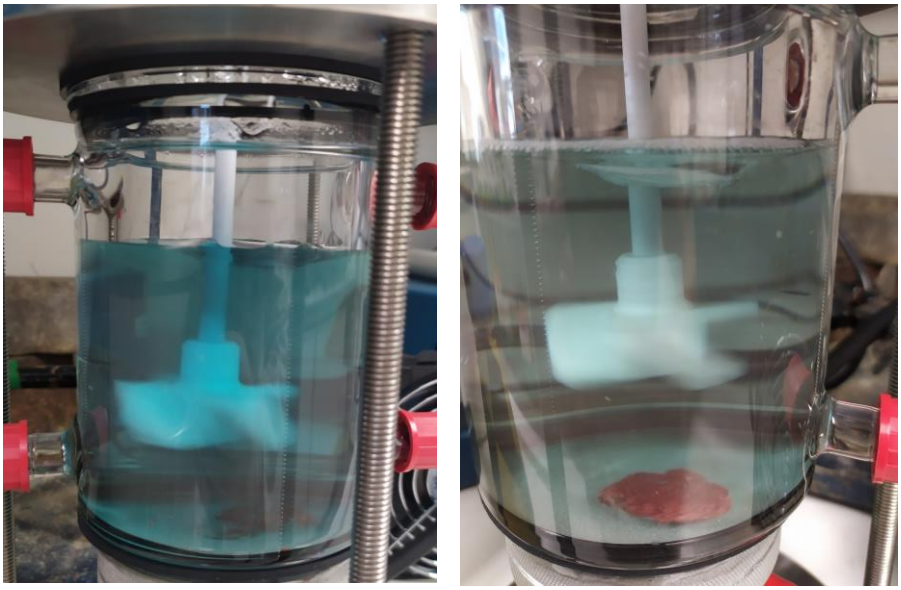

Figure 48 Agglomeration of the beads, cemented together, seen in assay 92 (left) and 93 (right).

The major difference between these examples is that only 6 minutes after the left picture was taken (11 minutes into the experiment), a sudden reaction took place that displaced all the cemented copper and dispersed it in the liquid, making it opaque. This can very clearly be seen in fig. 49. The amount of cementation is not drastically different between the two photos, as only six minutes separate them. It just came loose from the steel beads. A critical mass of copper was deposited, after which the cavitation events

managed to interfere with the cementation. As the copper layer grows thicker and the iron beads are dissolved, gaps form in the copper matrix, which give it its porous aspect. In these conditions bubbles growth is asymmetrical, which as discussed previously is greatly beneficial to produce jet streaming events. These are destructive to the copper shells and might have resulted in the "snowball" effect that totally disrupted the copper matrix.

Figure 49 Assay 92, little over 11 minutes into the reaction

Assay 93 on the other hand, did not manage to have the same disruptive effect. The beads remained clumped during the 3 h. If a non-resonating sonication had more intense results, it's likely because at resonance, the energy was absorbed or dispersed less efficiently. Indeed, looking at the PPT evolution of assay 93, the first hour of reaction showed PPT over 20% that of the non-resonance sonication. Parasitic reactions were initially enhanced during resonance. Although this effect stopped 1h30 into the reaction, when PPT decreased to lower values.

3.5.4 Energetic consumption

Table 11 Energetic consumption of the equipment used for copper cementation, silent and sonicated

Equipment	Nominal Voltage (V)	Max power rating (W)	Power consumed (W)	Energetic consumption (Wh)		
Time	-	-	-	2h	3h	4h
Transducer	1-1.9	120	14	28	42	56
Stirrer	230	176	176	352	528	704

Cooler	230	23	23	46	69	92
Wave gen.	230	30	10	20	30	40
Heater	230	2000	2000	814*	-	-

The stirrer operated between 200 and 500 RPM, which corresponds to 10 to 25% of the maximum rated output of 2000 RPM, respectively. This means that throughout the experiments, the maximum power of the equipment wasn't being consumed. However, estimating how this translates to power consumed is not linear; 25% of max load/RPM does not correspond to 25% of power consumption. Because calculating power consumption requires knowledge of the torque exerted by the paddles of the stirrer on the liquid, and that is not possible to do accurately in conditions of this work, the worst-case scenario was assumed, where the stirrer consumed the full 176 watts during the totality of assays.

The wave generator is rated to maximum 30 watts under peak load, however, upon inspection of the user manual, the standard use of a sinusoidal wave input, at 100 kHz and 10V consumes 10 watts. The true value is undoubtably lower than this, due to the lower voltages and frequencies used, but it sets the worst-case scenario, which will be also used for further calculations.

The temperature control, heater, was used in both types of assays. However, as it is not a variable in the silent vs sonicated assays and as it requires knowledge of complex variables to accurately measure power dissipation of the heater/water tank system to the environment, the temperature control wasn't taken into consideration when comparing silent and sonicated experiments.

*It's acknowledged that, despite only taking 10 Wh to heat the mass of water used in the assays, the heating control required at least 20 l of water to function, catapulting the heating requirements to 814 Wh of energy, not accounting the significant heat losses to the environment throughout the duration of the assay. In an industrial setting, this problem of exaggerated power requirements for heating wouldn't be such a problem, as the efficiency and effectiveness of industrial heaters is much greater.

Expected energetic advantages of using US

The cooler used for the transducer, a computer fan, was turned on during the totality of the experiments to prevents efficiency/performance drops from the transducer. However, as explained in section 1.1.2, if a pulsed mode was used to generate the sonication, the transducer probably would not require active cooling. Its own thermal mass would be enough to dissipate the heat.

In a pulsed mode, the wave generator would, probably, not require as much energy as in steady state. However, the degree of beneficiation to power usage is unclear. Similarly, when using the stirrer in a

sonicated experiment, a lower RPM could be achieved while maintaining similar results. The degree of advantage is once again not clear.

It's clear that if ultrasounds make copper recovery faster, the equipment does not need to be used for as long as in silent tests, reducing their energetic consumption. Silent assay 90 reached 80% copper recovery after 180 minutes, whereas 91 sonicated reached the same recovery at 30 minutes.

Taking the previously described advantages it's possible to plot a range of energetic scenarios for the used setup, figure 50. Diagonal lines progress until the peak recovery of each scenario is reached, and horizontal ones represent energy consumption correspondent to 80% copper recovery. The silent assay required 540 Wh of energy while the US, in the worst-case scenario, required 125 Wh. Over 4 times less energetic consumption, in a very conservative scenario.

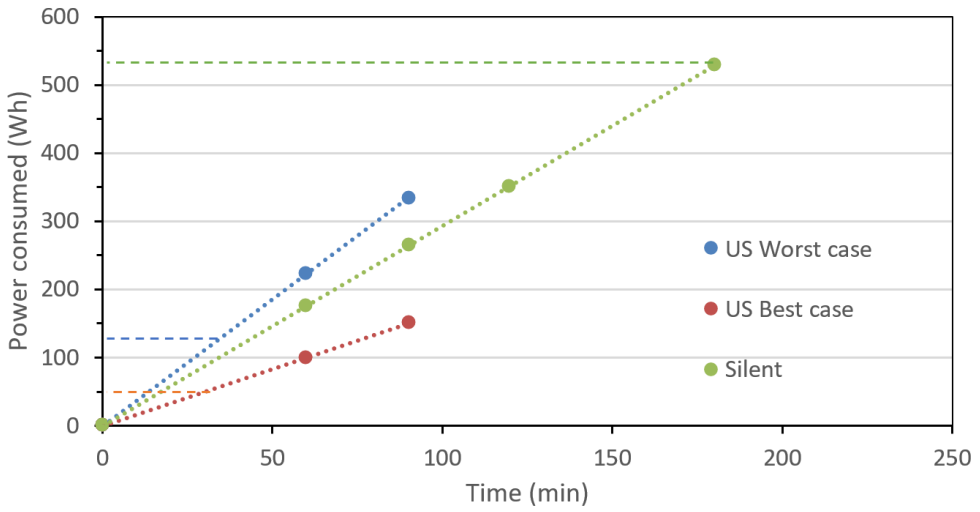

Figure 50 Energetic/power consumption estimates for silent (assay 90) and sonicated trials (assay 92).

The worst-case scenario assumes that neither the stirrer, wave generator, or transducer had any energy savings, compared to the silent assay, incurred by working at fewer RPM or at pulsed mode instead of continuous. The best case takes an arbitrary 50% cut in power consumption. This is not being proposed as a real-life behavior, it serves only to illustrate the possible range of power savings.

If this work is to be continued, further energetic insights will be had if electricity meters are placed in every equipment to quantify their consumption under different scenarios, and better understand the energetic dynamics at play.

3.6 Optical observation of the cemented copper and of the fine powder

Table 12 Optical characteristics of cemented copper. Left images are the filter aspect after filtration; right images show copper covered beads. (RPM, pH, kHz)

Temp	Assay 3	Assay 5	Assay 8	Assay 10
40°C	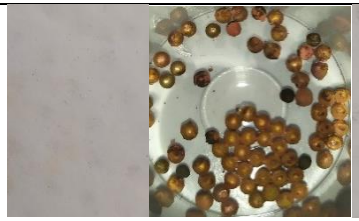	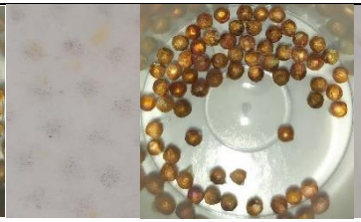		
	(200, 2.5, -)	(500, 2.5, -)	(200, 2.0, -)	(500, 2.0, -)
	Assay 13	**Assay 16**	**Assay 19**	**Assay 22**
60°C	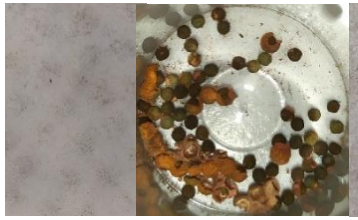		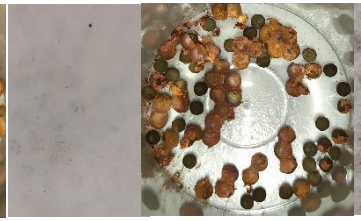	
	(200, 2.5, -)	(500, 2.5, -)	(200, 2.0, -)	(500 ,2.0, -)
	Assay 90	**Assay 91**	**Assay 92**	**Assay 93**
60 °C	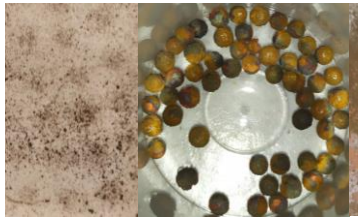		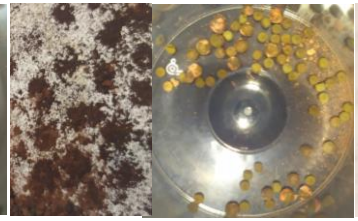	
	(500 ,2.0, -)	(500, 2.0, 20)	(200, 2.0, 20)	(200, 2.0, 40)

Chapter 4

4. EiT Chapter

Having participated on this master thesis, one realizes all the resources, both monetary, material, and social, required to technologically advance in science. But it's necessary, and the omnipresent word that is "transition" is the key to that necessity. Global CO_2 emissions are not close to peaking (as some of the most populous regions in the world will industrialize themselves in the next 50 years), yet climate phenomena regularly reach new records worldwide. But how is it fair that countries such as China represented 30% of the 2020 share of CO_2 emissions worldwide, whereas the EU didn't emit more than 8%. This would seem unfair without looking at embedded emissions in trade. The EU imports most of its emissions from countries such as China and India, and the results is that both the EU and China had similar per capita CO_2 emissions, resulting from consumption, at 7.7 and 6.6 tons per capita in 2019, respectively. This debunks the idea that some Asiatic nations are somehow much worse for the environment than the EU counterparts (Ritchie et al., 2020, p. 2).

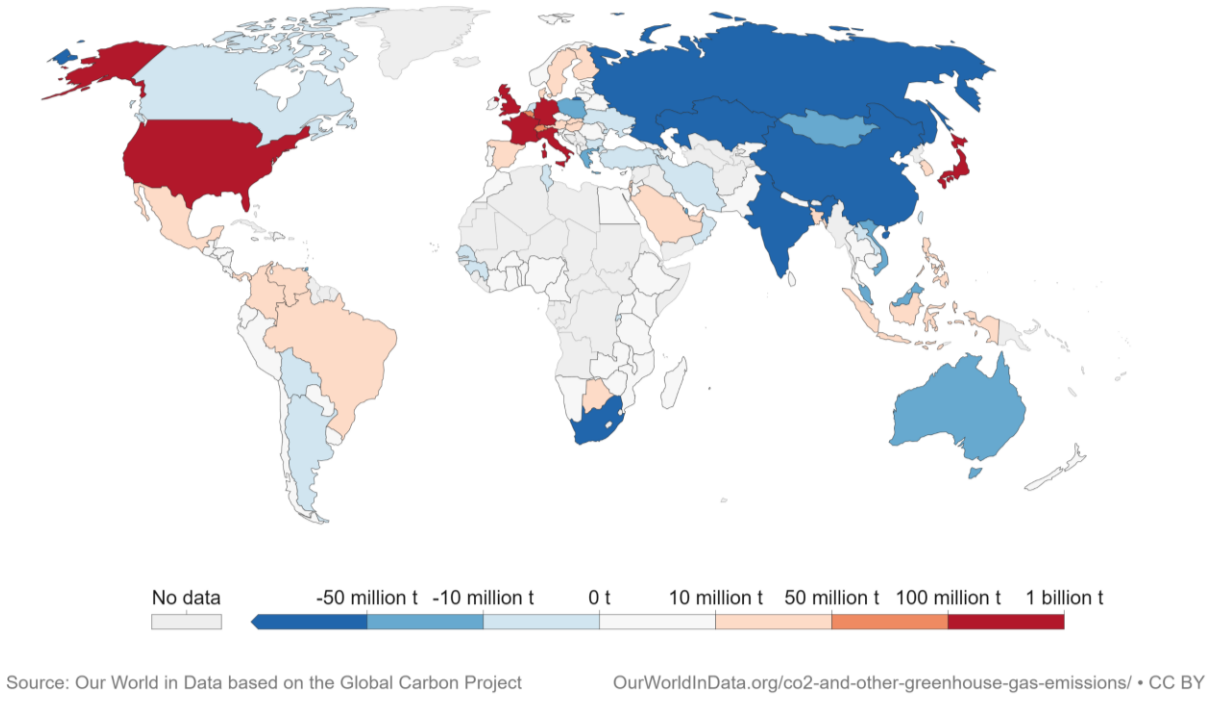

Figure 51 CO2 emissions embedded in global trade in 2019. Positive values (red) represent net importers of CO2, and negative values (blue) represent exporters (Ritchie et al., 2020, p. 2).

Having assessed the guilt, the problem must be fixed. And that's what this organization wants to achieve. The EIT RawMaterials' goal, is one based on improving the sustainability and viability of the European

based raw materials market, which at the moment is almost completely reliant on the importation of raw materials. So, the future relies on advancements made in exploration, mining, processing, recycling, substitution, and in the circular economy.

Within these categories, this work falls into the processing and recycling technical aspects of the EIT mission. The materials necessary to realize this work comprise concentrated sulfuric acid, copper sulfate, deionized water, energy, and the equipment. It has been assumed that sonication contributes to a decrease in energy requirements, and an increase in process and resource (iron and copper sulfate) efficiency, while increasing the equipment necessary. The remaining resources are unchanged between silent and sonicated assays, as far as this work was able to clarify.

In an industrial wastewater plant this would mean lower energy consumption and therefore CO_2 consumption, together with faster processing, which might reduce the scale of the plant, simplifying it and reducing its costs. However, the US EPA ranks the safety limit concentration of copper at 1.0 mg/l and of iron at 0.3 mg/l. By using the method in this work, the cementation of the copper would incur in the dissolution of 0.88 to 1.09 g/l of iron depending on the amount of copper which needs to be removed. In case the water stream in question is already at the maximum allowed iron, then other precipitant metals should be used, such as zinc (US EPA, 2015).

When recycling some alloys, such as steel, the PLS obtained are often too contaminated with impurities that reduce overall efficiency of the process and sometimes decrease the mechanical properties, which is an effect of copper as a contaminant. Manually sorting waste before it's leached could help, but many times, especially with wiring, the copper is embedded and hard to access. Leaching all the metal is not an option, but selectively leaching the copper followed by cementation a process intensified by ultrasounds, significant amounts of copper contaminant could be quickly removed.

With current needs, it's possible to divert the EoL (End-of-Life) copper contaminated steel (which has 0.1 to 0.4% copper weight per ton) to be recycled into products with higher tolerance, which under ideal management is feasible until 2050, as discussed by (Daehn et al., 2017) and can be seen in fig. 52 on the right by the same author. On the left, current techniques used to reduce copper concentration and their relative cost is shown. The more thoroughly the copper needs to be removed from steel before or during recycling, the highest it's energy consumption and cost. By possibly improving this process, sonicated copper cementation undoubtably contributes to the progression of a circular economy (CE). This expression referring to "an economic system that replaces the 'end-of-life' concept with reducing, (…), recycling, and recovering materials in production (…) and processes. (…) With the aim to accomplish sustainable

development, (…) environmental quality, economic prosperity, and social equity. (…) It is enabled by novel business models and responsible consumers." as described by (Kirchherr et al., 2017).

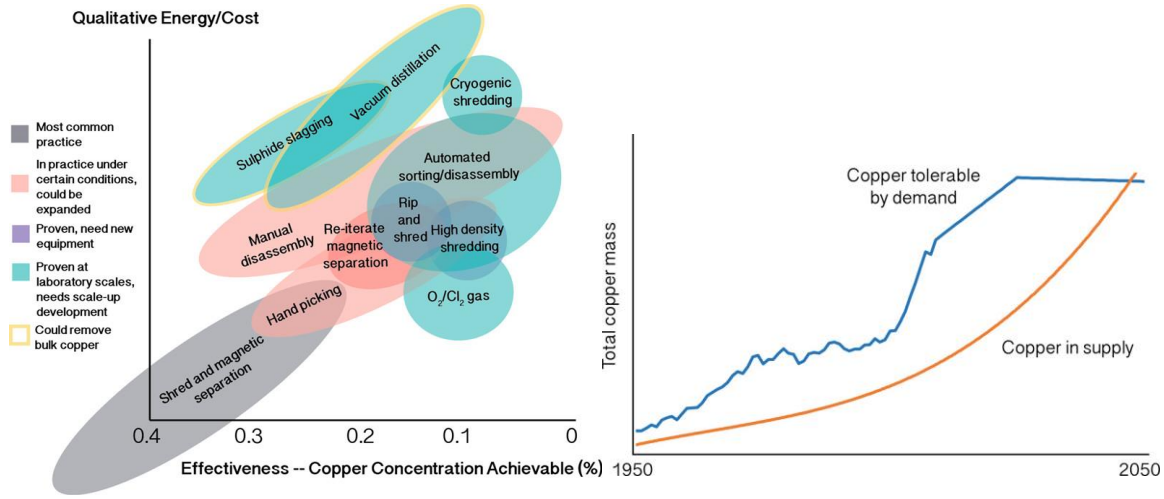

Figure 52 Left, cost/benefit plot for copper removal techniques; Right, cumulative copper which "sequestrated" within the steel supply chain, in line blue. In orange is the copper which needs to be removed from the same supply chain. (Daehn et al., 2017)

Despite not being confirmed as feasible in this work, the possible production of copper nanoparticles (NPs) is in line with EITs objectives and a CE. Namely due to their relative ease of synthesis and catalytic properties in: Organic transformations, which often replace standard processes by green ones; in electrocatalysis; in photocatalysis for hydrogen generation from water, for self-cleaning, and CO_2 reduction; and in gas-phase catalysis, where they have taken the role of replacing solvents. All these NP's applications and some more can be fully understood in the work by (Gawande et al., 2016). One other reason cited for why specifically copper NPs are so alluring, is copper's availability.

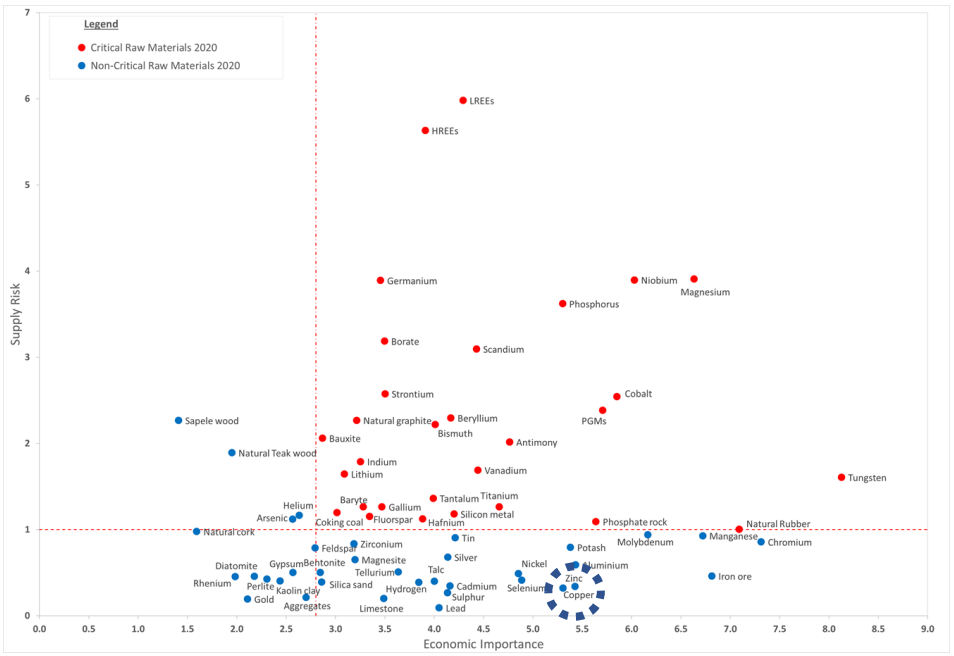

Figure 53 CRM assessment map. Materials above and to the right of the red dotted line are considered critical. Copper is highlighted, and it's not a CRM (European Commission, 2020).

In fact, despite having an economic importance more significant than 23 out of the 30 critical raw materials (CRMs) assessed in 2019 (fig. 53), it is also one of the elements with the smallest supply risk (*European Commission*, 2020). Similar can be said about iron ore. Despite contributing for process and raw material efficiency, this work does not greatly impact raw material availability, and especially not critical raw material availability. Similarly, no CRMs were used as principal raw materials in this work. Chromium was used for titration, and despite not being a CRM, it's on the verge of becoming one, especially due to its year-on-year increase in economic importance seen in the European Commission's report. The omnipresence of several CRMs in the electronics industry means that the heater, cooler, stirrer, wave generator, and power supply are all dependent on those them, without which no work would have been possible.

4.1 Life cycle analysis – Environmental benefits of sonication in cementation

To completely assess the environmental impacts of copper cementation and how they change by using ultrasonic energy, openLCA 1.10.3 was used. The Ecoinvent 3.6 database and the openLCA LCIA methods version 2.05 were used for the flows and processes information and for the impact assessment methods, respectively. These two databases are precisely that, libraries where a lot of information is stored. As this analysis proceeds, specific "books" of the library will be chosen, according to their relevance to this specific

topic and to the comprehensiveness of their information. Ecoinvent is one of the most robust and complete databases used in the industry. The construction of the silent and sonicated process can be seen in annex A.

A product system was created for both scenarios using the impact assessment "book" IPCC 2013, cost calculation was also performed. These systems were compared using CML-IA baseline. As the focus of this work is not to create an in depth LCA study, only 5 indicators were used: Acidification; Eutrophication; Global warming (GWP100a), where the '100a' refers to its time scope of 100 years since the emission of the pollutant; Human toxicity; and Ozone layer depletion (ODP). These categories were the most relevant to the Belgian environmental context. Their units and values can be found in the below.

Indicator	Silent	Sonicated	Unit
Acidification	3.25480e-1	2.87917e-1	kg SO2 eq
Eutrophication	1.35474e-1	1.18762e-1	kg PO4--- eq
Global warming (GWP100a)	2.73932e+1	7.18844e+0	kg CO2 eq
Human toxicity	3.90509e+2	3.78363e+2	kg 1,4-DB eq
Ozone layer depletion (ODP)	1.22912e-5	1.89980e-6	kg CFC-11 eq

Figure 54 Calculated values for impact indicators of silent and US cementation of 1 kg of copper at 80% efficiency

What is clearly seen is that on all categories the silent test is a better choice, especially in terms of global warming and ozone layer depletion. For every kg of cemented copper, 27.4 kg of CO_2 eq. are released with the silent setup, whereas only 7.2 kg of CO_2 eq. are released in the sonicated one.

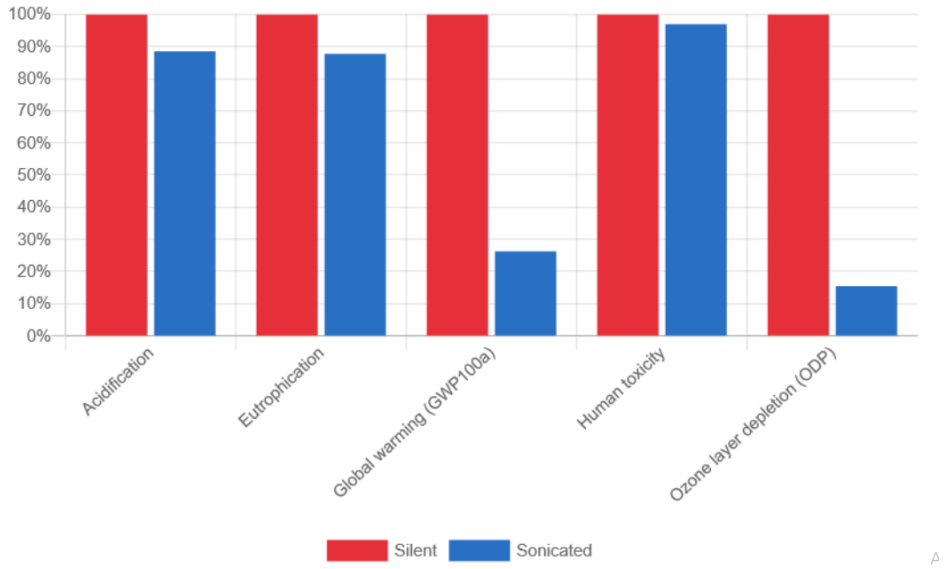

Figure 55 Relative comparison between the previously obtained results for the different eco indicators.

4.4.1 Structure of sonicated assay emissions

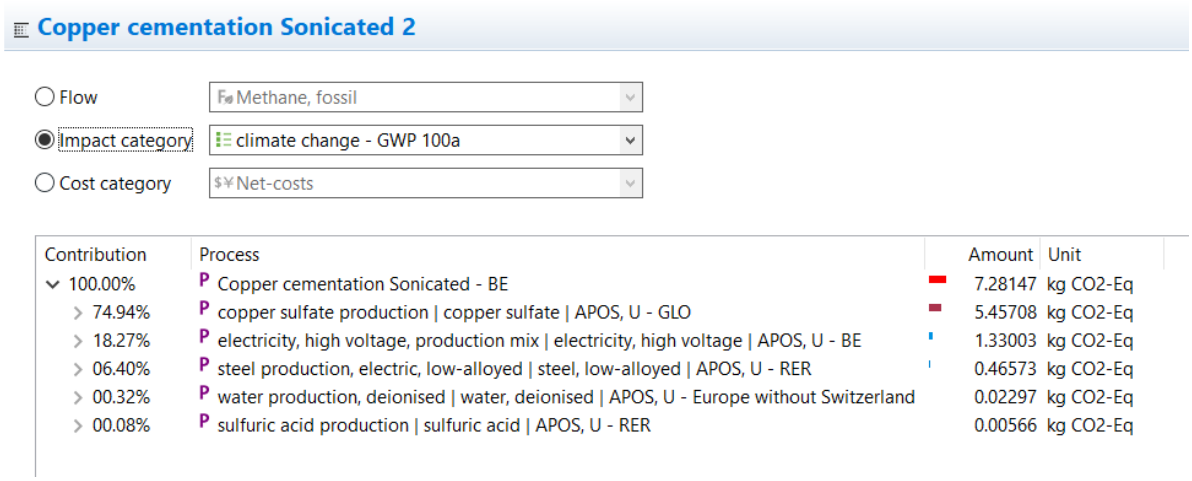

Figure 56 Relative contribution of the sonicated process components on the GWP

In the sonicated setup, the processes which contribute the most for the 7.2 kg of emissions are the electrical consumption, at 18.3 % and the copper sulfate production at 74.9 % (a detailed list and Sankey diagram can be seen in annex B. Furthermore, not accounting for equipment, nor the technical analysis and characterizations, nor for the steel balls, 322€ / kg of cemented copper were spent in the sonicated trials.

4.4.1 Structure of silent assay emissions

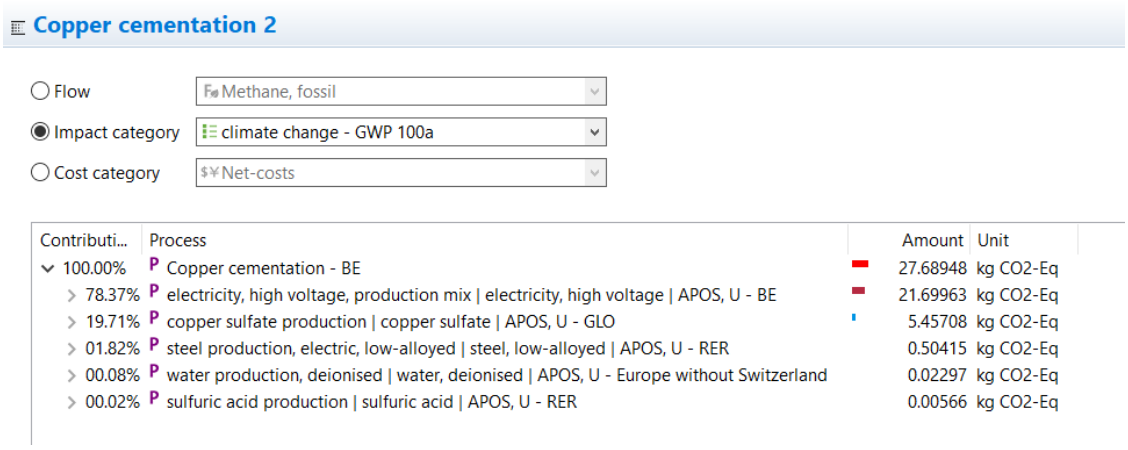

Figure 57 Relative contribution of the silent process components on the GWP

In the silent trials, electricity accounted for 78% of CO_2 eq. emissions. More detailed information and the Sankey diagram can be found in annex C. In the same conditions as previously, 416€ / kg of cemented copper were spent in the silent trials.

This simplified LCA study reveals that both in cost and in environmental impacts, the lab scale sonication of a copper cementing reaction is advantageous.

4.4.2 Limitations of the life cycle assessment

Using a software such as openLCA to assess all things within a process such as copper cementation is empowering. Like everything, attention and critical thinking must be employed. A LCA relies on previously gathered data that is generalized and overlaid on each life cycle. This probably works best on a large-scale approach, but results in big uncertainties at smaller scales.

Another issue is that with different databases and especially with different methods, different results are obtained. Knowing which method is more adequate is not always obvious, especially with small scale and niche processes, such as the case in this work. A consequence of this is the uncertainty of the data, which clearly exists, but is hard to quantify or to assimilate.

The impacts of building the different equipment, maintaining them, adjusting of their predicted lifespans, and for losses in efficiency, as well as obtaining company-specific data for each of the reactants bought and used should all be considered for a more realistic LCA. Of course, this would add extra complexity and costs to produce the LCA, so this hyper-realistic study is only feasible, probably, on a large industrial scale. For the comparison purposes and scope of this work, the results are deemed acceptable.

4.2 Techno-economic analysis

This analysis consists in identifying and discussing the economic advantages and tradeoffs of employing variations within a reference technology, using ultrasounds to enhance cementation in this case. The reference is the silent cementation as described in the methodology in this work.

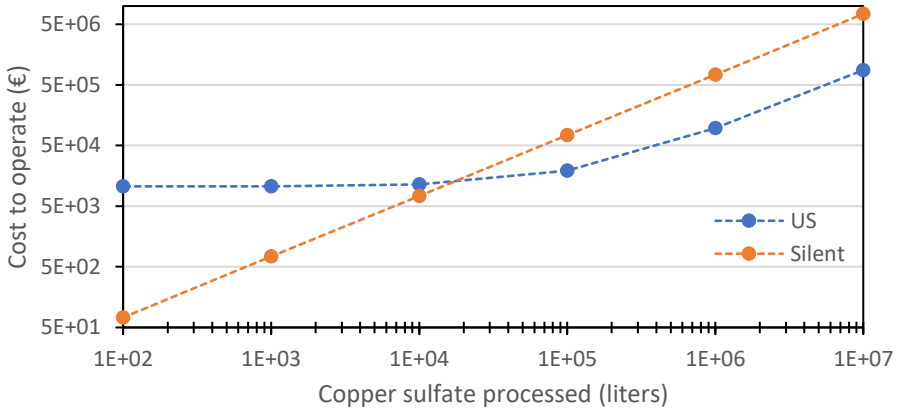

Figure 58 Predicted cost of operation in a laboratory setting at different handling scales

Having made a prediction on the energetic consumption of this technology and its reference, and knowing the material costs, it's possible to predict how do costs increase at lab scale. The equipment and materials in common between the reference and the sonicated trials has not been considered, such as heater, stirrer, reactor, and all raw materials. Energy predictions, and therefore costs, were made for the parameters: 300-500 RPM, 60°C, pH 2, and $[Cu^{2+}] \approx 5.2$ g/l, while achieving 80% copper recovery. From the graph it's noticeable that the ultrasonic technology presents much higher additional costs, at 10500 €, for the transducer, power supply and wave generator. After roughly 1500 liters of copper solution having been processed, equivalent to 8kg of copper cemented, the application of ultrasounds becomes economically more viable than the reference process. It should be noted that maintenance of the equipment and their estimated lifespan has not been considered. To process 1000 liters of solution it could take anywhere from 5 to 10 years. It's likely that within that time frame some or several equipment need to be fixed or replaced.

4.2.1 Conversion from lab to industrial scale – Considerations

The usage of ultrasounds warrants some safety measures to be taken. The human body absorbs US waves, and from reports, the apparent health effects resulting from exposure go from positive to very negative. When workers are exposed to those waves in high enough dosages, 21 kHz at a level of 110 dB for 3h a day for 10-15 days (Moyano et al., 2022), functional changes happen to the central nervous system, as well becoming irritated and having memory problems. When comparing audible sounds and ultrasounds, the former cause hearing damage above 120 dB, while the latter may cause damage starting at lower dBs (fig. 59, from Moyano et al., 2022.)

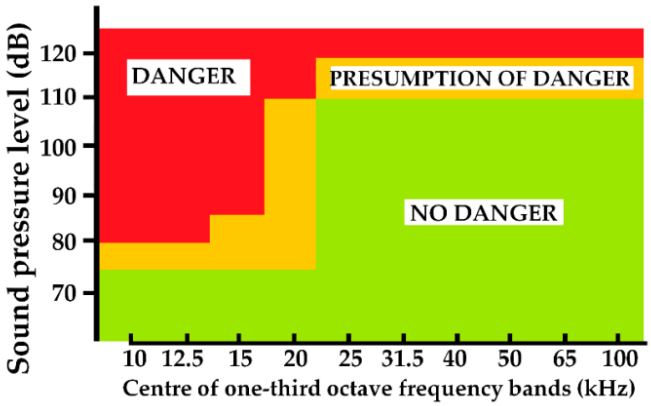

Figure 59 Dangers of US exposure of in terms of frequency and decibels (Moyano et al., 2022)

What this results in, is the need to use protection and prevention equipment, having smaller shifts and more workers, and even dedicated facilities with sound protection. These measures add costs and must be

considered for a future and complete techno-economic analysis, where they'd be considered a cost of ownership (CoO).

From the work done and the literature consulted, it's evident that US have not been widely studied in the field of electrochemical reactions. Significant research and money must be employed to develop the technology, as scalability is a limiting factor, but also to better assess feasibility. These fall in the research and development (R&D) category.

However, it's also common that costs of processing at laboratory scales are higher than the cost dynamics achieved at higher scales. This is due to the increased scale which reduces raw material costs, also due to equipment, which in industry becomes highly specific and efficient at specific tasks, as well as due to increased process optimization. At the laboratory, some examples of inefficiencies are:

- Precautions were not taken to reduce heat dissipation in the heater – vessel system
- The parameters used were not optimized to be maximally efficient. Improvements can likely be made regarding optimal agitation, not just regarding RPM but also stirrer shape and height, regarding temperature, pH, ultrasonic frequency and voltage
- Placement of the transducer on the vessel and type of sonification, either pulsated or continuous

4.3 Entrepreneurial prospects – Business plan and SWOT analysis

Product: The products would be ultrasonic related services. 1) Offering deep cleaning services would generate cash flow and make further transducer investments viable, 2) followed by implementations in residual water treatment plants or in tailings processing. High power (kW range) transducers are mostly built in China, so they would be manufactured there and imported. The transducer used in this work was not specially made to enhance electrochemical reactions, its main purpose was for ultrasonic deep cleaning, and yet, it worked remarkably well. So, for an initial market implementation, the struggles of developing working equipment are already overcome. With time this design would be adapted and optimized.

Market: The main costumers would be: The medical industry, as they have rigorous cleaning standards for surgical, medical, and dental equipment; The automotive and aerospace industry, due to complex engine parts which deteriorate in performance due to buildup of oils on the surface; and electronic manufacturing and repair industry, which can use this technology in the cleaning of PCBs. European mines and municipalities would be the late-stage costumers, whose waste streams need to be processed, specifically of copper contaminants, but this can be broadened to other contaminants after further studies.

Prospects: As the world population collectively increases its environmental awareness, environment friendly alternatives and technologies present great growing potential. Ultrasonic cleaning uses little or no

solvents and cleaning products when compared to traditional cleaning alternatives. From the results in this work, sonicated copper cementation also benefits the environment. The market of ultrasonic cleaning is already well established in some countries but not saturated worldwide.

Regulations: Some ultrasonic exposure limits have been setup by the International Non-Ionizing Radiation Committee in 1984 and by the Canadian government in 1991, that limit work exposure between 16 and 20 kHz to 75 dB. No further limitations have been found. Having all the above notions in mind, it's possible to perform a swot analysis to better understand the dynamics of an eventual business activity.

Table 13 Swot analysis of a simulated start-up focused on sonicated Cu cementation and US cleaning

S	W	O	T
Strengths	**Weaknesses**	**Opportunities**	**Threats**
● Early market for cement. intensification ● Existing technology ● Existing scientific and practical knowhow	● Expensive initial capital investment ● Difficult scale up ● Geographically disperse costumers	● Marketing of the ecological advantages ● Hiring US experts ● Reverse engineering of existing products	● Mature US cleaning market ● Niche cementation market susceptible to other intensification technologies

Chapter 5

5. Conclusion

This master thesis had the objective of characterizing a new ultrasonic setup and to study the possible ultrasonic intensification of the copper cementation reaction. The characterization was achieved successfully. Several characterization techniques were studied, and calorimetry was chosen as the most suitable and then performed. The initial protocol, that was shown to work in some literature, was inadequate for this setup. The source of inadequacy was found, and the protocol was adapted. Significantly more reproducible results were then obtained. Under the right circumstances and with the correct resources, I would have performed sonoluminescent characterization of the vessel. This might have facilitated the observation of differences between sonication at different frequencies, including RF. The possibility of observing a phenomenon as unusual and extraordinary as light emission from repeated bubble collapses is of great enthusiasm.

Regarding the setup, some parameters could be changed in a future work. The borosilicate glass layer between transducer and solution can probably be safely reduced in thickness. If this has significant influence in ultrasonic transmittance is to be seen. For a medium scale setup, the glass nature of the vessel and protective layer could pose to be a problem due to the required dimensions. Heating the solution to the desired 40 or 60°C sometimes took up to an hour, especially at 60°C. Finding a quicker heating alternative would facilitate future works. Despite this, the setup did not pose any problem and facilitated temperature readings, pH adjustments, and overall manipulation of the reaction. For these reactions it's well recommended for any future work. The type of transducer used, langevin, appears to be the best choice for this type of reaction. It indirectly sonicates the solution, as there is the borosilicate glass between, but this can be made thin and likely doesn't absorb a lot of energy. Additionally, the ultrasonic field generated is distributed in one vessel that sits right on top of the transducer, which is likely optimal when comparing to ultrasonic baths, in which multiple fields cross a significant mass of water and interact, positively or not, with each other. For contamination and costs, titanium horn transducer would have probably not been suitable either.

The best values for the copper cementation parameters were temperature of 60°C, pH of 2.00, and agitation of 500 RPM. These were not obtained through a sensitivity analysis, and so for future work or for a pilot scale implementation they should be further optimized with literature review and experimentation. The effects of agitation need to be explained by much more than rotations per minute, with characteristics such as volume and viscosity of solution, geometry of vessel and paddles, and depth of the paddles, which together form complex fluid dynamics. Silent cementation had an average activation energy ranging from

6 to 24 Kcal/mol, which is classified as an intermediate controlled process. However, this value varies during the reaction, and the Ea graphs show that an inversion in the slope corresponds to the point of maximum recovery.

The best value for the ultrasonic frequency appears to be around 20 kHz. Ideally, resonance should be obtained at this frequency, but the impedance analysis did not show this to be true. Modifications could be made to attempt to achieve RF at 20 kHz. The ultrasonic effects of cavitation, jet streaming, micro mixing, and degassing, likely contributed to the vastly superior maximum copper recovery of 96%, reduced time to achieve it at 1h30min, and reduced PPT at 1.02, compared to the best silent results at 83% after 4 h, with PPT of 1.07. Future work should cover the effects of sonication produced via pulsed mode to assess if similar results are found.

It became very apparent that after reaching maximum recovery, the system continued to use its resources to make unproductive reactions that consume already deposited copper, as well as solid iron and ferrous ions to produce ferric ones. So, it's very important that in a potential industrial application the maximum copper recovery is well defined to prevent those unproductive reactions from taking place. In a silent reaction, the factors that limit the main reaction are the lack of access to the solid iron due to the passivation layer, and when the ratio Cu^{2+}/Fe^{2+} is below the minimum. That minimum will depend on factors such as temperature, so it needs to be defined for every setup, although in theory this ratio is so small that the reaction should happen to completion. In a sonicated reaction, the passivation layer is destroyed, so it's the Cu^{2+}/Fe^{2+} ratio that's at least partially determining the limit.

Lastly, the sonicated reaction shows a great reduction in energy consumption. To achieve 80% recovery, the silent assay required 540 Wh, and the sonicated one required, in a very conservative scenario, 125 Wh. A continuation of this work should measure energy consumption to further cement these claims, but the ultrasonic enhancement shows very promising results regarding energy consumption. This translates to a significantly better carbon footprint and fewer costs associated to the reaction, which stand at 7.2 kg CO_2 and 322€ per kg of cemented copper respectively. The silent assay required 27.4 kg of CO_2 and 416 € / kg of cemented copper (the price does not account for equipment, technical analysis, or precipitant metal).

US intensified copper cementation can be used to improve wastewater purification (where copper is toxic), to recover copper from tailings (and obtain it as raw material), and to better recycle metals due to removal of copper (which is a contaminant), all the while reducing their energetic consumption and carbon footprint. These applications benefit raw materials recovery, recycling, and human and environmental health, areas which are now more important than ever.

Bibliography

Adibekyan, A., Kononogova, E., Hameury, J., Lauenstein, M., Monte, C., & Hollandt, J. (2021). Emissivity measurements on reflective insulation materials. *Tm - Technisches Messen*, *88*(10), 617–625. https://doi.org/10.1515/teme-2021-0049

Ammann, A. A. (2007). Inductively coupled plasma mass spectrometry (ICP MS): A versatile tool. *Journal of Mass Spectrometry*, *42*(4), 419–427. https://doi.org/10.1002/jms.1206

Awaad, I. M., Nosier, S. A., Hussein, M., Elnahrawy, M. S., Sedahmed, G. H., Abdel-Aziz, M. H., & El-Naggar, M. A. (2022). Copper Extraction from Dilute Solutions by Cementation in a Gas-Sparged Helical Coil Reactor. *JOM*, *74*(3), 963–970. https://doi.org/10.1007/s11837-021-05102-1

Capelo-Martínez, J.-L. (Ed.). (2009). *Ultrasound in chemistry: Analytical applications*. Wiley-VCH.

Castro, L. de, & Capote, F. P. (2007). Chapter 1 Introduction: Fundamentals of ultrasound and basis of its analytical uses. In *Techniques and Instrumentation in Analytical Chemistry* (Vol. 26, pp. 1–34). Elsevier. https://doi.org/10.1016/S0167-9244(07)80017-5

Chen, J., Lei, Y., Zhu, C., Sun, C., Xu, Q., Cheng, H., Zou, X., & Lu, X. (2022). Morphology and distribution of cemented product formed via cementation over Zn in zinc sulfate solution relevant to roast-leach-electrowin process. *Hydrometallurgy*, *210*, 105847. https://doi.org/10.1016/j.hydromet.2022.105847

Choi, J., & Son, Y. (2022). Quantification of sonochemical and sonophysical effects in a 20 kHz probe-type sonoreactor: Enhancing sonophysical effects in heterogeneous systems with milli-sized particles. *Ultrasonics Sonochemistry*, *82*, 105888. https://doi.org/10.1016/j.ultsonch.2021.105888

Critical materials for strategic technologies and sectors in the EU - a foresight study. (2020). European Commission. https://rmis.jrc.ec.europa.eu/uploads/CRMs_for_Strategic_Technologies_and_Sectors_in_the_EU_2020.pdf

Daehn, K. E., Cabrera Serrenho, A., & Allwood, J. M. (2017). How Will Copper Contamination Constrain Future Global Steel Recycling? *Environmental Science & Technology*, *51*(11), 6599–6606. https://doi.org/10.1021/acs.est.7b00997

Dong, Z., Delacour, C., Mc Carogher, K., Udepurkar, A. P., & Kuhn, S. (2020). Continuous Ultrasonic Reactors: Design, Mechanism and Application. *Materials*, *13*(2), 344. https://doi.org/10.3390/ma13020344

Fouad, O. A., & Abdel Basir, S. M. (2005). Cementation-induced recovery of self-assembled ultrafine copper powders from spent etching solutions of printed circuit boards. *Powder Technology*, *159*(3), 127–134. https://doi.org/10.1016/j.powtec.2005.08.001

Fragassa, C., & Ippoliti, M. (2016). *Failure mode effects and criticality analysis (fmeca) as a quality tool to plan improvements in ultrasonic mould cleaning systems*. 25. https://doi.org/10.18421/IJQR10.04-14

Gawande, M. B., Goswami, A., Felpin, F.-X., Asefa, T., Huang, X., Silva, R., Zou, X., Zboril, R., & Varma, R. S. (2016). Cu and Cu-Based Nanoparticles: Synthesis and Applications in Catalysis. *Chemical Reviews*, *116*(6), 3722–3811. https://doi.org/10.1021/acs.chemrev.5b00482

Habashi, F. (2006). Cementation of Copper—The End of an Era. *Metallurgy*, 4.

Hayes, P. (2021). *Metal Production and Recycling* (4th ed.). HAYES PUBLISHING CO.

Henglein, A. (1987). Sonochemistry: Historical developments and modern aspects. *Ultrasonics*, *25*(1), 6–16. https://doi.org/10.1016/0041-624X(87)90003-5

Kimura, T., Sakamoto, T., Leveque, J.-M., Sohmiya, H., Fujita, M., Ikeda, S., & Ando, T. (1996). Standardization of ultrasonic power for sonochemical reaction. *Ultrasonics Sonochemistry*, *3*(3), S157–S161. https://doi.org/10.1016/S1350-4177(96)00021-1

Kirchherr, J., Reike, D., & Hekkert, M. (2017). Conceptualizing the circular economy: An analysis of 114 definitions. *Resources, Conservation and Recycling*, *127*, 221–232. https://doi.org/10.1016/j.resconrec.2017.09.005

Kiss, A. A., Geertman, R., Wierschem, M., Skiborowski, M., Gielen, B., Jordens, J., John, J. J., & Van Gerven, T. (2018). Ultrasound-assisted emerging technologies for chemical processes: Ultrasound-assisted emerging technologies for chemical processes. *Journal of Chemical Technology & Biotechnology*, *93*(5), 1219–1227. https://doi.org/10.1002/jctb.5555

Margulis, I. M., & Margulis, M. A. (2005). *Measurement of acoustic power in studying cavitation processes*. *51*(6), 10.

Michaud, D. (2017, August 17). Copper Cementation System for Small Scale Mining Operations. *Metallurgist & Mineral Processing Engineer*. https://www.911metallurgist.com/copper-cementation-system

Mierzwa, J., Sun, Y.-C., & Yang, M.-H. (1997). Determination of Co and Ni in soils and river sediments by electrothermal atomic absorption spectrometry with slurry sampling. *Analytica Chimica Acta*, *355*(2–3), 277–282. https://doi.org/10.1016/S0003-2670(97)00483-2

Moreno, E., Acevedo, P., Fuentes, M., Sotomayor, A., Borroto, L., Villafuerte, M. E., & Leija, L. (2005). Design and Construction of a Bolt-Clamped Langevin Transducer. *2005 2nd International Conference on Electrical and Electronics Engineering*, 393–395. https://doi.org/10.1109/ICEEE.2005.1529652

Moyano, D. B., Paraiso, D. A., & González-Lezcano, R. A. (2022). Possible Effects on Health of Ultrasound Exposure, Risk Factors in the Work Environment and Occupational Safety Review. *Healthcare*, *10*(3), 423. https://doi.org/10.3390/healthcare10030423

Mukaka, M. M. (2012). *Statistics Corner: A guide to appropriate use of Correlation coefficient in medical research*. 3.

Ono, K. (2020). A Comprehensive Report on Ultrasonic Attenuation of Engineering Materials, Including Metals, Ceramics, Polymers, Fiber-Reinforced Composites, Wood, and Rocks. *Applied Sciences*, *10*(7), 2230. https://doi.org/10.3390/app10072230

Perry, S. C., Gateman, S. M., Stephens, L. I., Lacasse, R., Schulz, R., & Mauzeroll, J. (2019). Pourbaix Diagrams as a Simple Route to First Principles Corrosion Simulation. *Journal of The Electrochemical Society*, *166*(11), C3186–C3192. https://doi.org/10.1149/2.0111911jes

Pflieger, R., Nikitenko, S. I., Cairós, C., & Mettin, R. (2019). *Characterization of Cavitation Bubbles and Sonoluminescence*. Springer International Publishing. https://doi.org/10.1007/978-3-030-11717-7

Rajamma, D. B., Anandan, S., Yusof, N. S. M., Pollet, B. G., & Ashokkumar, M. (2021). Sonochemical dosimetry: A comparative study of Weissler, Fricke and terephthalic acid methods. *Ultrasonics Sonochemistry*, *72*, 105413. https://doi.org/10.1016/j.ultsonch.2020.105413

Ren, M., & Jacobsen, F. (1993). A method of measuring the dynamic flow resistance and reactance of porous materials. *Applied Acoustics*, *39*(4), 265–276. https://doi.org/10.1016/0003-682X(93)90010-4

Riesz, P., & Berdahl, D. (1985). Free Radical Generation by Ultrasound in Aqueous and Nonaqueous Solutions. *Environmental Health Perspectives*, 20.

Ritchie, H., Roser, M., & Rosado, P. (2020). CO_2 and Greenhouse Gas Emissions. *Our World in Data*. https://ourworldindata.org/co2-emissions

Rochebrochard d'Auzay, S. de L., Blais, J.-F., & Naffrechoux, E. (2010). Comparison of characterization methods in high frequency sonochemical reactors of differing configurations. *Ultrasonics Sonochemistry*, *17*(3), 547–554. https://doi.org/10.1016/j.ultsonch.2009.10.024

Rooze, J., Rebrov, E. V., Schouten, J. C., & Keurentjes, J. T. F. (2011). Effect of resonance frequency, power input, and saturation gas type on the oxidation efficiency of an ultrasound horn. *Ultrasonics Sonochemistry*, *18*(1), 209–215. https://doi.org/10.1016/j.ultsonch.2010.05.007

Ruiz-Jiménez, J., & Luque de Castro, M. D. (2003). Flow injection manifolds for liquid–liquid extraction without phase separation assisted by ultrasound. *Analytica Chimica Acta*, *489*(1), 1–11. https://doi.org/10.1016/S0003-2670(03)00715-3

Santos, H., & Capelo, J. (2007). Trends in ultrasonic-based equipment for analytical sample treatment. *Talanta*, *73*(5), 795–802. https://doi.org/10.1016/j.talanta.2007.05.039

Shamsuddin, M. (2016). *Physical Chemistry of Metallurgical Processes: Shamsuddin/Physical Chemistry of Metallurgical Processes*. John Wiley & Sons, Inc. https://doi.org/10.1002/9781119078326

Shishkin, A., Mironovs, V., Vu, H., Novak, P., Baronins, J., Polyakov, A., & Ozolins, J. (2018). Cavitation-Dispersion Method for Copper Cementation from Wastewater by Iron Powder. *Metals*, *8*(11), 920. https://doi.org/10.3390/met8110920

Taylor, A. A., Tsuji, J. S., Garry, M. R., McArdle, M. E., Goodfellow, W. L., Adams, W. J., & Menzie, C. A. (2020). Critical Review of Exposure and Effects: Implications for Setting Regulatory Health Criteria for Ingested Copper. *Environmental Management*, *65*(1), 131–159. https://doi.org/10.1007/s00267-019-01234-y

US EPA, O. (2015, September 3). *Drinking Water Regulations and Contaminants* [Collections and Lists]. https://www.epa.gov/sdwa/drinking-water-regulations-and-contaminants

Yagi, S. (2011). Potential-pH Diagrams for Oxidation-State Control of Nanoparticles Synthesized via Chemical Reduction. In *Thermodynamics—Physical Chemistry of Aqueous Systems*. IntechOpen. https://doi.org/10.5772/21548

Annexes

Annex A

Inputs/Outputs: Copper cementation

Inputs

Flow	Category	Amount	Unit	Costs/Reven...	Provider
copper sulfate	201:Manufacture of basic ...	1.25000	kg	187.50000 G...	copper sulfate production | copper sulfate | APOS, U - GLO
electricity, high voltage	351:Electric power genera...	134.60000	kWh	42.40000 EUR	electricity, high voltage, production mix | electricity, high voltage | APOS, U - BE
steel, low-alloyed	241:Manufacture of basic ...	1.05000	kg		steel production, electric, low-alloyed | steel, low-alloyed | APOS, U - RER
sulfuric acid	242:Manufacture of basic ...	0.06541	kg	1.71000 EUR	sulfuric acid production | sulfuric acid | APOS, U - RER
water, deionised	360:Water collection, treat...	63.48000	kg		water production, deionised | water, deionised | APOS, U - Europe without Switzerla...

Outputs

Flow	Category	Amount	Unit	Costs/Reven...	Uncertainty	Avoided pro...	Provider	Data quality...	Description
Copper cementation		**1.00000**	**kg**		**none**				

Inputs/Outputs: Copper cementation Sonicated

Inputs

Flow	Category	Amount	Unit	Costs/Revenu...	Provider
copper sulfate	201:Manufacture of basic ch...	1.25000	kg	187.50000 GBP	copper sulfate production | copper sulfate | APOS, U - GLO
electricity, high voltage	351:Electric power generatio...	8.25000	kWh	2.60000 EUR	electricity, high voltage, production mix | electricity, high voltage | APOS, U - BE
steel, low-alloyed	241:Manufacture of basic iro...	0.97000	kg		steel production, electric, low-alloyed | steel, low-alloyed | APOS, U - RER
sulfuric acid	242:Manufacture of basic pre...	0.06541	kg	1.71000 EUR	sulfuric acid production | sulfuric acid | APOS, U - RER
water, deionised	360:Water collection, treatm...	63.48000	kg		water production, deionised | water, deionised | APOS, U - Europe without Switzerland

Outputs

Flow	Category	Amount	Unit	Costs/Reven...	Uncertainty	Avoided pro...	Provider	Data quality...	Description
Copper cementation		**1.00000**	**kg**		**none**				

Annex B

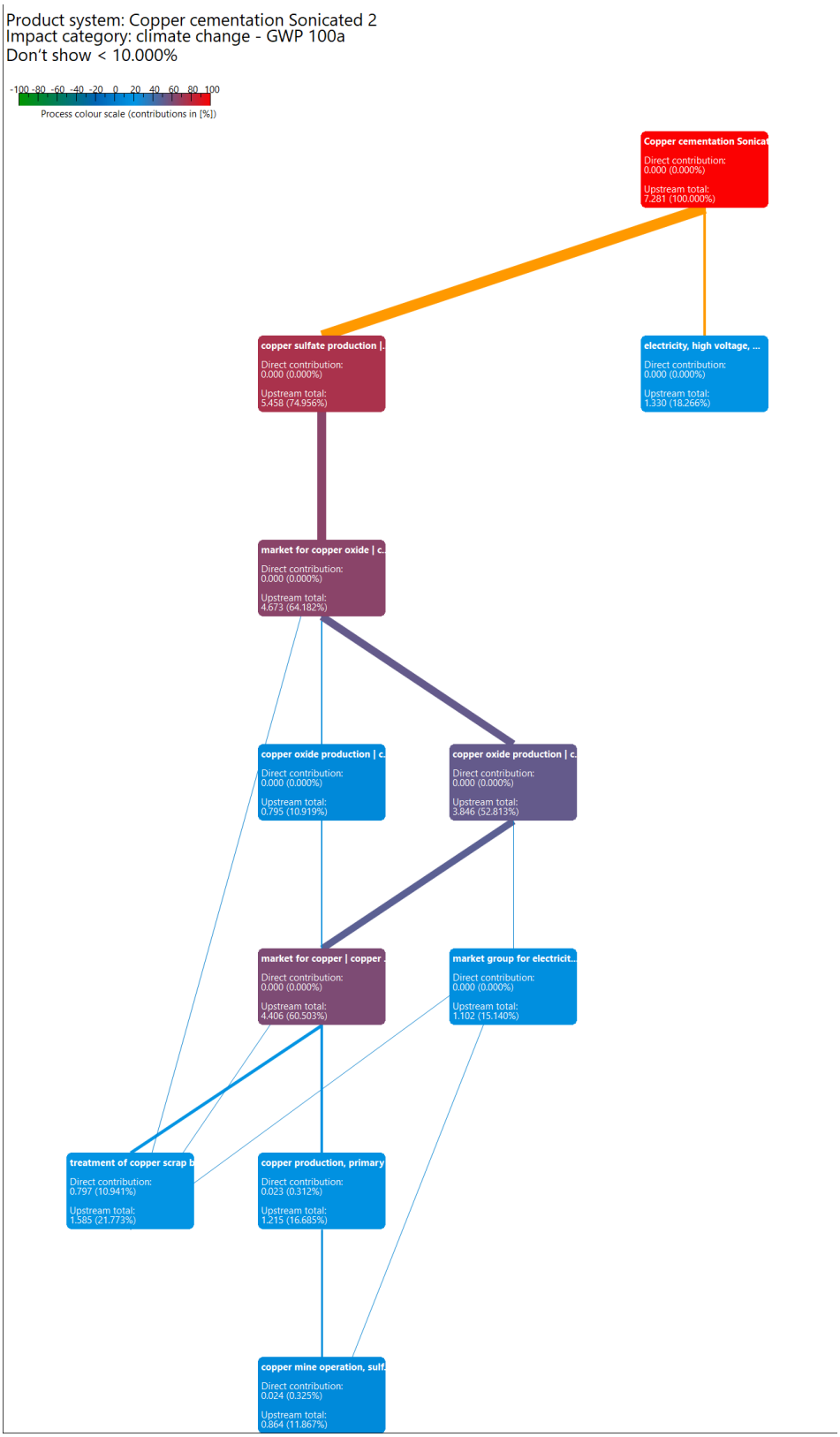
Product system: Copper cementation Sonicated 2
Impact category: climate change - GWP 100a
Don't show < 10.000%
-100 -80 -60 -40 -20 0 20 40 60 80 100
Process colour scale (contributions in [%])
Copper cementation Sonicat
Direct contribution:
0.000 (0.000%)
Upstream total:
7.281 (100.000%)
copper sulfate production |.
Direct contribution:
0.000 (0.000%)
Upstream total:
5.458 (74.956%)
electricity, high voltage, ...
Direct contribution:
0.000 (0.000%)
Upstream total:
1.330 (18.266%)
market for copper oxide | c..
Direct contribution:
0.000 (0.000%)
Upstream total:
4.673 (64.182%)
copper oxide production | c..
Direct contribution:
0.000 (0.000%)
Upstream total:
0.795 (10.919%)
copper oxide production | c..
Direct contribution:
0.000 (0.000%)
Upstream total:
3.846 (52.813%)
market for copper | copper ..
Direct contribution:
0.000 (0.000%)
Upstream total:
4.406 (60.503%)
market group for electricit..
Direct contribution:
0.000 (0.000%)
Upstream total:
1.102 (15.140%)
treatment of copper scrap b
Direct contribution:
0.797 (10.941%)
Upstream total:
1.585 (21.773%)
copper production, primary
Direct contribution:
0.023 (0.312%)
Upstream total:
1.215 (16.685%)
copper mine operation, sulf..
Direct contribution:
0.024 (0.325%)
Upstream total:
0.864 (11.867%)

Annex C

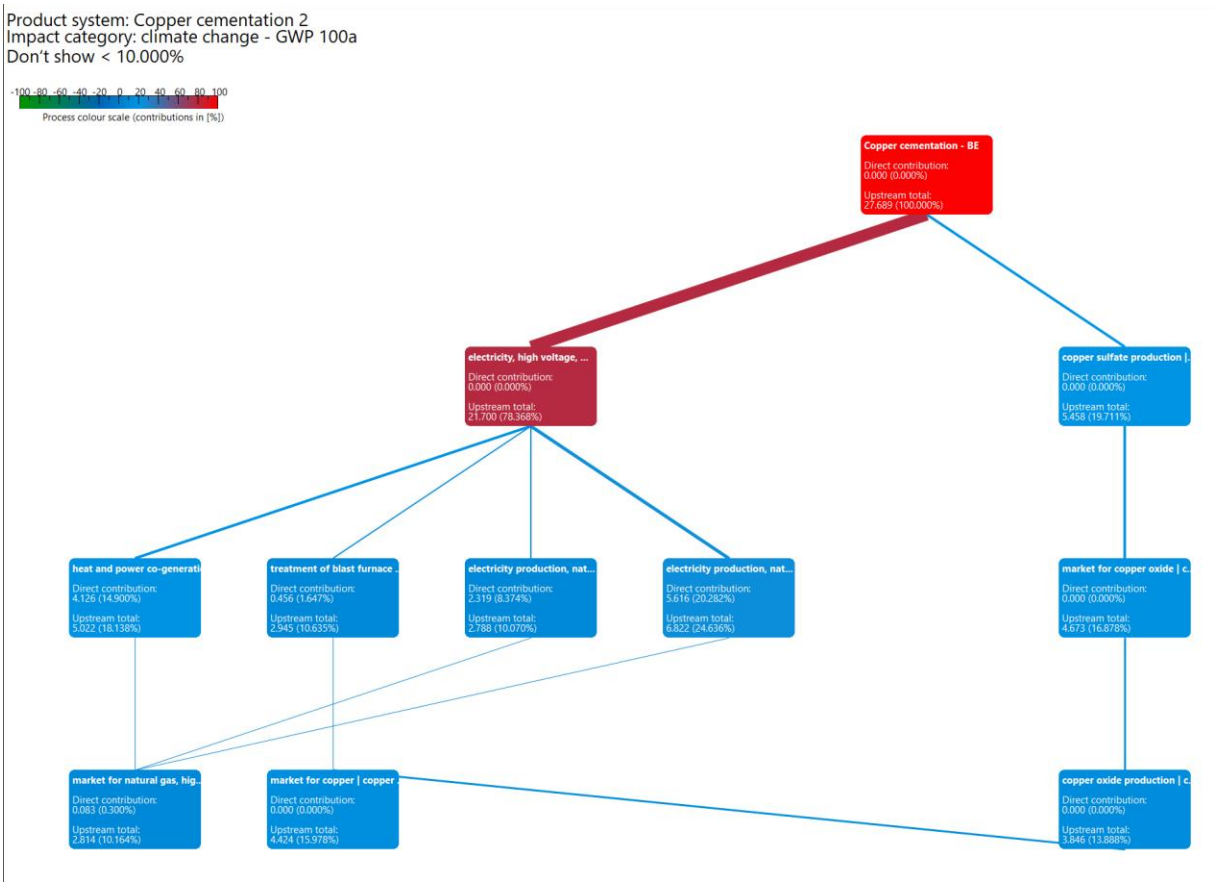
Product system: Copper cementation 2
Impact category: climate change - GWP 100a
Don't show < 10.000%
-100 -80 -60 -40 -20 0 20 40 60 80 100
Process colour scale (contributions in [%])
Copper cementation - BE
Direct contribution:
0.000 (0.000%)
Upstream total:
27.689 (100.000%)
electricity, high voltage, ...
Direct contribution:
0.000 (0.000%)
Upstream total:
21.700 (78.368%)
copper sulfate production |...
Direct contribution:
0.000 (0.000%)
Upstream total:
5.458 (19.711%)
heat and power co-generati...
Direct contribution:
4.126 (14.900%)
Upstream total:
5.022 (18.138%)
treatment of blast furnace ...
Direct contribution:
0.456 (1.647%)
Upstream total:
2.945 (10.635%)
electricity production, nat...
Direct contribution:
2.319 (8.374%)
Upstream total:
2.788 (10.070%)
electricity production, nat...
Direct contribution:
5.616 (20.282%)
Upstream total:
6.822 (24.636%)
market for copper oxide | c...
Direct contribution:
0.000 (0.000%)
Upstream total:
4.673 (16.878%)
market for natural gas, hig...
Direct contribution:
0.083 (0.300%)
Upstream total:
2.814 (10.164%)
market for copper | copper ...
Direct contribution:
0.000 (0.000%)
Upstream total:
4.424 (15.978%)
copper oxide production | c...
Direct contribution:
0.000 (0.000%)
Upstream total:
3.846 (13.888%)